Non-perturbative Studies of QED in (2+1) dimensions

A thesis submitted for the degree of Doctor of Philosophy

at The Australian National University

Chong-Ming Yung

August, 1990

This thesis reports work carried out while I was a student in the Department of Theoretical Physics, RSPhysS, The Australian National University between November 1986 and August 1990 under the supervision of Dr. Christopher J. Hamer and Dr. Conrad J. Burden.

Chapters 1,2,3 and 5 are mostly reviews whereas Chapters 4,6 and 7 present work done in collaboration with Dr. Hamer.

None of the work reported here has been submitted to any other institution of learning for any degree.

Chong-Ming Yung

3rd September 1990

Acknowledgements

I would first like to record my indebtedness to my parents for their support, without which none of this would have been possible.

I owe a great deal to Chris Hamer who has been a kind and generous supervisor and a patient teacher. It has been a real pleasure to learn from him. I am also grateful to Conrad Burden for his helpful advice, general and particular. It was also very enjoyable to collaborate with Chris Allton when he was in the Department.

Various members of the Department have made my stay here enjoyable; in particular, the Head of Department, Brian Robson, and my fellow dungeon dwellers.

I have benefited from conversations or written communications with Drs. F. A. Alcaraz, M. N. Barber, S. J. Brodsky, M. Burkardt, W. A. Coppel, and L. C. Hollenberg.

Finally, but by no means least, I would like to thank *mijn vriendin*, Kirsten Verburg, for her emotional support which has been invaluable during the few months it has taken to write this thesis.

Abstract

This thesis consists of two connected parts. In the first part a brief overview of lattice gauge theory is given. The Hamiltonian formulation of lattice gauge theory together with methods of calculation are reviewed in some detail. Emphasis is placed on the Hamiltonian lattice formulation of QED in (2+1) dimensions.

In the major project connected with the first part of this thesis, a stochastic extension of the exact finite-lattice method of calculation is presented and applied with some success to several models leading up to lattice QED in (2+1)D.

In the second part of the thesis, the Discretized Light Cone Quantization method is reviewed as a competitor to lattice gauge theory as a non-perturbative method for field theories. For QED in (1+1)D we obtained the mass spectrum with antiperiodic boundary conditions for the independent field. We also presented evidence of confinement and checked the non-relativistic limit.

The major project connected with the second part of the thesis is the application of Discretized Light Cone Quantization to QED in (2+1)D. We aimed at obtaining the bound state mass spectrum in the non-relativistic limit. In this limit we obtained the bound state mass spectrum independently via a Schrödinger equation approach. We found that with the most straightforward DLCQ scheme, namely regularization with momentum cutoffs, we were not able to obtain satisfactory continuum limit results.

Contents

Chapter 1

Introduction and Overview

The theory of Quantum Chromodynamics (QCD) is the quantum field theory of quarks and gluons. It is modelled on the theory of Quantum Electrodynamics (QED), with the quarks replacing the electrons and the gauge particles which mediate the interactions being gluons instead of photons. These quarks and gluons are believed to be the constituents of the nucleons and other hadrons seen in high energy experiments. Although first proposed by Gell-Mann and Ne'eman in the 60's, the quark picture of hadrons became generally accepted only after results from deep inelastic scattering experiments conducted in the early 1970's became available. These experiments involved the bombardment of nucleons with beams of electrons or positrons at very high energies. They indicated the existence of constituent particles within the nucleons, which come in three "colours". In QCD this colour SU(3) "charge" takes the place of the electric U(1) charge of QED. For detailed technical discussions of the physics and the history of these important developments, the texts of Close and Leader and Predazzi [1] are useful.

Calculations in QED have traditionally been of the perturbative type, and have had very great success. Some of the best agreement between theory and experiment in Physics has been achieved in this area. In fact, QED is conven-

tionally made into a sensible theory only within the framework of perturbation theory, with the procedure of renormalization being used to get rid of divergences occurring at each order. QCD also falls into the class of theories which become meaningful after renormalization is done [2]. For this theory, too, there is a regime in which perturbation theory allows contact with experiments. This is the high momentum transfer or short distance limit, as occurs in deep inelastic scattering experiments. For QED, on the other hand, it is the low momentum or large distance limit for which perturbation theory applies. The difference between the two theories is in the way their coupling "constants" vary with the momentum scale under consideration. For QED the coupling constant is small, $\alpha = e^2/4\pi \approx 1/137$, at large distance scales, and perturbation theory can be applied. For QCD, on the other hand, the coupling constant decreases with an increase in momentum, leading to a free theory of quarks in the high momentum limit. This property of QCD, known as "asymptotic freedom" [3], is precisely that seen in experiments and perturbative QCD has been very successful in describing the experimental results. For a review of perturbative QCD see, for example, the lecture notes of Mueller [4]. This success has led to QCD being regarded as the unique and correct theory of hadrons. A standard reference for the field theoretic arguments involved is the tome of Itzykson and Zuber [5].

Away from the perturbative regime, where the coupling constant is of the order 1, new methods had to be developed. In particular this was necessary to explain why free quarks have never been seen in nature. The non-existence of free quarks in the low energy limit (or at large distances), in distinct contrast to the case of electrons in QED, is known as the problem of "confinement". In the last 15 years or so, much effort has gone into the development and use of non-perturbative techniques in quantum field theory, with the main aim of

demonstrating confinement in QCD. The potential capacity to compute the mass spectrum and the properties of the hadrons from "first principles" has also been a major incentive.

The most familiar non-perturbative technique is Lattice Gauge Theory (LGT), developed by Kenneth Wilson [6] in 1974. Defining QCD on a discrete spacetime lattice, making use of equivalences with statistical mechanics and applying statistical mechanical methods like Monte Carlo, much progress has been made towards showing that QCD confines and showing that the hadron mass spectrum can be obtained from QCD. This has been at the expense of using up a not insignificant portion of all supercomputing time available to now. However, simulations of the full theory on lattices large enough to ignore finite-size effects are not yet available. Most of the reliable data has been obtained using the "quenched approximation", in which the quark dynamics are ignored. This is a reasonable approximation for fermions of large mass but not for the quarks we have to deal with. For some up to date results, consult the proceedings of the Lattice '88 and Lattice '89 [7] conferences. Opinions differ on how soon it will be before lattice gauge theory results can be accurately compared with experiments. Wilson [8] himself believes that a 10^8 increase in computing power and significant algorithmic advances are required.

In the first half of this thesis, we shall concern ourselves with the "Hamiltonian" formulation of LGT due to Kogut and Susskind [9]. Though it is not as popular as the "Euclidean" formulation of Wilson, the Hamiltonian formulation allows consideration of many analytic and semi-analytic methods and may turn out to be a strong competitor. In particular, we will describe attempts to develop stochastic methods for Hamiltonian LGT, given that Monte Carlo methods have turned out to be the most powerful available in Euclidean LGT. Hamilto-

nian LGT has similar mathematical structures to many quantum problems on lattices. Any advances here can be expected to result in payoffs in the areas of Statistical Mechanics and Condensed Matter Physics.

At this stage in the development of non-perturbative techniques for quantum field theories, it may well become profitable to consider alternatives to LGT. One such alternative is the method of Discretized Light Cone Quantization (DLCQ), developed by Brodsky and Pauli [10]. This method is based on quantization at equal light cone time $x^+ = x^0 + x^1$ instead of at equal time, as in Hamiltonian LGT, and on using a lattice in light cone momentum space instead of in coordinate space. Quantizing at equal light cone time is essentially the same as considering the infinite momentum frame. In this frame the vacuum structure is simpler because light cone momenta p^+ take only positive values and hence pair production from the light cone vacuum is forbidden. Such an approach has been endorsed by Wilson [8], as a way of eventually moving away from the grid techniques which are predominant at present to techniques based on the use of basis functions which may turn out to be more efficient. Results obtained in (1+1) dimensions have been very impressive [11]. Some effort has been made to advance beyond (1+1) dimensions [12]. In the second half of the thesis, we will present some preliminary work done in this direction and evaluate future prospects for this method.

Throughout the thesis, we will work mainly with Quantum Electrodynamics (QED) in (2+1) dimensions as a toy model for QCD. This theory is also believed to be a confining theory, in distinct contrast to QED in (3+1)D, but lacks many of the complications of non-Abelian theories, of which QCD is one. It also has one fewer space dimension than QCD, resulting in a further simplication. It has been studied in the past, mainly as a testing ground for theoretical ideas. In the

lattice Hamiltonian studies carried out mostly by Hamer and his collaborators, in which the strategy has been to build up from simple models to more complicated ones, striving for maximum accuracy at each stage, QED in (2+1)D represents just about the most complicated model that can be handled with some success with the techniques available. Most of the previous studies of the model have been perturbative in nature [13, 14]. On a consideration of the mass dimension of its coupling, QED in (2+1)D is a "superrenormalizable" theory [5] and can be made meaningful using renormalization theory. There are no ultraviolet divergences [14] in the theory. The massless theory has been shown to be free of infrared divergences [14] but for the massive theory there is a divergence in the mass renormalization [13]. Provided one formulates the theory in a parity invariant way [15], it is expected to be confining, with a massless "photon". The spectrum of states is expected to consist of charge-neutral bound states of the "electrons" and "positrons". This has not been established as fact yet but there is strong evidence for it.

The pure gauge theory, which also goes by the name of the U(1) gauge theory has also been studied extensively. Most of the previous lattice studies have been with this theory rather than the full QED in (2+1)D [16, 17, 18, 19, 20, 21, 22] The reason is that it has proved somewhat awkward to do numerical calculations with fermions on a lattice in the Euclidean formulation. Adding fermions is relatively easier in the Hamiltonian formulation and has been one of the main attractions in considering this formulation for Burden and Hamer [23] and for us. For this pure gauge theory defined on a lattice, Göpfert and Mack [16] have shown rigorously that the "string tension" in the theory is finite for all couplings, a signal of confinement.

We will now briefly summarise the rest of the thesis. In chapter 2, we briefly

review Lattice Gauge Theory and the standard techniques used, with the help of the reviews of Kogut [24] and the monograph of Creutz [25] which form some of the standard references in the field. We will treat QED in (2+1)D in chapter 3, leading to its Hamiltonian lattice formulation. In chapter 4, which forms the core of the first half of the thesis, we will develop Stochastic Truncation as a possible improvement on the well-tested techniques available in Hamiltonian LGT. We will describe tests on models leading up to QED in (2+1)D. In chapter 5, we will introduce DLCQ and describe its successes in (1+1)D. In chapter 6, we look at the non-relativistic limit of QED in (2+1)D using a Schrodinger equation approach, in order to compare with DLCQ results. In chapter 7, we will study QED in (2+1)D using the DLCQ formalism, concentrating on the non-relativistic limit.

Chapter 2

Lattice Gauge Theory

2.1 The Euclidean formulation

The key idea of Lattice Gauge Theory, or Lattice Field Theory (LFT) for field theories which are not gauge theories, is to replace continuum spacetime by a lattice, thus reducing the number of degrees of freedom to a countable number. The hope is that at the end of the day, by taking the continuum limit, where the lattice spacing goes to zero, one gets back continuum physics. In fact LFT can be viewed as an intermediate step in defining a continuum quantum field theory. An important property of this "regularisation" process is that local gauge invariance, believed to be a very important symmetry in nature and crucial to QED and QCD, can be maintained. Lorentz invariance, on the other hand, cannot be maintained on the lattice but it is expected to be recovered in the continuum limit.

Wilson's theory [6] was developed in the framework of path integral quantization. For a system of fields $\{\phi\}$ whose dynamics is specified by the action $S[\{\phi\}]$, the quantum mechanical object of central importance is Feynman's path integral Z, defined as being an integral over all "paths" $\{\phi(x)\}$ satisfying some boundary

conditions, of the exponentiated action multiplied by $i\hbar$:

$$Z = \int \{\mathcal{D}\phi\} \exp\left(\frac{i}{\hbar} S[\{\phi\}]\right). \tag{2.1}$$

All quantities of interest can be calculated from the path integral. In LFT one replaces continuum spacetime by a discrete regular lattice of spacing a and defines the fields on the lattice, with matter fields on the sites and gauge fields on the links joining the sites. In doing so, one can make rigorous the concept of "summing over all paths" since the number of "paths" then becomes countable. The action is replaced by a lattice action $S^{lattice}$ designed to recover the continuum action in the naive continuum limit. For instance one might make the substitution of derivatives with finite differences :

$$\partial_\mu \phi(x) \rightarrow \frac{\phi(x + a\hat{\mu}) - \phi(x)}{a} \tag{2.2}$$

and substitute for the integral over spacetime in the action a sum over lattice sites. Here $\hat{\mu}$ is a unit vector in the μ direction on the lattice. One also analytically continues to imaginary time via the Wick rotation $t \rightarrow it$ to obtain the Euclidean action $S_E^{lattice}$. The path integral Z then becomes the lattice path integral

$$Z_{lattice} = \sum_{\{\phi\}} \exp\left(-\frac{1}{\hbar} S_E^{lattice}\right) \tag{2.3}$$

where the sum is over all configurations of $\{\phi\}$ on the lattice. The Wick rotation makes the exponent in the path integral become purely real and easier to deal with than otherwise would be the case. The results are expected to be independent of whether we make the Wick rotation to Euclidean space or not. The terminology of "paths" is borrowed from Feynman's formulation of the quantum mechanics of

a point particle, discussed in the book of Feynman and Hibbs [26], in which the analogue of the field configuration $\{\phi\}$ is actually a path taken by the particle and the path integral gives the quantum amplitude for the propagation of a particle between two specified points.

$Z_{lattice}$ can be seen to have precisely the form of a partition function in Statistical Mechanics. We shall work in units in which $\hbar = 1$. Lattice spin models like the Ising model, in which the continuous fields $\{\phi\}$ are replaced by spins σ taking discrete values have been studied for a long time in Statistical Mechanics. Techniques developed there, like high temperature and low temperature perturbation expansions and the Monte Carlo method can be carried over wholesale into LFT. The series of books edited by Domb and Green [27] and later Domb and Lebowitz are the standard references in the field. An introductory account of the ideas in statistical mechanics relevant to lattice field theory can be found in the books of Pfeuty and Toulouse [28] and Parisi [29]. In practice, the most useful computational technique in LFT has turned out to be Monte Carlo, simply because of the large number of degrees of freedom involved. Techniques developed in LFT in turn have been applied to Statistical Mechanical models and as a result the boundary between the two subjects have more or less disappeared.

In the study of spin models in statistical mechanics, most emphasis has been placed on understanding their phase structures and in particular in understanding continuous phase transitions. An important concept in these studies is that of the correlation length ξ. This is defined by the expression

$$< \phi(x_1)\phi(x_2) >= e^{-\frac{|x_1-x_2|}{\xi}} \tag{2.4}$$

where the 2-point correlation function is calculated from the partition function

via

$$< \phi(x_1)\phi(x_2) >= \frac{1}{Z}\sum_{\{\phi\}} \phi(x_1)\phi(x_2)\mathrm{e}^{-S[\{\phi\}]}. \tag{2.5}$$

The points in phase space at which second-order phase transitions occur are known as "critical points" and are characterized by a divergent correlation length ξ. The correlation functions at critical points have a power law fall-off instead. A knowledge of all n-point correlation functions is sufficient for a full understanding of the model. Such knowledge has now become possible for certain conformally invariant theories [30].

In LGT one also obtains physical information by calculating correlation functions. One typically calculates the correlation function $\langle \mathcal{O}(x)\mathcal{O}(y) \rangle$ of some local field $\mathcal{O}(x)$ with the quantum numbers of the (composite) particle in which one is interested and obtains its mass from the exponential falloff of the correlation function with separation $|x-y|$. Calculations are usually done using the Monte Carlo technique on finite lattices, the sizes of the lattices being constrained by available computing resources. Finite size effects would have to be accounted for later. The mass (of the lowest excitation) is related to the correlation length ξ by $m = (\xi a)^{-1}$. In taking the continuum limit, where the lattice spacing a vanishes, one must let the correlation length go to infinity in order to arrive at a finite particle mass. Hence one must search for critical points in coupling parameter space, where the correlation length diverges.

In fact, one must do "renormalization" in order to obtain the continuum limit. This is done by making the coupling g dependent on the lattice spacing a in such a way that in the continuum limit, $g(a)$ approaches a critical point g^* and physical quantities become independent of a. A popular physical quantity to fix for a confining theory like QCD is the string tension which is the energy per unit length of a flux tube. Another choice could be the mass of a bound state. The

"smaller lattice sizes" on the line third from the bottom should read "smaller lattice spacing".

information regarding renormalization can be coded into the Callan-Symanzik β function, defined as

$$\beta(g) = -a\frac{dg}{da}. \tag{2.6}$$

For an arbitrary regularization scheme used in defining a quantum field theory, the β function relates the coupling to the cutoff used in the regularization. In order to reach the continuum limit we must have a "flow" of the coupling g to a zero of the beta function.

We shall now consider the situation of renormalization by keeping the string tension constant and obtain the β function for the lattice theory. The string tension can be written in the form

$$\sigma = \frac{1}{a^2}T(g) \tag{2.7}$$

where T is a dimensionless quantity measured on the lattice. By demanding that σ be independent of a, ie. setting $\frac{d\sigma}{da} = 0$, one obtains $\beta(g)$ in terms of T and its derivative. On the other hand, the beta function for QCD is known for small g from classic perturbative calculations performed by Gross and Wilczek, and by Politzer [3]. It is given by [†]

$$\beta(g) = -\frac{g^3}{16\pi^2}\left(11 - \frac{2}{3}n_f\right) + O(g^5) \tag{2.8}$$

for the theory with n_f fermion species. A comparison between the lattice result for β, which is valid for all g, and the perturbative QCD result will tell us if we are close to the continuum limit or not. If not, then, in order to obtain agreement we would presumably have to go to smaller lattice sizes (which for asymptotically free theories means smaller couplings) and larger lattice sizes. Once agreement with the perturbative QCD result is obtained, we can then, with some confidence,

[†]The result to $O(g^7)$ is renormalization scheme independent, but not higher order terms.

use the lattice calculation of whatever physical quantity we are interested in. In fact, if we can obtain a lattice β function, from fixing the string tension, which matches the perturbative result and is zero only at $g = 0$, then we would have convincing proof that QCD is confining.

In practice, the way to check if we are at or near the continuum limit is to subject quantities like $T(g)$ and masses $M(g)$ calculated on the lattice to "scaling tests". The β function of equation (2.8) can be inverted to obtain a in terms of g and an undetermined multiplicative constant Λ. For instance , for the theory with no fermions, and considering the g^5 term as well [31], we can obtain

$$a\Lambda = \left(\frac{16\pi^2}{11g^2}\right)^{\frac{51}{121}} e^{-\frac{8\pi^2}{11g^2}}[1 + O(g^2)]. \tag{2.9}$$

To test for scaling in the lattice string tension, $T(g) = a^2\sigma$ with σ unknown, we see if it scales with g in the predicted manner of equation (2.9). If it does in a certain region of coupling space (called the "scaling window") then we extract $\sigma\Lambda^2$ from the data in that region. The undetermined constant Λ can be eliminated by considering dimensionless ratios of physical quantities. Much of the effort in recent years has gone into speeding up algorithms in order to consider lattices large enough that a "scaling window" can be reached.

2.2 The Hamiltonian formulation

The above discussion refers to the Euclidean path integral formulation of LGT. Just as there are alternatives to path integral quantization in continuum quantum field theory, there are alternatives to this formulation. The "Hamiltonian" LGT formulation, developed by Kogut and Susskind [9], involves canonical quantization on a spatial lattice. Here one considers field operators which live on a

spatial lattice and operate on states in a Hilbert space. One proposes equal time commutation relations for these lattice field operators, and expresses observables in terms of them. The Hamiltonian operator, which generates the time evolution of the states, is the most important of these observables. Its eigenvalues give the masses of all the physical states in the theory. Obtaining the eigenvalue spectrum of the Hamiltonian is therefore a key objective of work in this formulation of LGT. Other physical quantities which are not eigenvalues of the Hamiltonian can be obtained as expectation values of other observables in the Hilbert space on which the lattice operators operate. The results obtained using the Hamiltonian formulation are expected to be the same as those obtained in the Euclidean formulation, in the continuum limit.

Several calculational techniques have been used in Hamiltonian LGT with varying degrees of success. These techniques go under the names of (1) perturbation expansions [32, 37], (2) the exact finite-lattice method [34], (3) variational methods [17, 21, 35, 36], and (4) real space renormalization [22]. The first three methods have been developed the furthest and we shall concentrate on them.

Perturbation theory was one of the first techniques applied. This is because the Hamiltonians, up to a dimensionful quantity, have the general form $H = H_0 - xV$, where H_0 and V are dimensionless operators and x is a dimensionless combination of the coupling g and the lattice spacing a. Working in a basis in which H_0 is diagonal, quantities like the ground state energy and the mass gap, which is the difference in energies between the ground state and the first excited state, can be developed as power series in x. One refers to these as strong-coupling (small x, large g)[†] expansions. As discussed earlier, one is interested in the critical behaviour of the theory, in order to study the continuum limit. Padé approximants and the like are therefore used to analytically continue these series

[†] That small x corresponds to large g is true, at least for gauge theories in 3 and 4 dimensions. Refer to Chapter 3 for the case of QED in 3 dimensions.

beyond their radii of convergence and to mimic the non-analytic behaviour associated with critical points. For pure gauge QCD, strong-coupling expansions are available [32, 33] for the ground state energy to order g^{-32}, for the string tension to order g^{-28} and for the mass gap to order g^{-24}. These are not quite sufficient to demonstrate scaling at weak coupling but are broadly consistent with it, and with Euclidean Monte Carlo results. The state-of-the-art calculations performed by Hamer et al [33] make use of the linked cluster expansion technique [37]. A typical strong coupling series can be written as a diagrammatic expansion. In this technique, contributions from diagrams spanning connected subsets of the lattice, or clusters, are determined, and from these contributions the series are obtained. The entire calculation can be done efficiently on a computer. This technique has been applied to many other models including to QED in (2+1)D [23] and QED in (3+1)D [38] both of which include fermions. The strong-coupling expansion technique is, however, hampered by the difficulty of calculating higher order terms. In general, the CPU time needed to calculate the nth term grows at least exponentially with n.

The second well tried and tested technique is the exact finite-lattice technique [34]. Here one calculates exactly a sequence of eigenvalues of the Hamiltonian on a lattice of size $M \times M \times M$, for a (3+1)D model, for $M = 1, 2, 3, \ldots$ and uses finite-size scaling theory [39] to extract information for the infinite size lattice. Briefly, this theory says that for a system away from criticality, its energy eigenvalues scale as

$$\omega_M - \omega_\infty \sim \mathrm{e}^{-\alpha M} \tag{2.10}$$

where α is a constant, whereas at criticality the energy eigenvalues scale as

$$\omega_M - \omega_\infty \sim \frac{1}{M}. \tag{2.11}$$

By looking at the behaviour of ω_M with M, one can then get accurate information about the position of the critical point, and accurate estimates of the energies. For statistical mechanical discrete spin models on a finite lattice, the basis of states on which the Hamiltonian has to be diagonalized is finite. The Lanczos method [40] for obtaining the lowest few eigenvalues and eigenvectors has been found to be very effective and the results obtained, judging by the accuracy of the critical indices, are comparable to the best results obtained using Euclidean techniques. For gauge models or for continuous spin models, however, the basis is a priori infinite even on a finite lattice. Some kind of basis truncation procedure is then necessary, with the effect of the truncation having to be accounted for. Basis truncation procedures have been studied in detail in the thesis of Allton [41][42] who considered the continuous spin O(2) model in (1+1)D. For this model, very good results have been obtained. However, not much success has been achieved in higher dimensions. For instance, for pure gauge QED in (2+1)D it has not been possible [19] to get beyond a 5×5 lattice and the extrapolations based on finite-size scaling theory cannot be used with confidence. In chapter 4, we shall present some work done to develop a stochastic procedure for basis truncation, in the hope that such a development will allow the finite-lattice method to be used to study models like QCD in the future.

The third method that has been popular in Hamiltonian LGT is the variational method. Here one chooses a trial state $|\psi>$ parametrized by one or more variational parameters α_i. The quantity

$$E(\alpha_i) = \frac{\langle\psi|H|\psi\rangle}{\langle\psi|\psi\rangle} \tag{2.12}$$

is then minimized over possible values of α_i and gives an upper bound to the ground state energy. The results are, of course, dependent on the quality of

the trial state chosen. Trial states chosen using physical insight can sometimes give very good results. An example is the analytic "demonstration" of scaling in the mass gap in pure gauge QED in (2+1)D by Suranyi [17]. Usually, though, the matrix elements in the calculation of $E(\alpha_i)$ have to be done numerically, for instance using Monte Carlo integration [35].

The Hamiltonian formulation can also be considered as the extreme anisotropic limit of the Euclidean formulation, in which one direction, the time direction, is made continuous. Letting the lattice spacing in the time direction be τ, we can write the path integral as $Z = Tr\{\mathbf{T}^N\}$ where $\mathbf{T}$ is the "transfer matrix" of the system. The trace is taken over states defined on a periodic spatial lattice and the transfer matrix takes these states at one time to states a time τ later. The transfer matrix formalism is the starting point of many approaches for which exact solutions have been found [43]. In the limit of vanishing τ, the transfer matrix takes the form $\mathbf{T} = \mathrm{e}^{-\tau \mathbf{H}}$ where $\mathbf{H}$ is the Hamiltonian, or time evolution operator. Taking the "Hamiltonian limit" is not uncommon in studies of statistical mechanical spin models. For 2 dimensional models, Hamiltonian methods have proved to be as successful as Euclidean methods, if success is based on how accurately critical exponents can be determined. See, for instance, the review of Henkel [44]. For this reason we will work in the Hamiltonian formulation. It should perhaps be reiterated that the techniques involved are not restricted to particle physics problems and any improvement in techniques developed to study LGT will have payoffs in other areas of physics.

Chapter 3

QED in (2+1)D

3.1 The continuum Lagrangian formulation

As the theory of QED in (2+1)D has somewhat peculiar properties, we shall first review the Lagrangian formulation, paying special attention to the symmetries of the theory. In the simplest formulation [14], the Lagrangian is given by

$$\mathcal{L} = \frac{i}{2}(\overline{\psi}\gamma^\mu\partial_\mu\psi - \partial_\mu\overline{\psi}\gamma^\mu\psi) - m\overline{\psi}\psi - \frac{1}{4}F^{\mu\nu}F_{\mu\nu} - eA_\mu\overline{\psi}\gamma^\mu\psi. \tag{3.1}$$

Here the Dirac matrices are given by $\gamma^0 = \sigma^3$, $\gamma^1 = i\sigma^1$, and $\gamma^2 = i\sigma^2$ where the σ's are Pauli matrices. They satisfy the commutation relations $\{\gamma^\mu, \gamma^\nu\} = \eta^{\mu\nu}$ with $\eta^{\mu\nu} = \mathrm{diag}(1, -1, -1)$. Two component spinors are sufficient to describe spinorial representations of the Lorentz group. The Lagrangian (3.1) is invariant under the usual local gauge transformations

$$\begin{aligned} \psi(x) &\rightarrow e^{-ie\Lambda(x)}\psi(x) \\ \overline{\psi}(x) &\rightarrow e^{ie\Lambda(x)}\overline{\psi}(x) \\ A_\mu(x) &\rightarrow A_\mu(x) + \partial_\mu\Lambda(x), \end{aligned} \tag{3.2}$$

and is also invariant under global Lorentz transformations. The discrete space-time symmetries are more subtle. The Lagrangian is invariant under charge conjugation but under parity and time reversal transformations the situation is different from the normal situation in 4 spacetime dimensions.

In 3 spacetime dimensions, the parity transformation can be taken to be the transformation of the spatial variable

$$\mathbf{x} = (x, y) \qquad \rightarrow \qquad \mathbf{x}' = (-x, y), \tag{3.3}$$

and the fermion and gauge fields transform as

$$\begin{aligned} \psi(t, \mathbf{x}) &\rightarrow \sigma_1 \psi(t, \mathbf{x}') \\ A^0(t, \mathbf{x}) &\rightarrow A^0(t, \mathbf{x}') \\ A^1(t, \mathbf{x}) &\rightarrow -A^1(t, \mathbf{x}') \\ A^2(t, \mathbf{x}) &\rightarrow A^2(t, \mathbf{x}'). \end{aligned} \tag{3.4}$$

The kinetic, Maxwell and interaction terms in the Lagrangian (3.1) are all invariant. The mass term $m\overline{\psi}\psi$ for the fermions, however, is anti-symmetric under the parity transformation. If this fermion mass term is included in the theory then we can expect that other parity- violating terms which are also "relevant" in the language of renormalization theory will come into play. One such term is the Chern- Simons term, $\frac{1}{4}\mu\epsilon^{\alpha\beta\gamma}F_{\alpha\beta}A_\gamma$, which has the effect of giving the photon a mass [14]. This already occurs at the level of perturbation theory . The photon mass is then expected to give rise to a non-confining theory. The situation concerning time reversal transformations is similar.

In order to obtain a confining theory, we can consider the situation where

$\psi = \begin{pmatrix} \psi_1 \\ \psi_2 \end{pmatrix}$ is a four component spinor [13], rather than a two component spinor. The Dirac matrices then are

$$\gamma^0 = \begin{pmatrix} \sigma^3 & 0 \\ 0 & -\sigma^3 \end{pmatrix}, \quad \gamma^1 = i\begin{pmatrix} \sigma^1 & 0 \\ 0 & -\sigma^1 \end{pmatrix}, \quad \gamma^2 = i\begin{pmatrix} \sigma^2 & 0 \\ 0 & -\sigma^2 \end{pmatrix}. \tag{3.5}$$

With this modification, and the following modifications to the transformation properties of the fermion field,

$$\begin{aligned} \psi_1(t,\mathbf{x}) &\rightarrow \sigma^1\psi_2(t,\mathbf{x}') \\ \psi_2(t,\mathbf{x}) &\rightarrow \sigma^1\psi_1(t,\mathbf{x}') \end{aligned} \tag{3.6}$$

the mass term, $-m\psi_1^\dagger\sigma^3\psi_1 + m\psi_2^\dagger\sigma^3\psi_2$, becomes symmetric. All the other terms in the Lagrangian (3.1) remain symmetric. The Lagrangian, similarly, becomes invariant under time reversal transformations.

In addition, for the massless theory, there is an extra global U(2) "chiral" symmetry [45] whose generators are the four matrices

$$I, \ \gamma^4 = \begin{pmatrix} 0 & I \\ I & 0 \end{pmatrix}, \quad \gamma^5 = \begin{pmatrix} 0 & -iI \\ iI & 0 \end{pmatrix}, \quad \text{and} \quad \gamma^{4,5} = i\gamma^4\gamma^5, \tag{3.7}$$

which satisfy the same Lie algebra as $\{I, \sigma^1, \sigma^2, \sigma^3\}$. The spinors transform according to

$$\begin{aligned} \psi &\rightarrow e^{i\left(\alpha_0+\alpha_1\gamma^4+\alpha_2\gamma^5+\alpha_3\gamma^{4,5}\right)}\psi \\ \overline{\psi} &\rightarrow e^{i\left(-\alpha_0+\alpha_1\gamma^4+\alpha_2\gamma^5-\alpha_3\gamma^{4,5}\right)}\psi \end{aligned} \tag{3.8}$$

This symmetry, which is chiral in the sense that the massless theory has more

symmetry than the massive theory, is expected to be broken in the massless theory to a global U(1)xU(1) symmetry. Studying this phenomenon is expected to give some insight into the problem of chiral symmetry breaking in QCD.

3.2 The Hamiltonian formulation

3.2.1 The continuum Hamiltonian

From the Lagrangian density, we can obtain the Hamiltonian density $\mathcal{H}$ by a Legendre transformation

$$\mathcal{H} = \Pi_{A_\mu}\partial_0 A_\mu + \Pi_\psi \partial_0 \psi + \partial_0 \overline{\psi}\Pi_{\overline{\psi}} - \mathcal{L} \tag{3.9}$$

where the Π's are the canonical momenta

$$\Pi_{A_\mu} = \frac{\partial \mathcal{L}}{\partial(\partial_0 A_\mu)}, \qquad \Pi_\psi = \frac{\partial \mathcal{L}}{\partial(\partial_0 \psi)}, \qquad \Pi_{\overline{\psi}} = \frac{\partial \mathcal{L}}{\partial(\partial_0 \overline{\psi})} \tag{3.10}$$

It is usual to work in the axial $A_0 = 0$ gauge. Note that fixing this gauge does not completely eliminate all the gauge degrees of freedom because time-independent gauge transformations do not take us out of the axial gauge. This residual gauge degree of freedom will have to be taken care of later, at the level of the Hilbert space. The result for the Hamiltonian density is

$$\mathcal{H} = \frac{i}{2}(\partial_j \overline{\psi}\gamma^j \psi - \overline{\psi}\gamma^j \partial_j \psi) + m\overline{\psi}\psi + eA_j \overline{\psi}\gamma^j \psi + \frac{1}{2}(B^2 + E_k^2) \tag{3.11}$$

and its spatial integral $\int d^2x \mathcal{H}$ gives the Hamiltonian H. The pure gauge term $\frac{1}{2}(B^2 + E_k^2)$ is the Hamiltonian density for classical electromagnetism in 2 space dimensions with $B(\mathbf{x}) = \epsilon_{kl}\partial_k A_l(\mathbf{x})$ being the magnetic field and $E_k = \partial_0 A_k$ being

the electric field. The other terms in the Hamiltonian are the kinetic and mass terms for the fermions and the interaction term.

In order to quantize the theory we specify equal-time commutation relations for the field variables $\psi(\mathbf{x})$, $\overline{\psi}(\mathbf{x})$, $\mathbf{A}(\mathbf{x})$ and $\mathbf{E}(\mathbf{x})$ which are now field operators acting on some Hilbert space. These commutation relations are

$$\begin{aligned} [\mathbf{E}_k(\mathbf{x}), \mathbf{A}_j(\mathbf{x}')] &= i\delta_{kj}\delta(\mathbf{x}-\mathbf{x}') \\ \{\psi_j(\mathbf{x}), \psi_k^\dagger(\mathbf{y})\} &= \delta^2(\mathbf{x}-\mathbf{y})\delta_{jk}. \end{aligned} \tag{3.12}$$

with all other (anti-) commutators vanishing. To get rid of the residual gauge degrees of freedom, we impose the Gauss' law constraint as a condition on the physical states $|\chi>$ of the theory. The interpretation of Gauss' law is the usual one that the physical states are the gauge-invariant ones. Explicitly, the Gauss' law condition on physical states is

$$\mathbf{G}(\mathbf{x})|\chi>=0 \tag{3.13}$$

for all spatial points $\mathbf{x}$. Here $\mathbf{G} = \psi^\dagger\psi - \partial_k\mathbf{E}_k$. For a time-independent function $\Lambda(\mathbf{x})$ define

$$\mathbf{U}(\Lambda) = \exp i\int d^2\mathbf{x}\mathbf{G}(\mathbf{x})\Lambda(\mathbf{x}). \tag{3.14}$$

Using the fundamental commutation relations we can show that

$$\begin{aligned} \mathbf{U}(\Lambda)\mathbf{A}_k(\mathbf{x})\mathbf{U}(\Lambda)^{-1} &= \mathbf{A}_k(\mathbf{x}) + \partial_k\Lambda(\mathbf{x}) \\ \mathbf{U}(\Lambda)\mathbf{E}_k(\mathbf{x})\mathbf{U}(\Lambda)^{-1} &= \mathbf{E}_k(\mathbf{x}) \\ \mathbf{U}(\Lambda)\psi(\mathbf{x})\mathbf{U}(\Lambda)^{-1} &= \mathrm{e}^{-i\Lambda(\mathbf{x})}\psi(\mathbf{x}) \end{aligned} \tag{3.15}$$

indicating that $\mathbf{U}(\Lambda)$ is a unitary representation of the group of time-independent

gauge transformations. The Gauss' law condition then implies that

$$\mathbf{U}(\Lambda)|\chi>=|\chi> \tag{3.16}$$

indicating the gauge invariance of $|\chi>$.

3.2.2 The lattice Hamiltonian for the pure gauge theory

We now proceed to put this theory on a lattice of spacing a. The fermion operators now live on the sites of the lattice and the gauge field operators on the links joining the sites. We are interested in physical states with zero momentum, and so we will impose translational and rotational invariance. On the lattice, translations are by multiples of a and rotations are by multiples of $\pi/2$. We shall first consider the pure gauge part of the Hamiltonian. It is convenient to work with the dimensionless operators

$$\mathbf{\Theta} = ea\mathbf{A}, \qquad \mathbf{L} = \frac{a}{e}\mathbf{E} \tag{3.17}$$

A link l of the lattice is labelled by $(\mathbf{n}, \mathbf{n}+a\mathbf{i})$ where $\mathbf{i} = 1, 2$ are unit vectors in the two perpendicular directions along the lattice. The gauge fields on the lattice are assigned directions : $-\mathbf{\Theta}(\mathbf{n}, \mathbf{n}+a\mathbf{i})$ is identified with $\mathbf{\Theta}(\mathbf{n}+a\mathbf{i}, \mathbf{n})$ and points in the opposite direction to $\mathbf{\Theta}(\mathbf{n}, \mathbf{n}+a\mathbf{i})$. The boson commutation relation then becomes

$$[\Theta_l, \mathbf{L}_{l'}] = i\delta_{ll'} \tag{3.18}$$

It is conventional to write the latticized form of the pure gauge part of the Hamiltonian (3.11), which is

$$\mathbf{H} = \int d^2\mathbf{x}\frac{1}{2}\left(\mathbf{E}^2 + \mathbf{B}^2\right), \tag{3.19}$$

as

$$\mathbf{H} = e^2 \sum_l \mathbf{L}_l^2 - \frac{1}{e^2 a^2} \sum_P \cos(i\Theta_P) \tag{3.20}$$

where the second sum is over all "plaquettes", which are unit squares on the lattice. Θ_P is a directed sum of the Θ's on the 4 links of the plaquette P. See Figure 3.1. It can be shown that the continuum Hamiltonian is recovered in the

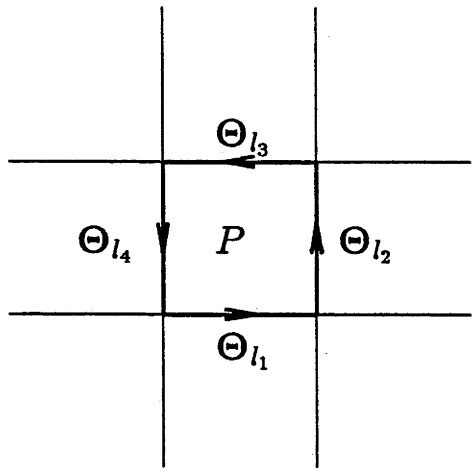

Figure 3.1: The definition of Θ_P $(= \Theta_{l_1} + \Theta_{l_2} - \Theta_{l_3} - \Theta_{l_4})$

"naive" continuum limit $a \to 0$. Note that the procedure of obtaining a lattice form of the Hamiltonian is not a unique one. Making the substitutions $g^2 = e^2 a$ and $x = g^{-4}$ the lattice Hamiltonian can be conveniently expressed as

$$\mathbf{H} = \frac{g^2}{2a} \left[\sum_l \mathbf{L}_l^2 - x \sum_p (\mathbf{Z}_p + \mathbf{Z}_p^\dagger) \right] \tag{3.21}$$

where $\mathbf{Z}_p = \mathbf{U}_{l_1} \mathbf{U}_{l_2} \mathbf{U}_{l_3}^\dagger \mathbf{U}_{l_4}^\dagger$ is a product of operators $\mathbf{U}_{l_j} = \exp(i\Theta_{l_j})$ around the links l_1, l_2, l_3, l_4 of plaquette P. This Hamiltonian is commonly referred to as the Hamiltonian for U(1) LGT.

On the lattice, the gauge field operators transform under time-independent

gauge transformations as

$$\begin{aligned} \Theta(\mathbf{n}, \mathbf{n}+a\mathbf{i}) &\rightarrow \Theta(\mathbf{n}, \mathbf{n}+a\mathbf{i}) + \mathrm{e}[\Lambda(\mathbf{n}+a\mathbf{i}) - \Lambda(\mathbf{n})] \\ \Theta_P &\rightarrow \Theta_P \\ \mathbf{L}(\mathbf{n}, \mathbf{n}+a\mathbf{i}) &\rightarrow \mathbf{L}(\mathbf{n}, \mathbf{n}+a\mathbf{i}) \end{aligned} \tag{3.22}$$

and the lattice Hamiltonian can be seen to be gauge invariant, as required. The physical states are again the gauge invariant states and the unitary represention of the group of gauge transformations is now given by

$$\mathbf{U}(\Lambda) = \exp i \sum_{\mathbf{n},j} \mathbf{L}(\mathbf{n}, \mathbf{n}+a\mathbf{j})\Lambda(\mathbf{n}), \tag{3.23}$$

the discretized version of equation (3.14) for the pure gauge theory.

3.2.3 The lattice Hamiltonian for the full theory

We are now ready to consider the remaining terms of the Hamiltonian of QED in (2+1)D which are, from (3.11),

$$\int d^2\mathbf{x} \left(m\overline{\psi}\psi - i\psi^\dagger \boldsymbol{\alpha} \cdot (\boldsymbol{\Delta} + ie\mathbf{A})\psi \right) \tag{3.24}$$

where $\alpha^i = \gamma^0\gamma^i$. Let us consider only the pure fermion terms for the moment. In order to avoid the fermion doubling problem (see e.g. [24]) which occurs when we just naively discretize the fermion Hamiltonian, we use the technique of "staggered fermions" due to Kogut and Susskind [9]. The idea is to distribute the fermion degrees of freedom into 2×2 cells on the lattice instead of into 1×1 cells. Consider the 4 sublattices labelled 1,2,3,4 in Figure 3.2.

Let $\boldsymbol{\xi}_p$ be a field living on sublattice p. Then let the field $\psi(\mathbf{R})$, which live on

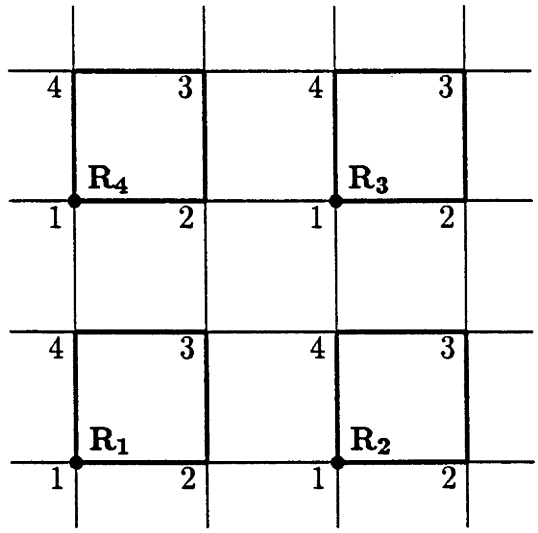

Figure 3.2: The four sublattices labelled 1,2,3,4 on which ξ_1, ξ_2, ξ_3, ξ_4 live. The four ξ's on each boldened plaquette are associated with $\psi(\mathbf{R})$ via equation (3.25).

the vertex $\mathbf{R}$ belonging to sublattice 1, be defined by

$$\begin{pmatrix} \psi_1 \\ \psi_2 \\ \psi_3 \\ \psi_4 \end{pmatrix} = \frac{1}{2\sqrt{2}a} \begin{pmatrix} 0 & -i & 0 & 1 \\ 1 & 0 & -i & 0 \\ -i & 0 & 1 & 0 \\ 0 & 1 & 0 & -i \end{pmatrix} \begin{pmatrix} \xi_1 \\ \xi_2 \\ \xi_3 \\ \xi_4 \end{pmatrix}. \tag{3.25}$$

$\psi(\mathbf{R})$ lives on a lattice of spacing $2a$ and in the limit of zero lattice spacing becomes the continuum fermion field. Note that with 4-spinors, this is very natural.

Define finite difference operators Δ_i by

$$\Delta_i \xi_p(\mathbf{n}) = \left[\xi_p(\mathbf{n} + a\mathbf{i}) - \xi_p(\mathbf{n} - a\mathbf{i})\right]/2a. \tag{3.26}$$

It can now be shown that the lattice Hamiltonian

$$\mathbf{H}_f^{kin} = -i\sum_{\mathbf{R}}(\xi_1\xi_2\xi_3\xi_4)\begin{pmatrix} 0 & -\Delta_1 & 0 & \Delta_2 \\ -\Delta_1 & 0 & \Delta_2 & 0 \\ 0 & \Delta_2 & 0 & \Delta_1 \\ \Delta_2 & 0 & \Delta_1 & 0 \end{pmatrix}\begin{pmatrix} \xi_1 \\ \xi_2 \\ \xi_3 \\ \xi_4 \end{pmatrix}. \tag{3.27}$$

is equivalent to

$$-4a^2 i\sum_{\mathbf{R}}\psi^\dagger(\mathbf{R})\left(\alpha_1\Delta_1+\alpha_2\Delta_2\right)\psi(\mathbf{R}) \tag{3.28}$$

which becomes the kinetic term in the pure fermion Hamiltonian in the naive continuum limit $a \to 0$. Furthermore, define the field $\boldsymbol{\xi}(\mathbf{n})$ which lives on all sites, to take the value of the field $\boldsymbol{\xi}_i$ at site $\mathbf{n}$ if $\mathbf{n}$ is on sublattice i and define the field $\boldsymbol{\chi}(\mathbf{n})$ by

$$\boldsymbol{\chi}(\mathbf{n}) = (-i)^{n_1+n_2}\boldsymbol{\xi}(\mathbf{n}). \tag{3.29}$$

Here the site vector is $\mathbf{n} = (n_1, n_2)$. In terms of the single fermion field $\boldsymbol{\chi}(\mathbf{n})$, the fermion Hamiltonian now becomes

$$\begin{aligned} \mathbf{H}_f &= \frac{1}{2a}\sum_{i,\mathbf{n}}\eta_i(\mathbf{n})\left[\boldsymbol{\chi}^\dagger(\mathbf{n})\boldsymbol{\chi}(\mathbf{n}+a\mathbf{i})+\boldsymbol{\chi}^\dagger(\mathbf{n}+a\mathbf{i})\boldsymbol{\chi}(\mathbf{n})\right] \\ &+ m\sum_{\mathbf{n}}(-1)^{n_1+n_2}\boldsymbol{\chi}^\dagger(\mathbf{n})\boldsymbol{\chi}(\mathbf{n}) \end{aligned} \tag{3.30}$$

where the mass term is obtained by following the same procedure as for the kinetic term. The auxiliary functions $\eta_i(\mathbf{r})$ are defined to be

$$\eta_1(\mathbf{r}) = (-1)^{r_2+1}, \eta_2(\mathbf{r}) = 1. \tag{3.31}$$

To include the interaction term it is customary [46] to insert the operator $U(\mathbf{n}, \mathbf{n}+a\mathbf{i})$ between the fermion operators $\boldsymbol{\chi}(\mathbf{n})$ and $\boldsymbol{\chi}(\mathbf{n}+a\mathbf{i})$. This ensures that gauge

invariance is maintained. The full Hamiltonian can then be written as

$$\mathbf{H} = \frac{g^2}{2a}\left(\mathbf{W}_0 + y\mathbf{W}_1 + y^2\mathbf{W}_2\right) \tag{3.32}$$

where

$$\begin{aligned}
\mathbf{W}_0 &= \sum_l \mathbf{L}_l^2 + \mu\sum_{\mathbf{n}}(-1)^{n_1+n_2}\chi^\dagger(\mathbf{n})\chi(\mathbf{n}) \\
\mathbf{W}_1 &= \sum_{i,\mathbf{n}}\eta_i(\mathbf{n})\left[\chi^\dagger(\mathbf{n})\mathbf{U}(\mathbf{n},\mathbf{n}+a\mathbf{i})\chi(\mathbf{n}+a\mathbf{i}) + \text{H.c.}\right] \\
\mathbf{W}_2 &= -\sum_P\left(\mathbf{Z}_P + \mathbf{Z}_P^\dagger\right)
\end{aligned}$$

Here the dimensionless coupling y is defined by $y = x^{1/2} = \frac{1}{e^2 a}$ and the dimensionless mass μ by $\mu = \frac{2am}{g^2}$.

To summarize, the Hamiltonian (3.32) is taken to be the lattice Hamiltonian for QED in (2+1)D. It is defined in terms of a single fermion field $\chi(\mathbf{n})$ living on the sites $\mathbf{n}$ and bosonic fields $\mathbf{L}_l$ and $\mathbf{U}_l$ living on the links l. The physical states $|\phi\rangle$ are the gauge invariant states satisfying $\mathbf{U}(\Lambda)|\phi\rangle = |\phi\rangle$, which come from the Gauss' law condition on states:

$$\mathbf{G}(\mathbf{n})|\phi\rangle = \left[\sum_j \mathbf{L}(\mathbf{n},\mathbf{n}+a\mathbf{j}) - \chi^\dagger(\mathbf{n})\chi(\mathbf{n})\right]|\phi\rangle = 0. \tag{3.33}$$

$\mathbf{U}(\Lambda) = \exp i\sum_{\mathbf{n}}\mathbf{G}(\mathbf{n})\Lambda(\mathbf{n})$ generates finite gauge transformations.

The lattice Hamiltonian (3.32) has been studied using the linked cluster expansion technique [23], briefly described in Section 2.2. In Chapter 4 we shall develop the method of stochastic truncation [47] and apply it to this Hamiltonian [48]. We shall test our methods on several models "leading up" to this Hamiltonian.

Chapter 4

Stochastic Truncation

4.1 Introduction

Let us begin this chapter by restating the problem : given a Hamiltonian operator of the form $H = H_0 - xV$ on a Hilbert space in which the "unperturbed" part H_0 is diagonal, determine its spectrum of eigenvalues. We treat the case where the Hilbert space is infinite, even though the Hamiltonian is defined on a lattice of finite size. This is the situation with continuous spin and gauge models. In order to obtain the eigenvalues numerically, we must truncate the chosen basis of states. If we choose a deterministic truncation scheme, the effect of the truncation must be accounted for. For instance, if we truncate the basis by allowing only states with "unperturbed" (ie. belonging to H_0) eigenvalues E_0 less than E_{max} [41], then we must extrapolate our results to $E_{max} \rightarrow \infty$. This has turned out to be difficult in practice, because of the large sizes of the basis required for obtaining results accurate enough to apply the theory of finite-size scaling.

It becomes important then, if one is to continue using the finite lattice approach coupled with finite size scaling on realistic models approaching lattice QCD, that other means of truncating bases be developed. Considering that

Monte Carlo is the most successful method in Euclidean LGT, it makes sense to search for a stochastic method of truncating a basis. One hopes to trade off the systematic errors involved with deterministic truncation schemes for random errors, which enter into any stochastic procedure. These random errors can be minimized with algorithmic improvement and by going to faster computers and hopefully the technique would then become competitive with standard Euclidean techniques. At this point, it might be worth mentioning that finite size effects are also corrected for in Euclidean lattice computations but there, the emphasis has not been on increasing the accuracy of the computations for smallish lattices but instead on getting to larger and larger lattices with moderate accuracy. Because the Hamiltonian formulation involves a continuous time direction and the lattices considered are effectively $\infty \times M^{d-1}$ compared to M^d for the Euclidean formulation, smaller lattices are sufficient to extract the same information. Of course, the data for a particular lattice are more difficult to extract in the Hamiltonian formulation than for a similar sized lattice in the Euclidean formulation. But results for the "exact" finite lattice method have been encouraging enough to warrant consideration of stochastic truncation.

We shall now briefly review the available "quantum Monte carlo" techniques that can be applied to Hamiltonian LGT. The motivation for these quantum MC algorithms initially came from studies in solid state physics where quantum mechanical problems defined on lattices are very natural. Particle physicists working in the Hamiltonian formulation of LGT have also been involved in recent developments. The two major approaches that can be discerned from the literature on the subject are the Green's function Monte Carlo (GFMC) method and the Projector Monte Carlo (PMC) method.

In the GFMC approach [49], the starting point is the eigenvalue equation

$$H|\phi\rangle = (H_0 - xV)|\phi\rangle = E|\phi\rangle \tag{4.1}$$

which can be written in the form

$$|\phi\rangle = (H_0 - E)^{-1} xV|\phi\rangle. \tag{4.2}$$

Choosing a basis $\{|i\rangle\}$ in which V is diagonal, we can write equation (4.2) as

$$|\phi\rangle = x \sum_{i,j} G(E;i,j)V_j\langle j|\phi\rangle|i\rangle \tag{4.3}$$

where the "Green's function" $G(E;i,j)$ is $\langle i|\,(H_0 - E)^{-1}\,|j\rangle$. To solve for x and $|\phi\rangle$ in equation (4.3) given E, the following iterative procedure is followed. Let $|\phi\rangle = \sum n_k|k\rangle$ where the n_k's are integers. We then obtain the right hand side of equation (4.3), to be called $|\phi'\rangle$, by the following two-step stochastic process. The first step is "branching", whereby for each state $|k\rangle$ in $|\phi\rangle$ we form an integer n'_k whose average is given by $V_k n_k$. We then let each of the n'_k states $|k\rangle$ "diffuse", that is we construct a probability function $P(i,j) = G(E;i,j)/\sum_i G(E;i,j)$ and let each state $|k\rangle$ diffuse to $|l\rangle$ with probability $P(l,k)$. We then gather all the states $|l\rangle$ to form $|\phi'\rangle$. In order that $|\phi\rangle$ is the solution of equation (4.2) we must have $|\phi\rangle = |\phi'\rangle$. To obtain a solution iteratively, x is modified at each iteration step such that the number of states $\sum_k n_k$ is kept relatively constant. The average of x over iteration steps then gives the value of x which corresponds to the energy E. The details of the iterative procedure and the averaging will be treated in detail in the algorithm that we will eventually adopt, which has these features in common with the GFMC method.

The PMC method [50] is based on the following theorem : given any states $|\phi\rangle$ and $|\chi\rangle$ which are not orthogonal to the ground state $|\psi_0\rangle$, the ground state energy E_0 is given by

$$\lim_{\alpha\to\infty} \frac{\langle\chi|e^{-(\alpha+\beta)H}|\phi\rangle}{\langle\chi|e^{-\alpha H}|\phi\rangle} = e^{-\beta E_0} \tag{4.4}$$

The PMC method involves setting $\alpha = M\Delta\tau$ and calculating

$$\langle\chi|\left(e^{-\Delta\tau H}\right)^M|\phi\rangle \tag{4.5}$$

by a stochastic process. This is done by inserting a complete set of states $\{|i\rangle\}$ into the matrix element (4.5) and factoring the matrix element in the form

$$\langle j|e^{-\Delta\tau H}|i\rangle = S_{ij}P_{ij} \tag{4.6}$$

where P_{ij} has the properties (1) $P_{ij} \geq 0$, (2) $\sum_j P_{ij} = 1$ and can be interpreted as the probability of obtaining state $|j\rangle$ from state $|i\rangle$. A "path" $|i_1\rangle \to \ldots \to |i_m\rangle$ of length M is then generated using the probability function P_{ij} and the product of the "scores" S_{ij} associated to the path. The ground state energy E_0 is then obtained, by means of equation (4.4), by summing over a collection of paths each weighted by a product of scores. A more efficient version, known as the Ensemble Projector Monte Carlo (EPMC) method [51], was also developed along lines similar to the GFMC method. Here one also makes use of the basic equation (4.4) but instead of generating paths, one iterates trial wavefunctions $|\psi\rangle$, as in the GFMC method. The iteration and averaging procedures are again similar to those in the algorithm we will describe later and will not be given here.

Both the GFMC and PMC/EPMC methods have the disadvantage that ma-

trix elements (of $(H_0 - E)^{-1}$ and $e^{-\Delta\tau H}$) are not easy to calculate. Usually tricks and approximations have to be used, making it difficult to evaluate their usefulness as general purpose algorithms. The algorithm that we shall adopt [47] involves only matrix elements of H which are easy to calculate. Similar methods have been considered in [52] and [53] for 2 dimensional spin models.

4.2 The Stochastic Truncation Method

4.2.1 The basic algorithm

Our method is based on the "power method" of obtaining the largest eigenvalue and associated eigenvector of a diagonalizable matrix H by repeated multiplication of H onto a trial vector $|\phi\rangle$. The basic relation is that, for large M,

$$H^M|\phi\rangle \propto E_0^M|\Phi_0\rangle + O\left(\frac{E_1}{E_0}\right)^M \tag{4.7}$$

where E_0 is the largest eigenvalue, $|\Phi_0\rangle$ is the corresponding eigenvector, E_1 is the next largest eigenvalue and $|\phi\rangle$ is a starting "trial vector" which is not orthogonal to $|\Phi_0\rangle$. The algorithm allows the extraction of E_0 and $|\Phi_0\rangle$ given $|\phi\rangle$.

Let $\{|i\rangle\}$ be a basis of states which is convenient to work with. Let $|\Psi^{(m)}\rangle = \sum_i n_i^{(m)}|i\rangle$ be a "trial state" at the mth iteration or "time" step, with the amplitudes $n_i^{(m)}$ taking only integer values. And let $S^{(m)}$ be a "score" at time m. The algorithm consists of the following two rules for generating $|\Phi^{(m+1)}\rangle$ and $S^{(m+1)}$ at time $m+1$ from $|\Phi^{(m)}\rangle$ and $S^{(m)}$ at time m :

$$n_k^{(m+1)} = \sum_i R\left(H_{ki}\frac{n_i^{(m)}}{S^{(m)}}\right) \tag{4.8}$$

$$S^{(m+1)} = S^{(m)}\frac{\sum_i |n_i^{(m+1)}|}{\sum_j |n_j^{(m)}|}. \tag{4.9}$$

Here H_{ki} is an element of the matrix H and the "stochastic rounding function" $R(x)$ is defined by

$$R(x) = \begin{cases} [x] & \text{with probability } 1-\delta \\ [x]+1 & \text{with probability } \delta \end{cases} \tag{4.10}$$

where $[x]$ is the largest integer less than or equal to the real number x, and $\delta = x - [x] \geq 0$ is the remainder. The function $R(x)$ can be implemented by generating a random number ϵ in the range $[0,1]$ and choosing

$$R(x) = \begin{cases} [x] & \text{if } \epsilon > \delta \\ [x]+1 & \text{otherwise} \end{cases} \tag{4.11}$$

$R(x)$ has the property that on averaging over many trials (or, equivalently, over iterations after equilibrium has been reached) denoted by angular brackets $< >$ we have

$$< R(x) > = x \tag{4.12}$$

We claim that for large m, $|\Phi^{(m)}\rangle$ is an approximation to the eigenvector $|\Phi_o\rangle$ and $S^{(m)}$ to the eigenvalue E_0 in the sense to be defined below. The first rule "truncates" the basis needed to represent the eigenvector because $n_i^{(m)} = 0$ is a possible (and even likely) outcome. The second rule is designed to ensure that the "ensemble size" $N^{(m)} = \sum |n_i^{(m)}|$ stays approximately constant for successive m.

4.2.2 Measurements

If the system comes to an "equilibrium", where the ensemble size $N^{(m)}$ and score $S^{(m)}$ fluctuate for successive m around some fixed values, then we can say the

following:

$$\langle n_k \rangle = \sum_i H_{ki} \langle \frac{n_i}{S} \rangle. \tag{4.13}$$

We also make the assumption that we can rewrite this as

$$\langle n_k \rangle = \sum_i H_{ki} \langle n_i \rangle \langle \frac{1}{S} \rangle. \tag{4.14}$$

This is not strictly correct because the n_k's and S's are correlated but for large enough ensemble sizes we believe that this is a fair assumption. Granted this, and on comparison with the eigenvalue equation

$$E_0 c_k^0 = \sum_k H_{ki} c_i^0 \tag{4.15}$$

where the c_i^0's are the amplitudes in the basis $\{|i\rangle\}$ of the eigenvector $|\Phi_0\rangle$, we have the result that

$$\langle n_k \rangle \propto c_k^0 \tag{4.16}$$

$$\langle \frac{1}{S} \rangle = \frac{1}{E_0}. \tag{4.17}$$

In other words, the averages over iterations m, after equilibrium has been reached, of the amplitudes $n_k^{(m)}$ and scores $S^{(m)}$ give the amplitudes c_k^0 and energy E_0.

An independent estimate of E_0, known in the EPMC literature as the "trial estimate" E_T, can be found from the average over iterations of the quantity

$$\frac{\langle \chi | H | \Psi^{(m)} \rangle}{\langle |\Psi^{(m)}\rangle} = \frac{\langle \sum H_{ij} n_i^{(m)} \rangle}{\langle \sum n_i^{(m)} \rangle}. \tag{4.18}$$

Here $|\chi\rangle = \sum |i\rangle$ is the "broad state". We have found that the trial estimate agrees well with the other estimate of the energy E_0 in equation (4.17), also

known as the "growth estimate", in cases where the amplitudes are non-negative. When negative amplitudes are required, difficulties can arise due to cancellation in the denominator of equation (4.18).

We can also calculate expectation values of operators Q other than the Hamiltonian in the state $|\Phi_0\rangle$. If Q commutes with H then we simply replace H by Q in the trial estimate. If Q does not commute with H then the expectation value is given by an average of

$$\frac{\langle \Psi'^{(m)}|Q|\Psi^{(m)}\rangle}{\langle \Psi'^{(m)}|\Psi^{(m)}\rangle} \approx \frac{\langle \Psi_0|Q|\Psi_0\rangle}{\langle \Psi_0|\Psi_0\rangle} \tag{4.19}$$

where $|\Psi^{(m)}\rangle$ and $|\Psi'^{(m)}\rangle$ are independently evolved trial states. We cannot let $|\Psi^{(m)}\rangle$ and $|\Psi'^{(m)}\rangle$ be the same state in equation (4.19) because even though we have $\langle n_k\rangle \propto c_k$ it is not true that $\langle n_k^2\rangle \propto c_k^2$ but it is true that

$$\langle n_k n_k'\rangle = \langle n_k\rangle\langle n_k'\rangle \propto c_k^2 \tag{4.20}$$

if $|\Psi^{(m)}\rangle$ and $|\Psi'^{(m)}\rangle$ are independent.

Because the data are correlated in time, the straightforward way of calculating errors is invalid. We calculate the variance using the standard procedure [55] of organizing the data into bins of size M, each bin containing the data from M successive iterations. The average value for each bin is recorded and the average and variance of these bin values taken. The bin size M is increased until the variance plateaus out and this value of the variance is used.

4.2.3 Variational Guidance

It is possible [53] to reduce the variance of the energy estimates calculated from data for a fixed time length if we know a good approximation to $|\Phi_0\rangle$ beforehand.

Suppose $|\chi_0\rangle$ is such a wavefunction. Then let U be an operator defined by $\langle\chi|U = \langle\chi_0|$ where $|\chi\rangle$ is the broad state defined in the previous subsection. Then we can see that the following holds:

$$\frac{\langle\chi_0|H|\Psi^{(m)}\rangle}{\langle\chi_0|\Psi^{(m)}\rangle} = \frac{\langle\chi|\tilde{H}|\tilde{\Psi}^{(m)}\rangle}{\langle\chi|\tilde{\Psi}^{(m)}\rangle} \tag{4.21}$$

where $\tilde{H} = UHU^{-1}$ and $|\tilde{\Psi}^{(m)}\rangle$ is obtained by starting with the initial state $U|\Psi^{(0)}\rangle$ instead of $|\Psi^{(0)}\rangle$. Hence we should get the same result for the trial estimate E_T regardless of whether we work with H and $|\chi\rangle$ or with $\tilde{H}$ and $|\chi_0\rangle$. But, if $|\chi_0\rangle$ is a better approximation to $|\Phi_0\rangle$ than is the broad state $|\chi\rangle$ then we can expect the variance to be reduced if we work with the transformed system. In fact, if $|\chi_0\rangle = |\Phi_0\rangle$ the left hand side of equation (4.21) gives E_0 exactly, regardless of what $|\Psi^{(m)}\rangle$ is. Similarly, we can expect a smaller variance for the growth estimate $\langle\frac{1}{S}\rangle^{-1}$ because now the amplitudes $n_i^{(m)}$ are biased towards the state $|\chi_0\rangle$ and changes in $n_i^{(m)}$ and hence in $S^{(m)}$ are now less likely. It should be emphasized, however, that the eigenvalues of the matrices H and $\tilde{H}$ are identical and that the "guided" estimates are *unbiased.*

4.2.4 Implementation

Because we are interested in the ground state of a Hamiltonian H, which has the lowest rather than the highest energy eigenvalue, we consider $E_{cut} - H$ rather than H where E_{cut} is a number larger than the largest eigenvalue of H, presuming there exists a largest eigenvalue. For the Hamiltonians of discrete spin models on finite lattices, such is always the case. However for a continuous spin model, the basis is infinite even for a finite lattice and there is no upper limit to the energy. In this case, there will be two steps to the approach. We first do a deterministic truncation of the basis. This we do by restricting the basis to states

with "unperturbed" energy less than E. So, in this case we do need a deterministic truncation in addition to a stochastic truncation. The difference between this approach and the exact finite lattice approach is that the deterministic truncation can be much less severe, ie. E_{cut} can be much larger than would be the case in the exact finite lattice approach. The hope is that now the systematic errors associated with deterministic truncation will be insignificant compared to the random errors introduced by stochastic truncation. The largest eigenvalue of the operator $E_{cut} - H$ obtained by stochastic truncation is then the ground state energy of the system and its associated eigenvector the ground state vector. Also, expectation values are now ground state expectation values.

We have found that variational functions of the form

$$|\chi_0\rangle = \sum_i e^{-\alpha\epsilon_i}|i\rangle \tag{4.22}$$

where ϵ_i is the "unperturbed energy" of the state $|i\rangle$ (ie. $H_0|i\rangle = \epsilon_i|i\rangle$) work well as guide wavefunctions. The U operator is diagonal and hence the transformed Hamiltonian $\tilde{H}$ is easily calculated. The variational parameter α is adjusted to minimize the variance for a set of values of the coupling and, for other couplings not in the set, the optimal values of α are determined by interpolation.

It is unfortunate that we have not been able to implement variational guidance for ground state expectation values $\langle Q \rangle$ in a similar fashion. The reason is that the U operator, being diagonal, is not unitary unless the variational parameter α is zero and so the expectation value of the transformed operator $\tilde{Q} = UQU^{-1}$ in the transformed ground state $|\tilde{\Phi}_0\rangle = U|\Phi_0\rangle$ is not equal to $\langle Q \rangle$.

In the exact finite-lattice method it is usual to make use of the translational, rotational and reflection symmetries (or rather, their remnants on the lattice) of the models to reduce the size of the basis we need to consider. One might

think that using such a basis of "symmetrized" states is useful for our stochastic truncation method as well. This has turned out not to be the case for the reason that the symmetrization process is too time consuming compared with the other steps in the algorithm.

In the next section, we describe applications of the Stochastic Truncation Method. We shall first test the algorithm on a 6×6 matrix for which exact results are known. Then we will apply it to the Z_2 gauge model in (2+1)D, the U(1) gauge model and finally QED in (2+1)D.

4.3 Applications of Stochastic Truncation

4.3.1 Tests on a small matrix

We begin by considering a 6×6 matrix obtained by using an energy cutoff of 5 in the antisymmetric sector of U(1) LGT (See Section 4.3.3). For the moment we need only be concerned with the matrix elements which are

$$\begin{pmatrix} 1 & -x & x & 0 & 0 & 0 \\ -x & 1 & 0 & x & -x & x \\ x & 0 & 1 & x & x & x \\ 0 & x & x & 1 & 0 & 0 \\ 0 & -x & x & 0 & 1 & 0 \\ 0 & x & x & 0 & 0 & 1 \end{pmatrix} \tag{4.23}$$

The largest eigenvalue can easily be found to be $1 + 2x$ with eigenvectors (1,-1,1,0,1,0) and (0,1,1,1,0,1). We apply our stochastic truncation method to obtain the largest eigenvalue and corresponding eigenvector. The largest eigenvalue is degenerate but with a suitable starting state we will "project" out only one eigen-

vector.

We chose the initial state to be (1,0,0,0,0,0). We ran the program for 500 time steps, for an ensemble size of 12, trial eigenvalue of 6, and for $x = 1.6$. The score $S^{(m)}$ is plotted against iteration number m in Figure 4.1. The reason

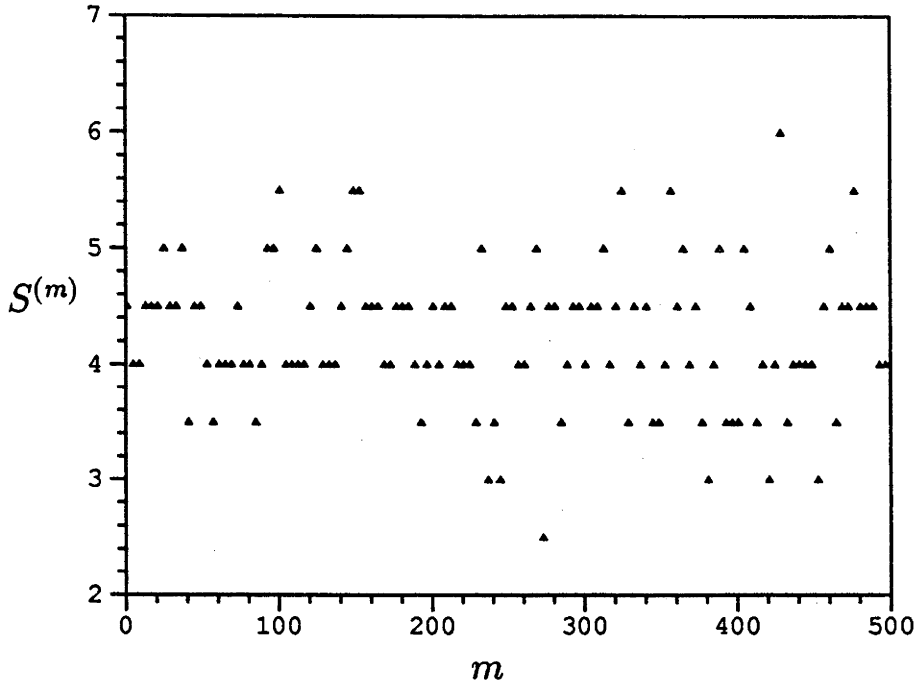

Figure 4.1: The score $S^{(m)}$ against iteration number m

that the scores take only half integer values is because of the combination of trial eigenvalue and starting ensemble size, which is purely coincidental. As can be seen, "equilibration" takes place almost straight away. Nevertheless, we discard the first 100 data points and analyse the data using a bin size of 10. We obtain the largest eigenvalue to be 4.229 with a standard error of 0.0211 and the associated

(unnormalized) eigenvector to be

$$\begin{pmatrix} 1.61 & (0.06) \\ -1.95 & (0.16) \\ 1.24 & (0.18) \\ -0.35 & (0.15) \\ 1.61 & (0.05) \\ -0.37 & (0.17) \end{pmatrix} \tag{4.24}$$

These are in good agreement with the exact values. The error is expected to decrease with the square root of the iteration length. The error was found to decrease with an increase in the ensemble size, as can be seen from Figure 4.2.

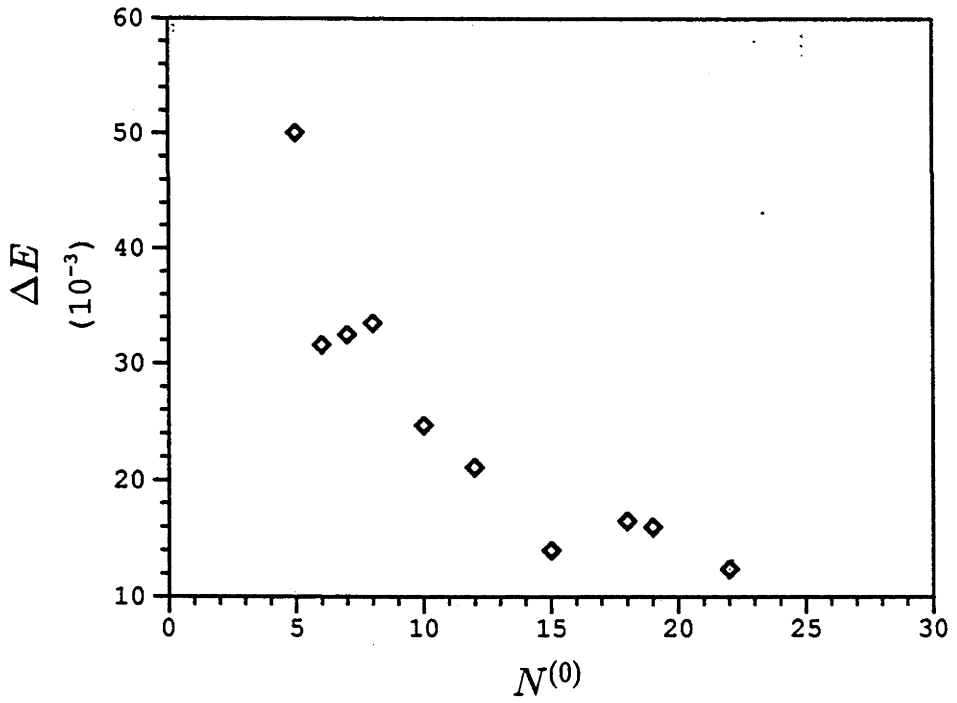

Figure 4.2: The dependence of the standard error of the eigenvalue estimate on the starting ensemble size $N^{(0)}$.

4.3.2 Z_2 Gauge Model in (2+1)D

The next model we considered was the Z_2 gauge model [24] in (2+1)D which is the simplest model with independent gauge field degrees of freedom. It is dual to the 3D Ising model and its phase structure has been well studied. It is known to exhibit a second order phase transition and its string tension undergoes a "roughening transition" [56] which forms a barrier to the analytic continuation of strong coupling series for the string tension. However, the exact finite lattice method is known [57] to be able to handle the problem well. The results available allows us to check our stochastic truncation method. The Hamiltonian is very much like that of the U(1) gauge model and is given by [58]

$$H = \sum_l [1 - \sigma_1(l)] - x \sum_p \sigma_3(l_1)\sigma_3(l_2)\sigma_3(l_3)\sigma_3(l_4) \tag{4.25}$$

We work in a basis in which the Pauli matrix σ_1 is diagonal. We then have two possible states at each link, corresponding to the two eigenvalues of σ_1 and the effect of σ_3 is to flip between these two states. At strong coupling, ie. at $x = 0$, the ground state of the model has eigenvalue 1 for σ_l at each link l and the ground state energy is zero. The physical states $|\phi\rangle$ of the theory are again the gauge invariant states characterized by

$$G(n)|\phi\rangle = |\phi\rangle \tag{4.26}$$

where $G(n) = \prod_i \sigma_1(l_i)$ for all links l_i terminating at the site n. A basis for the physical states can be generated as follows. We start from the strong coupling ground state and apply to it the non-diagonal part V of the Hamiltonian to form new states. These states are then acted on by V to form other states, etc. All these states are automatically gauge invariant. We work with a periodic lattice

of size $M \times M$.

The physical quantities of interest are the ground state energy per site ω_0 and the axial string tension T given by

$$\omega_0 = \frac{E_0}{M^2}, \qquad T_A = \frac{E_A - E_0}{M}. \tag{4.27}$$

Here E_A is the lowest energy in the "axial string sector", which contains the "strong coupling string state". This is defined as the state with a line of "flux" (ie. σ_l has eigenvalue -1) of length M running along one row of links of the lattice. This axial string sector is disjoint from the "vacuum sector" which contains the ground state. To calculate ω_0 using the stochastic truncation method, we simply apply the algorithm starting from the strong coupling ground state, which is the state without any flux. To calculate E_A we simply start from the strong coupling string state instead.

We do this for lattice sizes $M = 2, 3, 4$. Our calculations were done with an ensemble size of 1000, discarding the first 100 to allow for equilibration. Doing the statistical analysis as described earlier, the following results were obtained [42]. See Figures 4.3 and 4.4.

These are in excellent agreement with the exact results of Hamer and Irving [57]. Random errors are smaller than the symbols in all cases. With the exception of the value for the string tension for $M = 4$, there is total agreement with the results in [57], up to random errors. The results were good enough to do a finite-size scaling analysis [39] but that was not the point of the exercise. The success of the Stochastic Truncation Method encouraged us to do a similar calculation on the U(1) model and QED in (2+1)D.

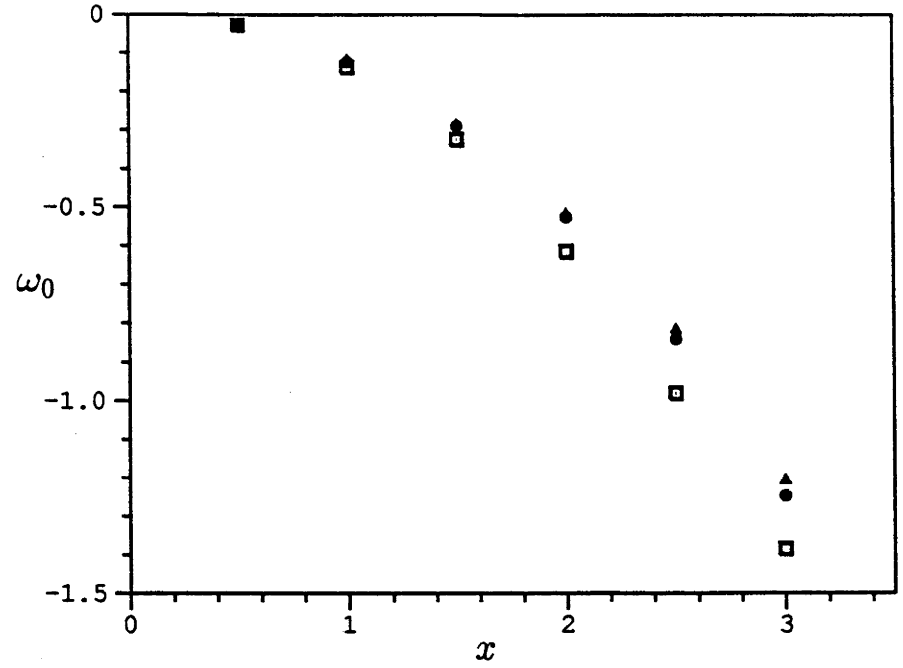

Figure 4.3: The ground state energy per site of the Z_2 gauge model versus coupling x, for lattice sizes $M = 2(\square), 3(\bullet)$ and $4(\triangle)$.

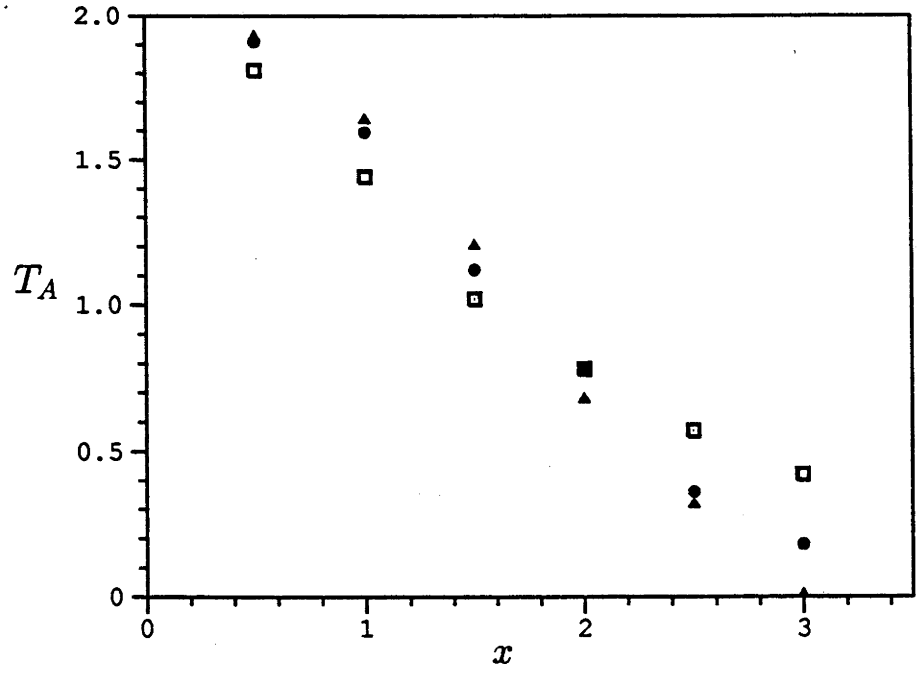

Figure 4.4: The axial string tension of the Z_2 gauge model versus coupling x, for lattice sizes $M = 2(\square), 3(\bullet)$ and $4(\triangle)$.

4.3.3 The U(1) Gauge Model in (2+1)D

We recall from Section 3.2 that the Hamiltonian for U(1) LGT in (2+1)D is given by

$$\mathbf{H} = \frac{g^2}{2a}\left[\sum_l \mathbf{L}_l^2 - x\sum_p(\mathbf{Z}_p + \mathbf{Z}_p^\dagger)\right] \tag{4.28}$$

Much work has been done already on this model, in both the Euclidean [16, 18] and Hamiltonian [17, 19, 20, 21, 22] formulations. A good test for any numerical technique would be to calculate the string tension or mass gaps for the model, for which analytic results are available. In the Euclidean formulation Gopfert and Mack [16] made a rigorous study of the theory with Villain action and obtained the mass gap M as

$$M^2a^2 \underset{g\to 0}{\approx} \frac{8\pi^2}{g^2}\exp\left(-\frac{2v(0)\pi^2}{g^2}\right) \tag{4.29}$$

where $v(0) = 0.2527$ and a lower bound to the string tension σ as

$$\sigma a \geq C\frac{g^2}{\pi^2}M \tag{4.30}$$

where C is a constant. In the Hamiltonian formulation, Suranyi [17] obtained via a variational approach the relation

$$\sigma a = 2\frac{g^2}{\pi^2}M \tag{4.31}$$

between the string tension and the mass gap, valid in the weak-coupling limit. He also found the mass gap M to be

$$M^2a^2 \underset{g\to 0}{\approx} c_1 g^{-n_1}\exp\left(-\frac{5.7\pm 0.1}{g^2}\right) \tag{4.32}$$

where c_1 is dependent on the approximation used and n_1 is probably 2. These expressions for the string tension and mass gap are analogous to equation (2.9), the scaling relation for the string tension in QCD. Numerical work by Hamer and Irving [20] using linked cluster expansions, by Heys and Stump [21] using a multiparameter variational wavefunction and evaluating the expectation of the Hamiltonian using Monte Carlo and by Lana [22] using the block-renormalization group all confirm the scaling relations

$$M^2a^2 \underset{g\to 0}{\approx} \frac{x_1}{g^2}\exp\left(-\frac{x_2}{g^2}\right) \tag{4.33}$$

$$\sigma^2a^4 \underset{g\to 0}{\approx} x_3g^2\exp\left(-\frac{x_4}{g^2}\right) \tag{4.34}$$

but quote different values for the constants x_1 to x_4. See Table 4.1.

	x_1	x_2	x_3	x_4
Hamer and Irving [20]	470 ± 200	5.3 ± 0.5	7.8 ± 2	4.5 ± 0.3
Heys and Stump [21]	500 ± 30	4.97 ± 0.05	114 ± 22	5.0 ± 0.4
Lana [22]	145 ± 15	4.1 ± 0.2		

Table 4.1: The constants obtained by fitting the mass gap and string tension to the forms (4.33) and (4.34) by various authors.

The values obtained for the constants x_2 and x_4 in the exponents are consistent with each other and with the calculations of Suranyi. There is discrepancy between the values for the constants x_1 and x_3 multiplying the exponentials, but this is not unexpected as they are very sensitive to the constants in the exponents, even when fitting the same set of data. Hamiltonian Monte Carlo calculations [51, 54] have also been performed but the results are not good enough

to compare with those mentioned above. The exact finite-lattice method has also been applied to this problem [19] but due to limitations placed on the size of the basis the results are also not good enough beyond $g^2 \approx 1$.

We used the stochastic truncation method to calculate [48] the string tension T and "antisymmetric" mass gap M_A for the model defined on a periodic lattice of size $M \times M$, for $M = 3, 4$, and 5. The string tension is defined, as before, as

$$T = \frac{\omega_{str} - \omega_0}{M} \tag{4.35}$$

and is related to the physical string tension σ by

$$\sigma = \lim_{M \to \infty} \frac{g^2}{2a^2} T \tag{4.36}$$

To obtain the string energy density ω_{str}, we start from the strong coupling string state with a "string" of flux running along one row of links, as in the Z_2 gauge model in Section 4.4.2. To do the deterministic part of the truncation we used energy cutoffs E_{cutoff} in the range $50 \leq E_{cutoff} \leq 110$ for different values of the coupling x. We did not extrapolate to $E_{cutoff} \to \infty$ because we expected our systematic errors to be much smaller than the random errors. We used ensemble sizes of about 2000 for the 3×3 lattice, about 3000 for the 4×4 lattice and about 4000 for the 5×5 lattice and the errors for the energies were usually within 1 %. Because the string tension is obtained as a difference between two energies, the errors there are considerably larger. The results for the string tension is plotted in Figure 4.5 and includes error bars for only the 5×5 lattice. The line is from the linked cluster expansions of Hamer and Irving [20]. The agreement is very good except at weak coupling. Finite size effects become important there. About 2 h CPU time on a VAX 11/785 was used in computing each string tension value

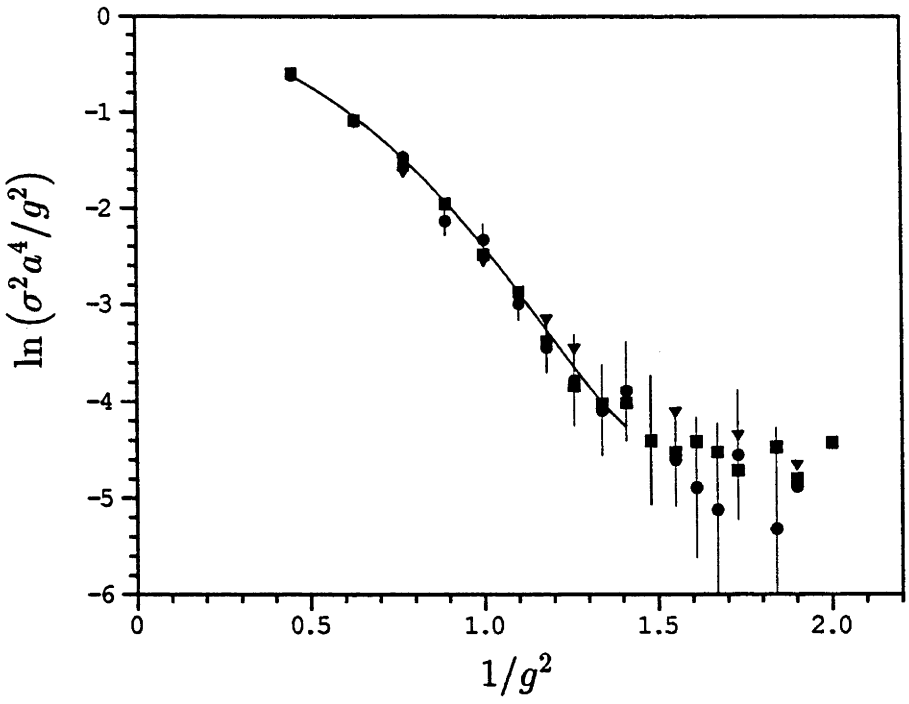

Figure 4.5: The string tension results fitted to the form (4.34) for lattice sizes $M = 3(\square), 4(\nabla)$ and $5(\bullet)$. The line is from the linked cluster expansions of [20]

for the 5×5 lattice. This represents a significant improvement in quality over previous Hamiltonian Monte Carlo calculations.

We were also able to do a calculation for the antisymmetric mass gap M_A of the U(1) model. Now, any basis state $|i\rangle$ has the same energy at strong coupling as the basis state $|i'\rangle$, which is $|i\rangle$ with the sign of the gauge field variables on all its links reversed. We can thus divide the basis into 2 disjoint sectors, one containing states which are symmetric combinations $|i\rangle + |i'\rangle$ and another which are antisymmetric combinations $|i\rangle - |i'\rangle$. The difference between the energies of the lowest state in the symmetric and antisymmetric sector is known as the antisymmetric mass gap. The symmetric mass gap M_S, on the other hand, is the difference in energies between the lowest two states in the symmetric sector. Hamer and Irving [20] have performed calculations using linked cluster expansions for both M_A and M_S. Only M_A can be calculated using our stochastic truncation program. We found that it is important to enforce translational and

rotational symmetry on the lattice in the antisymmetric sector. A quick hand calculation on a 2×2 lattice, keeping only the lowest few basis states, shows that if symmetry is not maintained, the "ground state" obtained is not translationally and rotationally symmetric and the state which is, and thus should be the ground state, is not the lowest energy state. Presumably, this effect is due to the periodic boundary conditions used and is more serious for small, even lattices; it may have to do with the "torelon" states discussed by Michael [59].

With the proper choice of basis, we calculated M_A for a 4×4 lattice. Negative amplitudes are required in the calculation and so only the growth estimate can be used. Because symmetrization meant longer computing time, we used an ensemble size of around 1000, giving poorer statistics than for the case of the string tension. The results are shown in Figure 4.6 together with the series result of Hamer and Irving [20]. Agreement with the series result is very good at strong coupling. At weak coupling, the agreement is almost too good, because one expects finite-size effects to become important there. Nevertheless, within errors, the results are satisfactory.

4.3.4 QED in (2+1)D

We recall from Section 3.2 that the Hamiltonian for lattice QED in (2+1)D is given by [23]

$$\mathbf{H} = \frac{g^2}{2a}\left(\mathbf{W}_0 + y\mathbf{W}_1 + y^2\mathbf{W}_2\right) \tag{4.37}$$

where

$$\mathbf{W}_0 = \sum_l \mathbf{L}_l^2 + \mu \sum_{\mathbf{n}} (-1)^{n_1+n_2} \boldsymbol{\chi}^\dagger(\mathbf{n})\boldsymbol{\chi}(\mathbf{n}) \tag{4.38}$$

$$\mathbf{W}_1 = \sum_{i,\mathbf{n}} \eta_i(\mathbf{n}) \left[\boldsymbol{\chi}^\dagger(\mathbf{n})\mathbf{U}(\mathbf{n}, \mathbf{n}+a\mathbf{i})\boldsymbol{\chi}(\mathbf{n}+a\mathbf{i}) + \text{H.c.}\right] \tag{4.39}$$

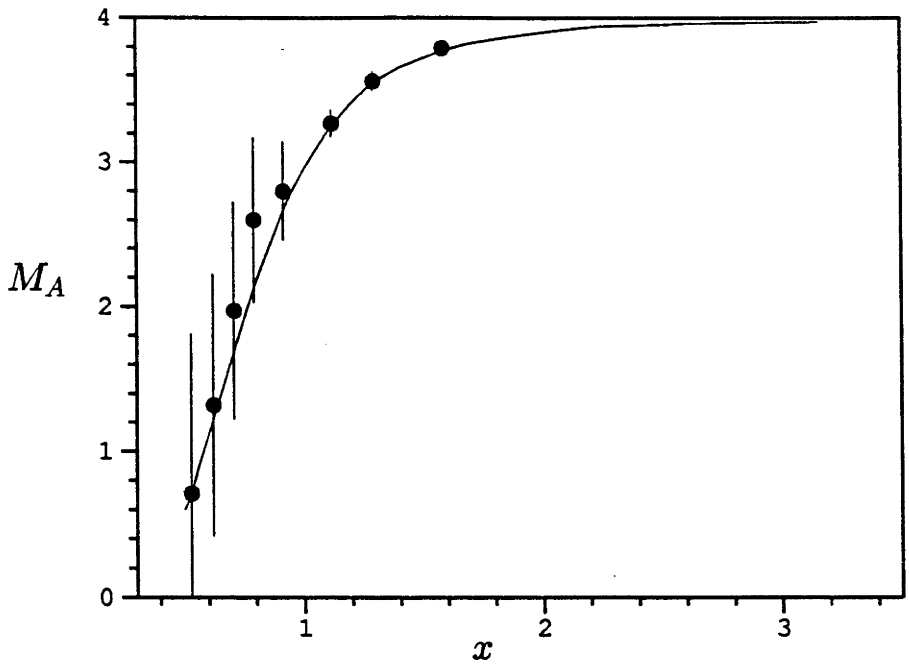

Figure 4.6: The antisymmetric mass gap of the U(1) gauge model against coupling x for lattice size $M = 4$ with error bars. The line is from the strong coupling expansions of [20]

$$\mathbf{W}_2 = -\sum_P \left(\mathbf{Z}_P + \mathbf{Z}_P^\dagger\right) \tag{4.40}$$

and $Z_P = U_{l_1} U_{l_2} U_{l_3}^\dagger U_{l_4}^\dagger$ with the l_i being the links of the plaquette P. We found that it is convenient to absorb the η's into the U's and for the massless theory, which is the only one that we will study, the modified Hamiltonian is given by

$$\mathbf{H} = \frac{g^2}{2a}\left(\mathbf{W}_0 + y\mathbf{W}_1 + y^2\mathbf{W}_2\right) \tag{4.41}$$

where

$$\begin{aligned}
\mathbf{W}_0 &= \sum_l \mathbf{L}_l^2 \\
\mathbf{W}_1 &= \sum_{i,\mathbf{n}} (\mathbf{n}) \left[\chi^\dagger(\mathbf{n}) \mathbf{U}(\mathbf{n}, \mathbf{n} + a\mathbf{i}) \chi(\mathbf{n} + a\mathbf{i}) + \text{H.c.}\right] \\
\mathbf{W}_2 &= \sum_P \left(\mathbf{Z}_P + \mathbf{Z}_P^\dagger\right)
\end{aligned}$$

The sign of the $\mathbf{W}_2$ term is now positive because of the η's. At each link l of the lattice there is an integer flux (eigenvalue of L_l) n_l, and at each site two states $|+\rangle$ and $|-\rangle$ are allowed which have the properties that

$$\chi^\dagger|-\rangle = |+\rangle,\ \chi^\dagger|+\rangle = 0,\ \chi|-\rangle = 0,\ \chi^|+\rangle = |-\rangle. \tag{4.42}$$

The strong coupling ground state of the model is chosen to be the state with $n_l = 0$ for all links l and $|+\rangle$ on odd sites and $|-\rangle$ on even sites, a site (n_1, n_2) being odd or even according to whether $n_1 + n_2$ is odd or even. We generate the basis for the physical states by applying the "perturbation" operators W_1 and W_2 to the strong coupling ground state, similar to what was done for the U(1) model in the previous section. We found that we could adjust the phase of each basis state such that all matrix elements of W_1 and W_2 in this basis are negative. This means that in this basis, all matrix elements of the "inverted" Hamiltonian $\tilde{H} = E_{cutoff} - H$ are positive. All the amplitudes of the ground state wavefunction are then positive.

We calculated the ground state energy for the model on lattices of size 2×2 and 4×4. The cutoff energies used were of the order of 50 and the ensemble sizes used were around 2000. We display the results in Figure 4.7. We also show the [4/4] Pade approximants to the ground state energy obtained using linked cluster expansions for an infinite lattice [23] and for a 2×2 lattice [60]. The agreement is excellent over the whole range of couplings considered. Evidently, as far as the stochastic truncation method is concerned, it is not more difficult to calculate ground state energies for the model with fermions than it is for the model without. This is to be contrasted with Monte Carlo calculations in the Euclidean formulation.

Unfortunately the string tension calculation for the pure gauge theory does

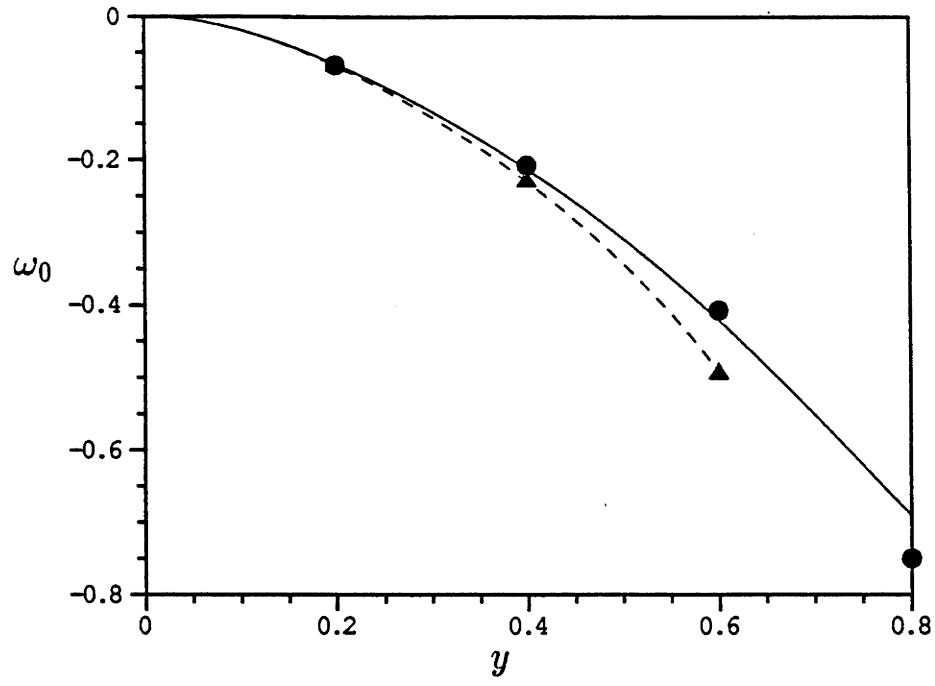

Figure 4.7: The ground state energy per site of lattice QED in (2+1)D against coupling y for lattice sizes $M = 2(\triangle)$ and $4(\bullet)$. The broken (unbroken) line is a [4/4] Pade approximant obtained using linked cluster expansions [23] for a 2×2 (infinite) lattice.

not generalize here as the strong coupling string state is "eaten up" by the fermion operator W_1 and stochastic truncation will lead us back to the ground state. In principle we can calculate the antisymmetric mass gap in the same way as was done for the pure gauge theory but this will not be done until the results for the pure gauge theory are completely satisfactory.

A quantity that we managed to calculate is the "chiral condensate" defined by

$$\langle \psi\overline{\psi} \rangle^{lattice} = \frac{1}{N} \sum_{\mathbf{n}} (-1)^{n_1+n_2} [\chi^\dagger(\mathbf{n}), \chi(\mathbf{n})] \tag{4.43}$$

A breakdown [45] of discrete "chiral symmetry" is expected to be manifested by a non-zero value of the chiral condensate in the continuum limit. Burden and Hamer [23] used the linked cluster expansion technique to calculate the series expansion for the chiral condensate up to $O(g^{-32})$. The Pade and Shafer approx-

imants they constructed were consistent, though not conclusively, with a nonzero limit of the chiral condensate. Euclidean Monte Carlo results [61][62] are also not inconsistent with dynamical chiral symmetry breaking.

We calculated the chiral condensate $\langle \overline{\psi}\psi \rangle$ using equation (4.19) for lattices of size 2×2 and 4×4. The results are shown in Figure 4.8 together with the [4/4] Pade approximants constructed from a series expansion to $O(g^{-32})$ by Burden and Hamer for an infinite lattice [23] and for a 2×2 lattice [60]. The two trial states

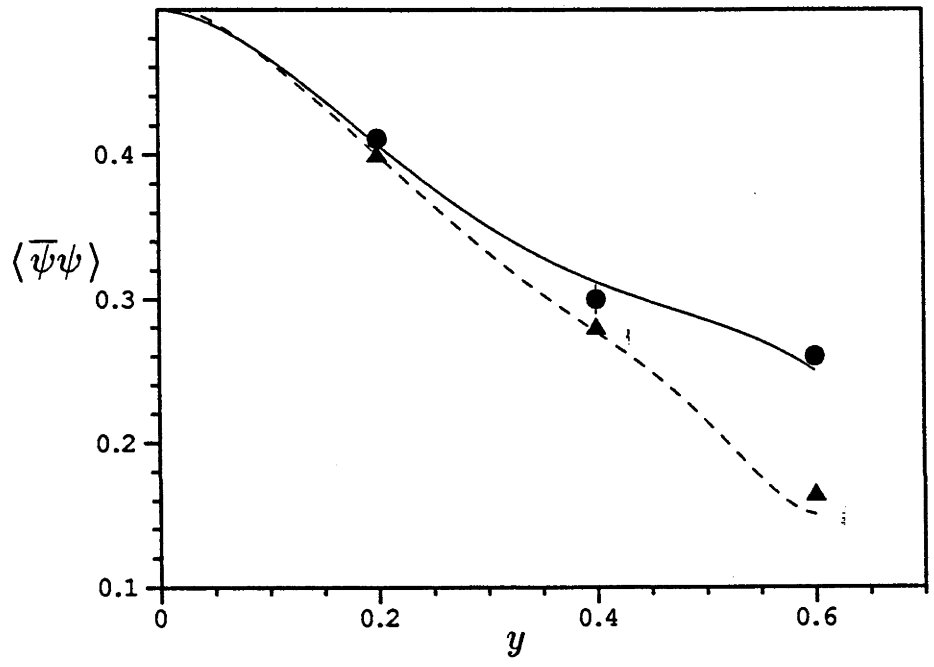

Figure 4.8: The chiral condensate of lattice QED in (2+1)D against coupling y for lattice sizes $M = 2(\triangle)$ and $4(\bullet)$. The broken (unbroken) line is a [4/4] Pade approximant obtained using linked cluster expansions [23] for a 2×2 (infinite) lattice.

$|\Psi'^{(m)}\rangle$ and $|\Psi^{(m)}\rangle$ needed for the computation of the expectation value had to have significant overlap; otherwise the statistical error will be large. We found that the ensemble sizes required to keep the errors down increased with lattice size and with coupling y. For $y = 0.6$ on the 4×4 lattice, we used an ensemble size of 3000. The agreement with the series result was good but we were unable to shed more light on the issue of chiral symmetry breaking by going to larger

lattices and larger y. With an ensemble size of 10000 and doing the calculation on a supercomputer, we were able to reach only $y \approx 2$. As mentioned earlier, we were unable to implement variational guidance to give unbiased results. Modest though the results are, they represent the first successful Monte Carlo calculations done in the Hamiltonian formulation for a (2+1)D model which includes dynamical fermions.

4.3.5 Outlook for Stochastic Truncation

Applications of the stochastic truncation method to other models have been made by Hamer and collaborators [63]. The models are the 3-state Potts model in (2+1)D and the Z_2 gauge model in (3+1)D, both of which are expected to exhibit a first order phase transition. For the 3-state Potts model they were able to obtain estimates of the ground state energy and mass gap with sufficient accuracy to do a finite size scaling analysis. The results were in agreement with strong coupling series results and provided evidence for the existence of a first order phase transition in the model. For the Z_2 model, they were also able to confirm that there exists a first order transition.

In the above calculations of Hamer et al, a faster version of the algorithm was used. Let us refer back to the algorithm of equations (4.8) and (4.9), namely

$$\begin{aligned} n_k^{(m+1)} &= \sum_i R\left(H_{ki}\frac{n_i^{(m)}}{S^{(m)}}\right) \\ S^{(m+1)} &= S^{(m)}\frac{\sum_i |n_i^{(m+1)}|}{\sum_j |n_j^{(m)}|}. \end{aligned}$$

Now, the amplitude $n_k^{(m+1)}$ will frequently be stochastically rounded to zero. In fact, at equilibrium, each initial state $|i\rangle$ will on average give rise to only one final state $|k\rangle$ with non-zero amplitude. The new version of the algorithm was

designed to eliminate the time wasted in generating states whose amplitudes end up being zero.

Let T be the quantity

$$T = \sum_k H_{ki} \frac{n_i^{(m)}}{S^{(m-1)}} \tag{4.44}$$

which is a sum over all possible final states $|k\rangle$ for a given initial state $|i\rangle$. Let P be the number of possible final states $|k\rangle$. Then the P values of $n_k^{(m+1)}$ are generated as follows:

1. Round T to an integer $\overline{T}$;

2. If $\overline{T}/P > 1$ (unlikely), then let $n_k^{(m+1)}$ take the value $[\overline{T}/P]$ for each k;

3. For the remainder $\overline{T}/P - \overline{T}/P$, choose randomly a set of $\overline{T} - P[\overline{T}/P]$ states out of the possible P states, and to the amplitude $n_j^{(m+1)}$ of each of these chosen states $|j\rangle$ add the number one.

For the Z_2 model in (3+1)D, each iteration took only 60μsec. per state on an IBM3090.

They found that variational guidance was necessary with this faster algorithm for large lattices. Otherwise there would be a "diffusion" of the initial ensemble of states into the large basis of possible states as the iteration proceeds, leaving none to sample the most important region. No equilibrium is achieved and no sensible estimate of the eigenvalue is obtained.

Based on these recent calculations of Hamer et al, it would seem that the prospects for further applications of the stochastic truncation method to discrete spin and gauge models are good. As far as continuous spin and gauge models are concerned, one could hope to obtain better statistics with a faster algorithm than the basic one and as a result study the effects of the deterministic part of the truncation. Nevertheless, the lack of an efficient method for calculating

expectation values will limit us to calculations of only energies for the moment.

Chapter 5

Discretized Light Cone Quantization

5.1 Introduction

The infinite momentum frame was studied extensively in the late 1960's and early 1970's in connection with deep inelastic scattering and lepton pair production. Weinberg [69] showed that in this frame ordinary perturbation theory has many simplifications. Susskind [46] and Bardakci and Halpern [71] suggested that similar simplifications could be obtained by a change of variables from the laboratory time x^0 and space coordinate x^1 to a new "light cone time" $x^+ = x^0 + x^1$ and light cone space coordinate $x^- = x^0 - x^1$, and quantizing the theory on an equal light cone time surface. Chang and Ma [72] and Kogut and Soper [73] showed that this is indeed the case and that the new light cone perturbation theory gives the same results as Weinberg's time-ordered perturbation theory in the infinite momentum frame.

The reason for the simplifications can be traced back to the energy-momentum relation $p^+p^- = m^2 + (p^2)^2 + (p^3)^2$ where $p^\pm = p^0 \pm p^1$ are the light cone energy

and momenta. In contrast to the situation in normal Minkowski spacetime, for each light cone momentum p^+ there corresponds only one light cone energy p^-. Furthermore, p^+ and p^- have the same sign. Hence, when negative p^- states are interpreted as antiparticles with positive energy, as is the usual case, the associated p^+ become positive too. Hence we have the situation in which all particles and antiparticles carry only positive light cone energy and momenta. This then means that there cannot be pair production from the light cone vacuum. This is in distinct contrast to the situation in Minkowski spacetime where the vacuum is a "soup" of virtual particle-antiparticle pairs. The number of diagrams that need to be considered in light cone perturbation theory to any order is then drastically reduced.

Pauli and Brodsky [10] introduced a non-perturbative formulation called Discretized Light Cone Quantization (DLCQ) which is based on quantization on an equal light cone time surface. They worked in (1+1) dimensions and obtained impressive results, especially [11] for QED in (1+1)D. They considered the theory in a finite "volume" with $-L \leq x^- \leq L$ and worked in the light cone gauge $A^+ = 0$. Periodic boundary conditions were imposed on the independent fields to discretize the light cone momenta. They also introduced an ultraviolet cutoff Λ for the light cone momenta. The independent fields were Fourier analysed into creation and annihilation operators and quantized at equal x^+ They then obtained the invariant mass squared operator as $M^2 = KH$ where the dimensionless light cone momentum operator K is defined as $K = \frac{L}{2\pi}P^+$ and the Hamiltonian H is defined as $H = \frac{2\pi}{L}P^-$. There is no *explicit* L dependence in M^2.The operator K is diagonal in Fock space and basically just sums the light cone momenta for each Fock state. Because light cone momentum is strictly positive and is discretized, the Fock space corresponding to an eigenvalue of K is finite. Diagonalizing the

Hamiltonian H in this Fock space then gives the invariant mass for that eigenvalue of K. The continuum limit $L \to \infty$ is obtained by taking K to infinity, thereby keeping P^+ finite.

For a finite K, the dependence on momentum cutoff Λ, once $\Lambda \geq K$, is solely in the "self-induced inertias" obtained after normal ordering the interaction term in the light cone Hamiltonian. This cutoff has to be lifted before the continuum limit $K \to \infty$ is taken. Good results were obtained for the bound state spectrum with fairly low values of K and by considering only Fock states with one fermion and one antifermion.

Our aim will be to apply DLCQ to (2+1) dimensions, in particular to QED in (2+1)D. Before we go on to study the (2+1) dimensional theory, we shall review the situation in (1+1) dimensions in more detail than was done above, with a choice of antiperiodic boundary conditions for the fermions. We will calculate the mass of the lowest bound state and also look at the charge 1 sector to try to obtain indications of confinement. From a computational point of view, this has proved to be a useful exercise in showing that the computer code for the (2+1)D theory, which can be easily modified to handle the (1+1)D theory, actually works.

5.2 The Pauli Brodsky approach

5.2.1 Light cone formulation of QED in (1+1)D

We shall now review the method of DLCQ and its application to QED in (1+1)D, following very closely the works of Eller, Pauli and Brodsky [11], Hornbostel [75] and Tang [12]. The Lagrangian density $\mathcal{L}$ for QED in (1+1)D is given by

$$\mathcal{L} = \frac{i}{2}(\overline{\psi}\gamma^\mu \partial_\mu \psi - \partial_\mu \overline{\psi}\gamma^\mu \psi) - m\overline{\psi}\psi - \frac{1}{4}F^{\mu\nu}F_{\mu\nu} - eA_\mu \overline{\psi}\gamma^\mu \psi. \qquad (5.1)$$

where the fermion field ψ is a two-component spinor. The Dirac matrices satisfy the commutation relations $\{\gamma^\mu, \gamma^\nu\} = 2g^{\mu\nu}$ and can be represented as

$$\gamma^0 = \begin{pmatrix} 1 & 0 \\ 0 & -1 \end{pmatrix}, \qquad \gamma^1 = \begin{pmatrix} 0 & 1 \\ -1 & 0 \end{pmatrix}. \tag{5.2}$$

We make a transformation to light cone coordinates x^+, x^- defined by $x^\pm = x^0 \pm x^1$. The metric $g^{\mu\nu}$, for $\mu, \nu = +, -$, becomes

$$g^{\mu\nu} = \begin{pmatrix} 0 & 2 \\ 2 & 0 \end{pmatrix} \tag{5.3}$$

and is used to raise and lower indices. The Dirac matrices become $\gamma^\pm = \gamma^0 \pm \gamma^1$ and can be used to define projection operators $\Lambda^{(\pm)}$ for the spinors. The projection operators are given by

$$\Lambda^{(\pm)} = \frac{1}{4}\gamma^\mp\gamma^\pm \tag{5.4}$$

and satisfy $\Lambda^{(+)} + \Lambda^{(-)} = 1$, $\Lambda^{(\pm)}\Lambda^{(\pm)} = \Lambda^{(\pm)}$ and $\Lambda^{(\pm)}\Lambda^{(\mp)} = 0$. They are used to separate ψ into the "components" $\psi_+ = \Lambda^{(+)}\psi$ and $\psi_- = \Lambda^{(-)}\psi$. These, together with the light cone gauge fields $A^\pm = A^0 \pm A^1$ are the basic fields in terms of which the Lagrangian (5.1) in light cone formulation is now defined.

5.2.2 Independent Degrees of Freedom

The equations of motion are Maxwell's equations

$$\partial_\mu F^{\mu\nu} = g\overline{\psi}\gamma^\nu\psi \tag{5.5}$$

and Dirac's equation

$$[(i\partial_\mu - gA_\mu)\gamma^\mu - m_0]\psi = 0. \tag{5.6}$$

which, in the light cone formulation, and in the light cone gauge $A^+ = 0$ become

$$-\partial_-\partial^+ A^- = 2e\psi_+^\dagger\psi_+ \tag{5.7}$$

$$\partial_\mu\partial^\mu A^- - \partial_-\partial^- A^- = 2e\psi_-^\dagger\psi_- \tag{5.8}$$

$$i\partial^+\psi_- - m_0\gamma^0\psi_+ = 0 \tag{5.9}$$

$$\left(i\partial^- - eA^-\right)\psi_+ - m_0\gamma^0\psi_- = 0. \tag{5.10}$$

In the Pauli-Brodsky approach, one treats ψ_+ as the only independent degree of freedom, with ψ_- and A^- being determined in terms of ψ_+ from the equations of motion. To justify this let us use the arguments of McCartor [74] and Hornbostel [75]. Let us put the system in a box with $-L \leq x^\pm \leq L$. See Figure 5.1. Consider only the classical free fermion theory for the moment, ie. equa-

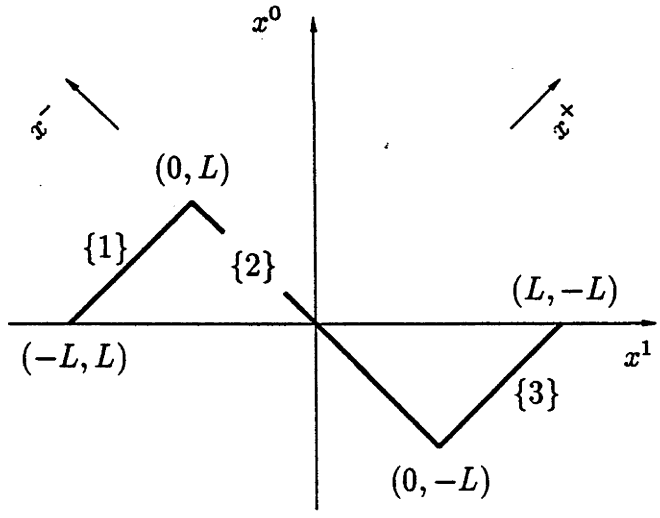

Figure 5.1: The segments $\{1\}$, $\{2\}$ and $\{3\}$ on which specifying ψ_+ and ψ_- would completely determine the initial value problem. See text.

tions (5.9) and (5.10) without the A^- term. McCartor pointed out that for a proper formulation of the initial value problem for the field theory it is not enough to specify only initial values for ψ_+ at an initial light cone time x_0^+. It

is necessary to specify ψ_- on, for instance, the segments $\{1\}$ and $\{3\}$ in Figure 5.1 in addition to ψ_+ on segment $\{2\}$, ie. at $x^+ = 0$. Given these initial values all the field values at other times can be obtained by integrating the equations of motion. For instance, knowing ψ_+ on $\{2\}$ and ψ_- on $\{3\}$ allows us to integrate equation (5.9) to obtain ψ_- on $\{2\}$. Equation (5.10) then integrates to give ψ_+ on the segment $\{2'\}$ defined by $x^+ = \delta > 0$. Repeating the steps gives us ψ_+ and ψ_- for all positive x^+ and for all x^-. Similarly, we obtain the field values for all negative x^+ by making use the initial values of ψ_- on segment $\{1\}$. In the corresponding quantum problem, one specifies commutation relations for ψ_+ on segment $\{2\}$ and ψ_- on segments $\{1\}$ and $\{3\}$ and constructs operators which generate translations in x^+ and x^-.

For the case of the gauge theory, Hornbostel quantized by specifying commutation relations for ψ_+ on segment $\{2\}$ and for ψ_- and A^- on segments $\{1\}$ and $\{3\}$. He worked in light cone gauge $A^+ = 0$ and imposed invariance under the residual x^--independent gauge transformations on the physical states. This is a standard procedure used in the equal time Hamiltonian formulation of gauge theories, as mentioned in Section 3. He was then able to show that, in the "continuum limit" $L \to \infty$, the sector of states containing only ψ_+ excitations is enough to describe the *massive* theory. This then forms the justification for the procedure of Eller, Pauli and Brodsky in which only the ψ_+ degrees of freedom are quantized. For the *massless* theory, however, this procedure is apparently not justified and boundary terms have to be explicitly included.

The dependent degrees of freedom ψ_- and A^- are obtained from the equations of motion as

$$A^- = 4g\frac{1}{(i\partial^+)^2}\left(\psi_+^\dagger\psi_+\right), \tag{5.11}$$

$$\psi_- = m_0\gamma^0\frac{1}{(i\partial^+)}\psi_+. \tag{5.12}$$

Here $\frac{1}{(i\partial^+)}$ and $\frac{1}{(i\partial^+)^2}$ are short hand notations for the operators defined by

$$\frac{1}{(i\partial^+)}F(x^-) = -\frac{i}{2}\int_{-L}^{x^-} F(y)dy + c_1 \tag{5.13}$$

$$\frac{1}{(i\partial^+)^2}G(x^-) = -\frac{1}{4}\int_{-L}^{x^-}\int_{-L}^{z} G(y)dydz + c_2x^- + c_3. \tag{5.14}$$

The constants c_1, c_2 and c_3 are related to the values of ψ_- and A^- at the boundaries and will, for the moment, be left unspecified.

Important observables of the theory are the conserved charges, which before quantization, are given by

$$Q = \frac{1}{2}\int_{-L}^{L} dx^- j^+(x^-, x_0^+) \tag{5.15}$$

and

$$P^\nu = \frac{1}{2}\int_{-L}^{L} dx^- T^{+\nu}(x^-, x_0^+) \tag{5.16}$$

where j^μ and $T^{\mu\nu}$ are, respectively, the charge current and the energy-momentum tensor. They are given by

$$j^\mu = \overline{\psi}\gamma^\mu\psi, \tag{5.17}$$

$$T^{\mu\nu} = \frac{i}{2}\left(\overline{\psi}\gamma^\mu\partial^\nu\psi - \partial^\nu\overline{\psi}\gamma^\mu\psi\right) + F^{\lambda\mu}\partial^\nu A_\lambda - g^{\mu\nu}\mathcal{L}. \tag{5.18}$$

After some algebra, in which ψ_- and A^- are eliminated in favour of ψ^+ by means of equations (5.11) and (5.12), the conserved charges can be shown to be given by

$$Q = \int dx^- \psi_+^\dagger\psi_+ \tag{5.19}$$

$$P^+ = i\int dx^- \psi_+^\dagger \partial^+ \psi_+ \tag{5.20}$$

$$P^- = m_0^2 \int dx^- \left\{ \psi^\dagger \frac{1}{(i\partial^+)} \psi_+ \right\}_{sym} + 2g^2 \int dx^- \left\{ \psi_+^\dagger \psi_+ \frac{1}{(i\partial^+)^2} \psi_+^\dagger \psi_+ \right\}_{sym} . \tag{5.21}$$

Here the symmetrized brackets [76] $\{\quad\}_{sym}$ are defined by

$$\left\{ A \frac{1}{i\partial^+} B \right\}_{sym} = \frac{1}{2}\left[A\left(\frac{1}{i\partial^+} B\right) - \left(\frac{1}{i\partial^+} A\right) B \right] \tag{5.22}$$

$$\left\{ A \frac{1}{(i\partial^+)^2} B \right\}_{sym} = A\left(\frac{1}{(i\partial^+)^2} B\right) + \left(\frac{1}{i\partial^+} A\right)\left(\frac{1}{i\partial^+} B\right) + \left(\frac{1}{(i\partial^+)^2} A\right) B \tag{5.23}$$

5.2.3 Light cone Quantization

We quantize at equal light cone time x^+ by specifying the (anti) commutation relations

$$\{\psi_+(x_0^+, x^-), \psi_+^\dagger(x_0^+, y^-)\} = \Lambda^{(+)} \delta(x^- - y^-) \tag{5.24}$$

In contrast to [11] and following [75] and [12] we impose anti-periodic boundary conditions on ψ_+ in the x^- direction, ie. we let $\psi_+(x^-) = -\psi_+(x^- + 2L)$. This leads to a discretization of the light cone momenta

$$p^+ = 2p^- = \frac{l\pi}{L} \qquad\qquad l = \frac{1}{2}, \frac{3}{2}, \frac{5}{2}, \ldots, \Lambda_+ \tag{5.25}$$

where Λ_+ is an odd multiple of $\frac{1}{2}$ and provides an upper cutoff to the light cone momenta. We then expand the field ψ^+ at time x_0^+ in terms of normal modes,

$$\psi^+(x_0^+, x^-) = u \frac{1}{\sqrt{2L}} \sum_{l=\frac{1}{2}}^{\Lambda_+} \left(\mathrm{b}_l e^{-il\xi} + \mathrm{d}_l^\dagger e^{il\xi} \right), \tag{5.26}$$

with $\xi = \pi\frac{x^-}{L}$. The operators $\mathbf{b}_l^\dagger$ ($\mathbf{d}_l^\dagger$) are creation operators for fermions (anti-fermions) with light cone momenta l and $\mathbf{b}_l$ ($\mathbf{d}_l$) are destruction operators. They satisfy the usual (anti) commutation relations

$$\left\{\mathbf{b}_n, \mathbf{b}_m^\dagger\right\} = \left\{\mathbf{d}_n, \mathbf{d}_m^\dagger\right\} = \delta_{n,m} \tag{5.27}$$

with all other (anti) commutators vanishing. The spinor u satisfies the relation $u = \Lambda^{(+)}u$ and is normalized by $u^\dagger u = 1$.

We next substitute the mode expansion (5.26) for ψ_+ in the expressions (5.19) to (5.21) for the conserved charges.

In doing so we will make use of the quantities

$$\{n|m\} = \frac{1}{2\pi}\int_{-\pi}^{\pi} d\xi \left\{e^{in\xi}\frac{1}{(i\partial_\xi)}e^{im\xi}\right\}_{sym} \tag{5.28}$$

$$[k|l] = \frac{1}{2\pi}\int_{-\pi}^{\pi} d\xi \left\{e^{ik\xi}\frac{1}{(i\partial_\xi)^2}e^{il\xi}\right\}_{sym} \tag{5.29}$$

where n and m are positive odd multiples of $\frac{1}{2}$ and k and l are integers. Following Hamer [76] and Tang [12], we show in Appendix A that we can consistently set

$$\{n|m\} = \frac{1}{n}\delta_{n+m,0} \tag{5.30}$$

$$[k|l] = \begin{cases} \frac{1}{k^2}\delta_{k+l,0} & k,l \neq 0 \\ 0 & k = 0,\ l \neq 0 \\ 0 & k \neq 0,\ l = 0 \\ 0 & l = k = 0 \end{cases} \tag{5.31}$$

It is important that we can do this because, as will be seen later, these particular values can be interpreted as making the interaction term conserve light cone momenta.

The conserved charges become

$$\mathbf{Q} = \sum_{l=\frac{1}{2}}^{\Lambda+} \left(\mathbf{b}_l^\dagger \mathbf{b}_l - \mathbf{d}_l^\dagger \mathbf{d}_l\right) \tag{5.32}$$

$$\mathbf{P}^+ = \frac{2\pi}{L} \sum_{l=\frac{1}{2}1}^{\Lambda+} l \left(\mathbf{b}_l^\dagger \mathbf{b}_l + \mathbf{d}_l^\dagger \mathbf{d}_l\right) \tag{5.33}$$

$$\mathbf{P}^- = \frac{L}{2\pi}\left\{m_0^2 \mathbf{H}_0 + \frac{g^2}{\pi}\left(\mathbf{V}_N + \mathbf{V}_C\right)\right\} \tag{5.34}$$

where

$$\mathbf{H}_0 = \sum_{l=\frac{1}{2}}^{\Lambda+} \frac{1}{l} \left(\mathbf{b}_l^\dagger \mathbf{b}_l + \mathbf{d}_l^\dagger \mathbf{d}_l\right) \tag{5.35}$$

$$\begin{aligned}\mathbf{V}_N = \frac{1}{2} \sum_{k,l,m,n=\frac{1}{2}}^{\Lambda+} \Big\{ & \left(\mathbf{b}_k^\dagger \mathbf{b}_l^\dagger \mathbf{b}_m \mathbf{b}_n + \mathbf{d}_k^\dagger \mathbf{d}_l^\dagger \mathbf{d}_m \mathbf{d}_n\right) [k-n|l-m] \\ & + 2\mathbf{b}_k^\dagger \mathbf{b}_l \mathbf{d}_m^\dagger \mathbf{d}_n \left([k+m|-l-n] - [k-l|m-n]\right) \\ & + \left(\mathbf{b}_k^\dagger \mathbf{d}_l^\dagger \mathbf{d}_m^\dagger \mathbf{d}_n + \mathbf{d}_n^\dagger \mathbf{d}_m \mathbf{d}_l \mathbf{b}_k\right) [k+m|l-n] \\ & + \left(\mathbf{d}_k^\dagger \mathbf{b}_l^\dagger \mathbf{b}_m^\dagger \mathbf{b}_n + \mathbf{b}_n^\dagger \mathbf{b}_m \mathbf{b}_l \mathbf{d}_k\right) [k+m|l-n]\Big\}\end{aligned} \tag{5.36}$$

$$\mathbf{V}_C = \sum_{n=\frac{1}{2}}^{\Lambda+} I_n \left(\mathbf{b}_n^\dagger \mathbf{b}_n + \mathbf{d}_n^\dagger \mathbf{d}_n\right). \tag{5.37}$$

$\mathbf{V}_N$ is the normal ordered interaction term whereas $\mathbf{V}_C$ is the term left over after normal ordering. The "self-induced inertias" I_n are given by

$$I_n = \frac{1}{2} \sum_{m=\frac{1}{2}}^{\Lambda+} \left([n-m|m-n] - [n+m|-n-m]\right). \tag{5.38}$$

Note that $\mathbf{Q}$ and $\mathbf{P}^+$ are diagonal in Fock space. $\mathbf{Q}$ measures the charge of a Fock state whereas $\mathbf{P}^+$ measures the total light cone momentum. The Fock space vacuum $|0\rangle$ which is annihilated by all the $\mathbf{b}_k$ and $\mathbf{d}_l$ operators can be seen to be an eigenstate of $\mathbf{Q}$, $\mathbf{P}^+$ and $\mathbf{P}^-$. $\mathbf{V}_N$ can be seen to conserve light cone momentum in the sense that it acts on a Fock state with momentum P^+, it will

only produce other Fock states with the same momentum P^+. This property of the vacuum is very nice computationally because we no longer have to obtain, for instance, bound state masses by subtracting two uncertain quantities as would be necessary in a normal spacetime approach.

5.2.4 The mass spectrum

We define the quantity $K = \frac{L}{2\pi}P^+$ and $H = \frac{2\pi}{L}P^-$. The invariant mass squared is then given by

$$\mathcal{M}^2 = \mathbf{P}^+\mathbf{P}^- = \mathbf{KH} \tag{5.39}$$

and is *independent* of L. Note that $\mathcal{M}^2$ in the space time formulation, as in Hamiltonian lattice gauge theory, is given by the square of the Hamiltonian if we work with physical states with zero momentum.

For a chosen value of the momentum cutoff Λ_+, we can obtain the mass spectrum for any charge $\mathbf{Q}$ by the following procedure. Form a subspace containing Fock states with the appropriate charge $\mathbf{Q}$ and with the eigenvalue of $\mathbf{K}$ equal to K. This subspace is finite dimensional because light cone momenta p^+ take only positive values. Diagonalize $\mathbf{H}$ in this subspace to obtain eigenvalues E_i. Then form $\mathcal{M}^2 = KE_i$ as the estimate of the invariant mass squared pertaining to light cone momentum cutoff Λ_+ and $\mathbf{K}$ eigenvalue K. In order to take the continuum limit, we must lift the cutoff Λ_+ to ∞ and also take K to ∞. K must be taken to ∞ in order to have a finite P^+ for $L \to \infty$. The order in which the two limits are taken is important. To get sensible results, Λ_+ must be taken to ∞ first.

EPB showed that the invariant mass squared can be conveniently expressed as

$$\mathcal{M}^2 = \tilde{m}^2 \left[(1-\lambda^2)\mathbf{KH}_0 + \lambda^2\mathbf{K}\left(\mathbf{V}_N + \mathbf{V}_C\right)\right] \tag{5.40}$$

where the dimensionless coupling λ is given by

$$\lambda = \sqrt{\frac{1}{1+\pi(\frac{m}{g})^2}} \tag{5.41}$$

and $\tilde{m} = \sqrt{1-\lambda^2}$. To renormalize the mass spectrum one could adjust $\tilde{m}$ so that the lowest energy bound state has unit mass for all coupling λ.

To obtain the charge neutral bound states we work in the $Q = 0$ sector and, furthermore, restrict ourselves to only Fock states of the form

$$\mathbf{b}^\dagger_\alpha \mathbf{d}^\dagger_\beta |0\rangle \tag{5.42}$$

or $(1f, 1\overline{f})$ states, where the f stands for *fermion*. EPB showed numerically that, for the low-lying states, this is a very good approximation. The (unrenormalized) mass for the lowest bound state is plotted against coupling λ in Figure 5.2, for $2K = 40$ and $2K = 80$ with a momentum cutoff $2\Lambda_+$ of 1999. The convergence with K is very rapid and the results agree very well with the EPB results obtained using periodic boundary conditions. For comparison, results obtained with a much lower momentum cutoff $2\Lambda_+ = 59$ and $2K = 80$ are also plotted, as points. This provides confirmation that the limit $\Lambda_+ \to \infty$ must be taken before $K \to \infty$. It is possible to check that QED in (1+1)D confines fermions by considering the $Q = 1$ sector. We restrict ourselves to Fock states of the form

$$\mathbf{b}^\dagger_\alpha |0\rangle$$

$$\mathbf{b}^\dagger_\alpha \mathbf{b}^\dagger_\beta \mathbf{d}^\dagger_\gamma |0\rangle.$$

The results are displayed in Figure 5.3 for $2K = 29, 39, 59$, and 69. Apart from $\lambda = 0$ and $\lambda = 1$, the results are indicative of confinement in that the mass of the

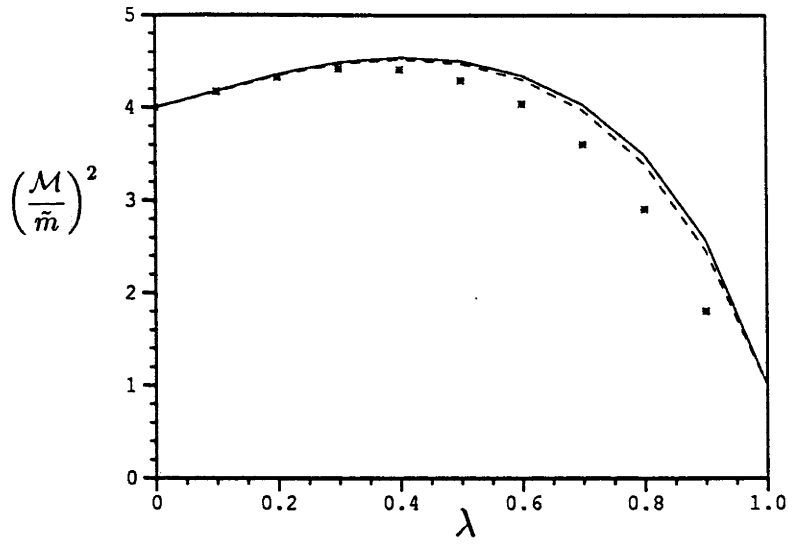

Figure 5.2: The lowest bound state mass versus coupling λ for $2K = 40$ (broken line) and $2K = 80$ (unbroken line) with $2\Lambda_+ = 1999$. The crosses are for $2K = 80$ with $\Lambda_+ = 59$.

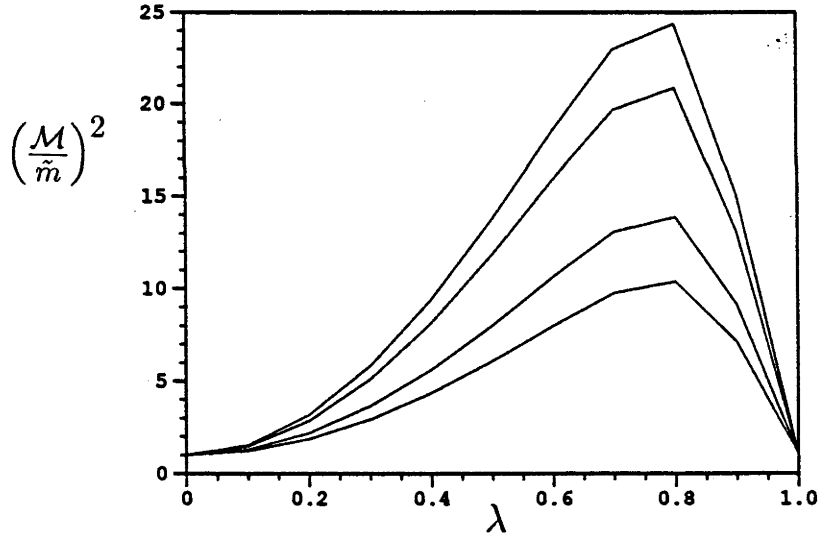

Figure 5.3: The lowest "mass" of the singly charged state for $2K = 29, 39, 59,$ and 69. The increase of the "mass" with K indicates that it is not a meaningful quantity in the continuum limit.

charged state diverges with K. In other words, the mass of the charged state is not a meaningful quantity in the continuum limit. At $\lambda = 0$ we have a free theory which obviously does not confine whereas at $\lambda = 1$ we have, from equation (5.41), a massless theory, or the Schwinger model. The Schwinger model is a confining

theory but because DLCQ as formulated above is not valid for massless theories, as discussed earlier, we are not surprised that we did not obtain the correct result. It is surprising, though, that the correct bound state mass is obtained for the Schwinger model in Figure 5.2

We shall now study in more detail the non-relativistic limit of the model, ie. the limit of large $\frac{m}{g}$. This limit has been studied by Hamer [64] who obtained exact results for the bound state masses. In particular he found the lowest two bound state masses to be

$$\begin{aligned} \frac{\mathcal{M}_0}{g} &= 0.642\left(\frac{g}{m_0}\right)^{\frac{1}{3}} \\ \frac{\mathcal{M}_1}{g} &= 1.473\left(\frac{g}{m_0}\right)^{\frac{1}{3}}. \end{aligned} \tag{5.43}$$

We computed the mass gap $\Delta E = \frac{\mathcal{M}_1}{g} - \frac{\mathcal{M}_0}{g}$ for values of $\frac{m_0}{g}$ in the range of 1 to 32. for $K = 40, 80$ and 120. The results are displayed in a log-log plot in Figure 5.4 together with the result of Hamer. A trend towards the non-relativistic limit is clearly evident, although it seems that as $\frac{m_0}{g}$ increases higher values of K are required. In other words, larger masses feel the finite size L first. A similar calculation will be attempted for QED in (2+1)D in Section 7.

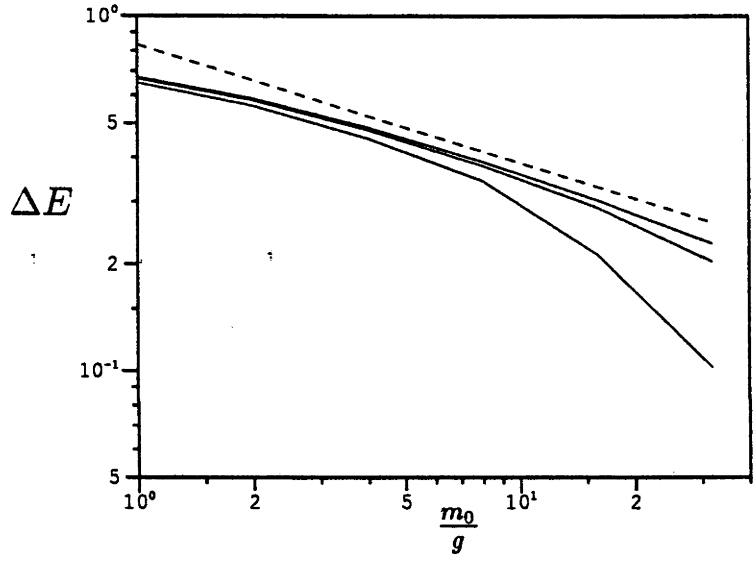

Figure 5.4: The dimensionless mass difference between the two lowest bound states versus dimensionless bare mass for $2K = 40, 80$, and 120 with the values tending towards the non-relativistic limit (broken line) for increasing K.

Chapter 6

Non-relativistic limit of QED in (2+1)D

6.1 Introduction

As described in the previous chapter, the main success of DLCQ for QED in (1+1)D has been the results for the bound-state problem, ie. the calculations of the masses of the low lying charge-neutral states. These were in very good agreement with Lattice Gauge Theory calculations performed by Hamer and collaborators. In (2+1)D the bound-state problem has not been considered satisfactorily before in lattice gauge theory, to the author's knowledge; at least in the Hamiltonian formulation. Our task in the DLCQ formulation of QED in (2+1)D is to consider this problem. As a check on the results, we first study the non-relativistic limit of the theory, where a Schrödinger equation approach is believed to be valid. This approach is the same one as that considered in (1+1)D by Hamer [64] and mentioned in the last chapter. The differential equation obtained in that case has an exact solution. In (2+1)D the differential equation obtained has to be solved numerically.

6.2 The Schrödinger equation

We derive the "potential" for the Schrödinger equation in two ways. Firstly, let us consider a purely classical approach. We consider a "quark" of mass m and charge g in the electric field produced by an "antiquark" of charge $-g$. The electric potential is then

$$V(r) = -\int_{r_0}^{r} E \cdot dr = -\frac{g}{2\pi}\int_{r_0}^{r} \frac{dr}{r} \tag{6.1}$$

on applying Gauss' law, and the potential energy is

$$U(r) = \frac{g^2}{2\pi}\log\left(\frac{r}{r_0}\right) \tag{6.2}$$

where the zero of the potential is arbitrarily chosen to be at r_0. Schrödinger's equation for the system in the centre of mass frame is then

$$\left\{-\frac{1}{m}\nabla_r^2 + \frac{g^2}{2\pi}\log\left(\frac{r}{r_0}\right)\right\}\Psi(\mathbf{r}) = E\Psi(\mathbf{r}). \tag{6.3}$$

This can be rewritten in terms of dimensionless variables $\mathbf{z} = (mg^2/2\pi)^{1/2}\mathbf{r}$ and $\lambda = 2\pi E/g^2$ as

$$\left\{-\nabla_z^2 + \log\left(\frac{z}{z_0}\right)\right\}\Psi(\mathbf{z}) = \lambda\Psi(\mathbf{z}). \tag{6.4}$$

Note that the binding energy is determined only up to a constant dependent on the zero of the potential r_0. Equation (6.4) will be solved numerically for $z_0 = 1$. The term dependent on r_0 is a constant and can be added on to the eigenvalues obtained.

An alternative way of studying the non-relativistic limit is to consider the "Coulomb potential" due to a 1-photon exchange between the quark and anti-

quark. It is given by

$$V(r) = -g^2 \int \frac{d^2\mathbf{k}}{(2\pi)^2} \frac{\exp(i\mathbf{k}\cdot\mathbf{r})}{k^2+\mu^2} = -\frac{g^2}{2\pi} K_0(\mu r). \tag{6.5}$$

where a photon mass μ has been used to regularize the infra-red divergence. $K_0(\mu r)$ is the MacDonald function. To order $(\mu r)^2$ the potential is [65]

$$V(r) = \frac{g^2}{2\pi} \log\left(\frac{\mu r}{2}\right) + \frac{g^2}{2\pi} 0.5772 + O(\mu^2 r^2). \tag{6.6}$$

This shows the same logarithmic behaviour as the classical result. The infrared divergence (as μ is taken to 0) will be seen later to be resolved when one calculates the total energy of the bound state.

By a separation of variables $\Psi(\mathbf{z}) = R(z)\Theta(\theta)$, equation (6.4) for $z_0 = 1$ leads to $\Theta(\theta) = \exp(\pm il\theta)$ and a differential equation for the radial part:

$$-\left\{R''(z) + \frac{1}{z}R'(z)\right\} + \left\{\frac{l^2}{z^2} + \log(z)\right\} R(z) = \lambda R(z). \tag{6.7}$$

Making the substitution $R(z) = z^{-1/2} f(z)$ we obtain a differential equation for f:

$$f''(z) + \left\{\frac{(1-4l)^2}{4z^2} - \log(z) + \lambda\right\} f(z) = 0. \tag{6.8}$$

To solve the bound state problem in the non-relativistic limit, all we need now is to solve the differential equation (6.8) as a boundary-valued eigenvalue problem for the binding energy E. However, we first need to determine all the boundary conditions which lead to normalizability of the radial wavefunction, that is to $\int_0^\infty \mid R(z) \mid^2 z dz < \infty$. This we can do using asymptotic analysis for large and for small z.

6.3 Asymptotic analysis of the Schrodinger equation

We first study the limit of small z. The log term is negligible and the differential equation (6.8) reduces to

$$f''(z) + \frac{1-4l^2}{4z^2} f(z) = 0. \tag{6.9}$$

This equation can be solved by trying solutions of the form $f(z) = z^\alpha$. For $l > 0$ we have the general solution

$$f(z) = c_1 z^{l+1/2} + c_2 z^{-l+1/2} \tag{6.10}$$

whereas for $l = 0$ we obtain

$$f(z) = c_1 z^{1/2} \log z + c_2 z^{1/2}. \tag{6.11}$$

To satisfy normalizability of the radial wavefunction $R(z) = z^{-1/2} f(z)$ we must reject the solution $f(z) = c_1 z^{-l+1/2}$ for $l > 0$. Hence the only boundary condition on f at $z = 0$ consistent with normalizability of $R(z)$ is $f(0) = 0$.

We next study the limit of large z. For this we make use of a theorem by Coppel [66]. This theorem states:

For $\phi(x)$ a positive, twice continuously differentiable function for $x \geq x_0$ such that

$$\int_{x_0}^{\infty} \mid \phi^{-3/2} \phi'' \mid dx < \infty \tag{6.12}$$

the equation $y'' - \phi(x) y = 0$ has a fundamental system of solutions (which form

a basis for the space of all solutions) satisfying for $x \to \infty$

$$y \sim [\phi(x)]^{-1/4} \exp\{\pm \int_{x_0}^{x} [\phi(\xi)]^{1/2} d\xi\} \tag{6.13}$$

and

$$y' \sim \pm[\phi(x)]^{1/4} \exp\{\pm \int_{x_0}^{x} [\phi(\xi)]^{1/2} d\xi\}. \tag{6.14}$$

We can check easily that our "potential" from equation (6.8)

$$\phi(z) = \log z - \frac{1 - 4l^2}{4z^2} \tag{6.15}$$

satisfies the condition of the theorem. We then have all the asymptotic solutions to the differential equation. For normalizability of the radial wavefunction $R(z) = z^{-1/2} f(z)$ we must reject the exponentially increasing solution. Hence our other boundary condition consistent with normalizability is $f(\infty) = 0$. For numerical purposes it is more useful to know that for physical solutions we have

$$\frac{f'(z)}{f(z)} \sim [\phi(z)]^{1/2} \tag{6.16}$$

as $z \to \infty$.

6.4 Numerical Results

We now solve the differential equation (6.8) with boundary conditions

$$f(0) = 0, \qquad \frac{f'(R)}{f(R)} = [\phi(R) - \lambda]^{1/2} \tag{6.17}$$

at a large "boundary" R by the numerical method of "shooting". (See, for example, Koonin [67]). The idea is to discretize the differential equation, by replacing

the real line by a grid of points $\{x_i\}$, $i = 1, \ldots, M$, and derivatives by finite differences, to obtain a three-step recursion relation for the wavefunction $f(x_m)$. Given $f(x_1 = 0)$ (from one boundary condition) and $f(x_1)$ (which can be arbitrary because for a linear, homogeneous differential equation the normalization of the eigenfunction is unspecified) we can then obtain $f(x_m)$ for all $m > 2$. This is known as "shooting from the left" to obtain the "left branch". Similarly one can "shoot from the right", starting from the other boundary condition. The strategy adopted to find eigensolutions is the following:

1. Guess an energy λ;

2. Choose a matching point x_P defined as that grid point x_i for which $\phi(x_i) - \lambda$ ($\phi(x)$ defined by equation (6.15)) is a minimum;

3. Shoot from the left with arbitrary normalization to obtain the left branch $\psi_<$;

4. Shoot from the right with normalization chosen so that the left and right branches meet at x_P and obtain the right branch $\psi_>$;

5. If the left and right branches match smoothly at x_P, ie. if they have the same derivatives, then λ is an eigenvalue; otherwise adjust λ and repeat the above steps until an eigenvalue is found.

We look for solutions of the finite difference form of the equation

$$\frac{d\psi_<}{dx}|_{x_P} - \frac{d\psi_>}{dx}|_{x_P} = 0. \tag{6.18}$$

Solutions of this equation are then the eigenvalues. We used the secant method to obtain eigenvalues to 5 significant figures, having first obtained approximate eigenvalues by scanning λ. We obtained the lowest 10 eigenvalues, using a step

size of 0.01 and 2000 steps. Decreasing the step size further and increasing the number of steps did not influence the results, to the degree of accuracy quoted. The solutions corresponding to the lowest two eigenvalues for $l = 0$ and $l = 1$ are displayed in Figures 6.1 to 6.4. It can be seen that they all have the correct

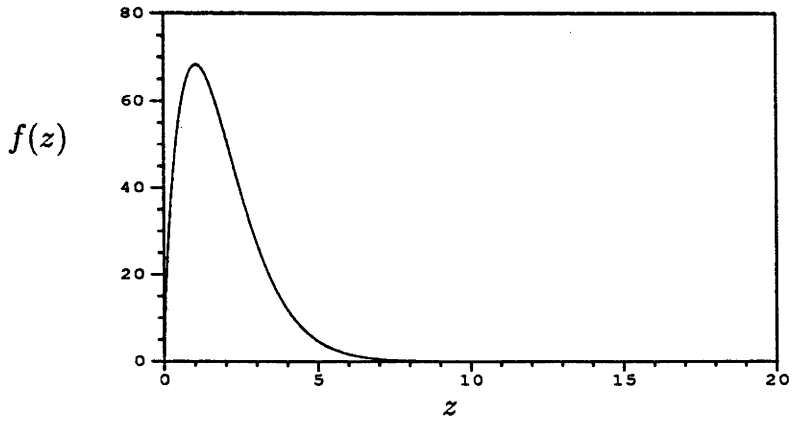

Figure 6.1: The (unnormalized) wavefunction $f(z)$ obtained by the shooting method for $l = 0$ and $\lambda = 0.69861$.

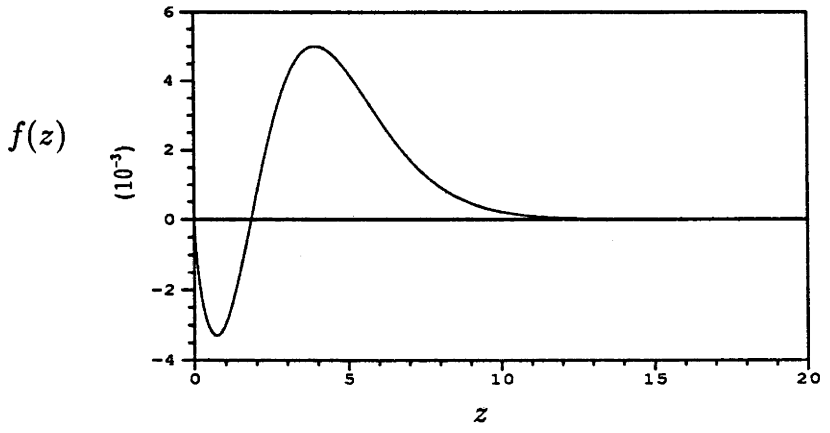

Figure 6.2: The (unnormalized) wavefunction $f(z)$ obtained by the shooting method for $l = 1$ and $\lambda = 1.3862$.

asymptotic behaviour. The eigenvalues are displayed in Table 6.1.

Having found the numerical eigensolutions to the differential equation (6.8) we are now in a position to calculate the energies of the bound states in the non-relativistic limit. In the purely classical approach, where the "quarks" are purely

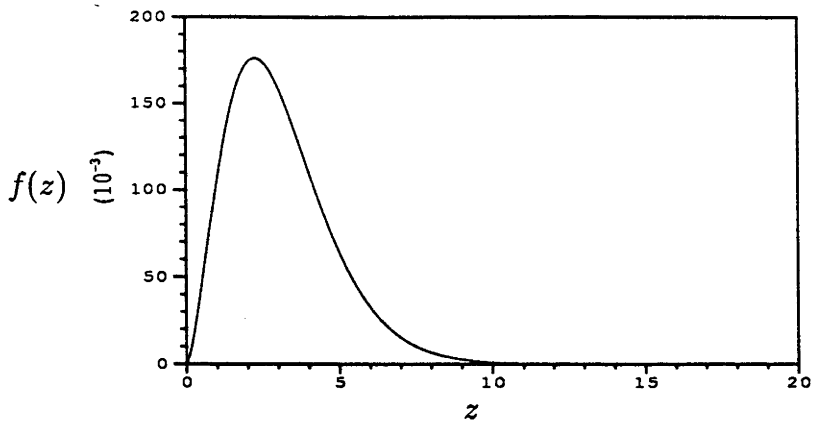

Figure 6.3: The (unnormalized) wavefunction $f(z)$ obtained by the shooting method for $l = 0$ and $\lambda = 1.7169$.

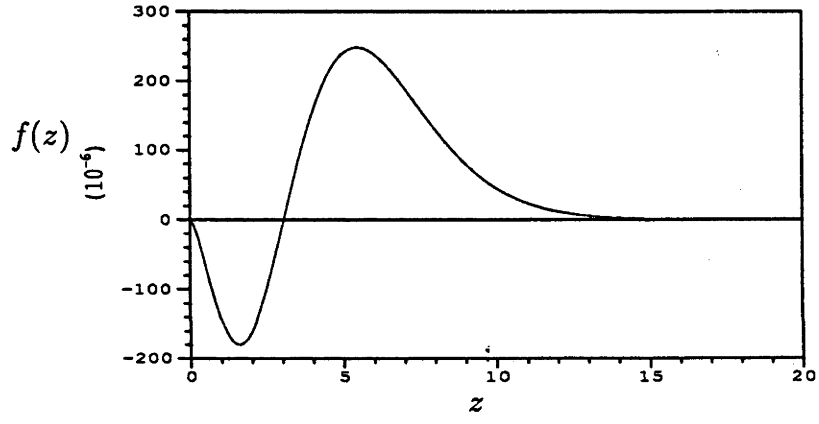

Figure 6.4: The (unnormalized) wavefunction $f(z)$ obtained by the shooting method for $l = 1$ and $\lambda = 2.0095$.

classical particles of mass m, the bound state energies are given by $E = 2m + E_b$ where the binding energy E_b is an eigensolution of the Schrodinger equation. Because of the arbitrariness in r_0, the zero of the potential, we know E only to an undetermined constant. However, the mass gaps are obtained as

$$E_i - E_j = \frac{g^2}{2\pi}(\lambda_i - \lambda_j) \tag{6.19}$$

where the λ_i's are from Table 6.1. They are independent of r_0 because the r_0 dependent term is the same for all physical states. Note that the mass gaps

l	λ
0	0.69861
1	1.3862
0	1.7169
2	1.8444
1	2.0095
3	2.1578
0	2.2103
2	2.2759
1	2.3943
4	2.3963

Table 6.1: The lowest ten eigenvalues λ of equation (6.8) together with their l mode numbers obtained by shooting.

depend only on the coupling g and not on the mass m.

In the second approach, where we introduce a mass μ for the photon and look at the non-relativistic limit of the field theory, we can follow similar discussions by Cornwall [13] and Sen [68]. These authors calculated the 1 and 2 loop corrections to the fermion mass, with a small photon mass μ included as an infra-red regulator, and arrived at a "renormalized mass" given by

$$m_R = m + \frac{g^2}{4\pi}\left[1 + O\left(\frac{g^2}{m}\right)\right]\log(\frac{m}{\mu}) \tag{6.20}$$

where the $O(g^2/m)$ terms are infrared finite. They then argued that the infrared divergences cancel in the sum of $2m_R$ and $V(r)$ from equation (6.6), which contribute to the mass of bound states. In other words, charge-neutral bound states have well defined physical masses whereas single fermion states do not, precisely as one would expect in a confining theory. We can use this argument to obtain the absolute energies of the bound states. For this we need to solve the Schrödinger equation with the potential $V(r)$ given by equation (6.6), ie. the equation

$$\left\{-\frac{1}{m}\nabla_r^2 + \frac{g^2}{2\pi}\log\left(\frac{\mu r}{2}\right) + \frac{g^2}{2\pi}0.5772\right\}\Psi(\mathbf{r}) = \tilde{E}\Psi(\mathbf{r}). \tag{6.21}$$

$\tilde{E}$ can be easily shown to be related to λ obtained by solving equation (6.8) by

$$\tilde{E} = \frac{g^2}{2\pi}\left[\lambda + 0.5772 + \log\left(\frac{\mu}{2}\sqrt{\frac{2\pi}{mg^2}}\right)\right]. \tag{6.22}$$

The bound state energies $E_i = 2m_R + \tilde{E}_i$ are then given by

$$\begin{aligned} E_i &= 2m_R + \frac{g^2}{2\pi}\left[\lambda_i + 0.5772 + \log\left\{\frac{\mu}{2}\sqrt{\left(\frac{2\pi}{mg^2}\right)}\right\}\right] \\ &= 2m + \frac{g^2}{2\pi}\left[\lambda_i + 0.5772 - \log 2 + \log\sqrt{\left(\frac{2\pi m}{g^2}\right)}\right] \end{aligned} \tag{6.23}$$

where λ_i is from Table 6.1.

One can say that the perturbative quantum field theory approach has in some sense determined the arbitrary zero of the potential, r_0, in the purely classical approach. We can use the results for the mass gaps in equation (6.19) and for the masses in equation (6.23) as checks for the DLCQ calculation of bound state masses.

Chapter 7

Application of DLCQ to QED in (2+1)D

7.1 Introduction

In this Chapter, we will apply DLCQ to QED in (2+1)D. An application of DLCQ to higher than (1+1)D has already been made by Tang [12] who considered QED in (3+1)D. Because we are eventually interested in applications to QCD, it would be interesting to consider the theory in (2+1)D as well. It might also turn out that different ways of extending the DLCQ procedure of [11] would be required for confining and non-confining theories in higher dimensions.

We will work with the most straightforward approach, namely regularization with momentum cutoffs. We again consider the theory in a finite volume, with $-L_+ \leq x^- \leq L_+$ and $-L_\perp \leq x^\perp \leq L_\perp$ where $x^\perp$ is the extra coordinate in (2+1)D, the transverse coordinate. We introduce a transverse momentum cutoff $\Lambda_\perp$ in addition to the light cone momentum cutoff Λ_+.

The results are expected to be very similar to those in (1+1)D. Both are ultraviolet finite [14] in normal perturbation theory and infrared divergences in

the fermion self-masses are expected to cancel in bound state masses. To arrive at the expression for the invariant mass squared $\mathcal{M}^2$, we will follow very closely the procedure used in (1+1)D.

7.2 Light cone formulation

We will again work with the four-component spinor theory of QED in (2+1)D which leads to confinement, as was discussed in Section 3.1. The Lagrangian density $\mathcal{L}$ is given by

$$\mathcal{L} = \frac{i}{2}(\overline{\psi}\gamma^\mu\partial_\mu\psi - \partial_\mu\overline{\psi}\gamma^\mu\psi) - m\overline{\psi}\psi - \frac{1}{4}F^{\mu\nu}F_{\mu\nu} - eA_\mu\overline{\psi}\gamma^\mu\psi. \tag{7.1}$$

where the fermion field ψ is a four-component spinor. The Dirac matrices are those given in (3.5). For definiteness we will choose the following representation of the Pauli matrices :

$$\sigma^1 = \begin{pmatrix} 0 & -i \\ i & 0 \end{pmatrix}, \quad \sigma^2 = \begin{pmatrix} 0 & 1 \\ 1 & 0 \end{pmatrix}, \quad \sigma^3 = \begin{pmatrix} 1 & 0 \\ 0 & -1 \end{pmatrix}. \tag{7.2}$$

We now make a transformation to light cone coordinates x^+, x^-, $x^\perp$ defined by $x^\pm = x^0 \pm x^1$, $x^\perp = x^2$. The metric $g^{\mu\nu}$, for $\mu, \nu = +, -, \perp$, becomes

$$g^{\mu\nu} = \begin{pmatrix} 0 & 2 & 0 \\ 2 & 0 & 0 \\ 0 & 0 & -1 \end{pmatrix} \tag{7.3}$$

The Dirac matrices become $\gamma^{\pm} = \gamma^0 \pm \gamma^1$ and $\gamma^{\perp} = \gamma^2$ and, once again, $\gamma^{\pm}$ are used to define projection operators

$$\Lambda^{(\pm)} = \frac{1}{4}\gamma^{\mp}\gamma^{\pm} \tag{7.4}$$

for the spinors. Explicitly, we have

$$\Lambda^{(+)} = \begin{pmatrix} 1 & 1 & 0 & 0 \\ 1 & 1 & 0 & 0 \\ 0 & 0 & 1 & 1 \\ 0 & 0 & 1 & 1 \end{pmatrix}, \qquad \gamma^{\perp} = \begin{pmatrix} 0 & i & 0 & 0 \\ i & 0 & 0 & 0 \\ 0 & 0 & 0 & -i \\ 0 & 0 & -i & 0 \end{pmatrix}. \tag{7.5}$$

The equations of motion are, again, Maxwell's equations

$$\partial_\mu F^{\mu\nu} = e\overline{\psi}\gamma^\nu\psi \tag{7.6}$$

and Dirac's equation

$$\left[(i\partial_\mu - eA_\mu)\,\gamma^\mu - m_0\right]\psi = 0, \tag{7.7}$$

which can be written in terms of $\psi_\pm = \Lambda^{(\pm)}\psi$ and the components A^- and $A^\perp$ of the photon field if we work in light cone gauge $A^+ = 0$. The fields ψ_+ and $A^\perp$ are treated as independent fields which will be quantized later. The dependent degrees of freedom ψ_- and A^- are obtained from the equations of motion as

$$A^- = 4e\frac{1}{(i\partial^+)^2}\left(\psi_+^\dagger\psi_+\right) - 2i\partial_\perp\frac{1}{(i\partial^+)^2}i\partial^+A^\perp, \tag{7.8}$$

$$\psi_- = m_0\gamma^0\frac{1}{(i\partial^+)}\psi_+ - \frac{1}{(i\partial^+)}\left(i\partial_\perp - eA_\perp\right)\alpha^\perp\psi_+ \tag{7.9}$$

where $\alpha^\perp = \gamma^0\gamma^\perp$.

The classical conserved charges are given by

$$Q = \frac{1}{2}\int_{-L_+}^{L_+} dx^- \int_{-L_\perp}^{L_\perp} dx^\perp j^+(x^-, x_0^+, x^\perp) \tag{7.10}$$

and

$$P^\nu = \frac{1}{2}\int_{-L_+}^{L_+} dx^- \int_{-L_\perp}^{L_\perp} dx^\perp T^{+\nu}(x^-, x_0^+, x^\perp). \tag{7.11}$$

where the charge current j^μ and the energy-momentum tensor $T^{\mu\nu}$ are defined as in equations (5.17) and (5.18). After some algebra, in which ψ_- and A^- are eliminated in favour of ψ^+ and $A^\perp$ by means of equations (7.8) and (7.9), the conserved charges can be shown to be given by

$$Q = \int dx^- dx^\perp \psi_+^\dagger \psi_+ \tag{7.12}$$

$$P^+ = \int dx^- dx^\perp \left[\psi_+^\dagger i\partial^+ \psi_+ + \frac{1}{2}\left(\partial^+ A^\perp\right)^2\right] \tag{7.13}$$

$$\begin{aligned} P^- = \int dx^- dx^\perp \Bigg[& 2g^2 \left\{\psi_+^\dagger \psi_+ \frac{1}{(i\partial^+)^2} \psi_+^\dagger \psi_+\right\}_{sym} \\ & + g^2 \left\{\psi_+^\dagger A_\perp \alpha^\perp \frac{1}{(i\partial^+)} A_\perp \alpha^\perp \psi_+\right\}_{sym} \\ & + 2g \left\{\psi_+^\dagger \psi_+ \frac{1}{(i\partial^+)^2} i\partial^+ i\partial^\perp A^\perp\right\}_{sym} \\ & + \frac{1}{2}\left\{i\partial^+ i\partial^\perp A^\perp \frac{1}{(i\partial^+)^2} i\partial^+ i\partial^\perp A^\perp\right\}_{sym} \\ & + g \left\{\psi_+^\dagger A_\perp \alpha^\perp \frac{1}{(i\partial^+)} \left(-i\partial_\perp \alpha^\perp + \beta m_0\right)\psi_+\right\}_{sym} \\ & + g \left\{\psi_+^\dagger \left(i\partial_\perp \alpha^\perp + \beta m_0\right) \frac{1}{(i\partial^+)} A_\perp \alpha^\perp \psi_+\right\}_{sym} \\ & + \left\{\psi_+^\dagger \left(i\partial_\perp \alpha^\perp + \beta m_0\right) \frac{1}{(i\partial^+)} \left(-i\partial_\perp \alpha^\perp + \beta m_0\right)\psi_+\right\}_{sym} \Bigg] \end{aligned} \tag{7.14}$$

The assumption of periodic boundary conditions for ψ_+ and $A^\perp$ was used in obtaining the above expressions.

We quantize at equal light cone time x^+ by specifying the (anti) commutation

relations [73] at equal light cone time

$$\left\{\psi_{+\alpha}(x_0^+,x^-,x^\perp),\psi^\dagger_{+\beta}(x_0^+,y^-,y^\perp)\right\} = \Lambda^{(+)}_{\alpha\beta}\delta(x^- - y^-)\delta(x^\perp - y^\perp) \quad (7.15)$$

$$\left[A^\perp(x_0^+,x^-,x^\perp),A^\perp(x_0^+,y^-,y^\perp)\right] = -i\frac{1}{4}\epsilon(x^- - y^-)\delta(x^\perp - y^\perp) \quad (7.16)$$

where the step function $\epsilon(x)$ is defined such that $\epsilon'(x) = 2\delta(x)$.

We again impose anti-periodic boundary conditions for ψ_+ in the x^- direction. As mentioned above, we impose periodic boundary conditions in the $x^\perp$ direction for ψ_+. For $A^\perp$ we impose periodic boundary conditions in both the x^- and $x^\perp$ directions. This leads to a discretization of the light cone and transverse momenta. For fermions, the light cone momenta p^+ take the values

$$p^+ = 2p_- = \frac{2l\pi}{L_+} \qquad l = \frac{1}{2},\frac{3}{2},\frac{5}{2}\ldots\Lambda_+ \quad (7.17)$$

while for the "photons" the light cone momenta are

$$k^+ = 2k_- = \frac{2l\pi}{L_+} \qquad l = 1,2,\ldots,\Lambda_+. \quad (7.18)$$

The transverse momenta of both fermions and photons take the values

$$p^\perp = \frac{m\pi}{L_\perp} \qquad m = 0,\pm1,\pm2,\ldots\pm\Lambda_\perp. \quad (7.19)$$

Λ_+ is an odd multiple of $\frac{1}{2}$ and provides an upper cutoff to the light cone momenta and $\Lambda_\perp$ is an integer and provides an upper and lower cutoff to the transverse momenta. We expand the fields ψ^+ and $\mathbf{A}^\perp$ at time x_0^+ in terms of normal modes,

$$\psi_+(x_0^+,x^-,x^\perp) = \frac{1}{2\sqrt{L_+L_\perp}}\sum_{l=\frac{1}{2}}^{\Lambda_+}\sum_{m=-\Lambda_\perp}^{\Lambda_\perp}\sum_{j=1}^{2}\chi^j\left(\mathrm{b}^j_{lm}\mathrm{e}^{-i(l\xi-m\eta)}+\right.$$

$$\mathrm{d}^{j\dagger}_{lm}\mathrm{e}^{i(l\xi-m\eta)}\Big)\,, \tag{7.20}$$

$$A^{\perp}(x^{+}_{0},x^{-},x^{\perp}) = \frac{1}{\sqrt{8\pi L_{\perp}}}\sum_{l=1}^{\Lambda_{+}}\sum_{m=-\Lambda_{\perp}}^{\Lambda_{\perp}}\frac{1}{\sqrt{l}}\Big(\mathbf{a}_{lm}\mathrm{e}^{-i(l\xi-m\eta)}+ \mathbf{a}^{\dagger}_{lm}\mathrm{e}^{i(l\xi-m\eta)}\Big) \tag{7.21}$$

with $\xi = \pi\frac{x^{-}}{L_{+}}$ and $\eta = \pi\frac{x^{\perp}}{L_{\perp}}$. The operators $\mathbf{b}^{j\dagger}_{lm}$ ($\mathbf{d}^{j\dagger}_{lm}$) are creation operators for fermions (anti-fermions) with light cone momenta l and transverse momenta m while $\mathbf{b}^{j}_{lm}$ ($\mathbf{d}^{j}_{lm}$) are destruction operators. $\mathbf{a}^{\dagger}_{lm}$ and $\mathbf{a}_{lm}$ are, respectively, creation and destruction operators for "photons" with light cone momenta l and transverse momenta m. They satisfy the usual (anti) commutation relations

$$\begin{aligned}\left\{\mathbf{b}^{j}_{lm},\mathbf{b}^{j'\dagger}_{l'm'}\right\} &= \left\{\mathbf{d}^{j}_{lm},\mathbf{d}^{j'\dagger}_{l'm'}\right\} = \delta_{l,l'}\delta_{m,m'}\delta_{j,j'} \\ \left[\mathbf{a}_{lm},\mathbf{a}^{\dagger}_{l'm'}\right] &= \delta_{l,l'}\delta_{m,m'}\end{aligned} \tag{7.22}$$

with all other commutators vanishing. These commutation relations can be shown to be consistent with the commutation relations (7.16). The spinors χ^{j} in the fermion mode expansion (7.20) are chosen to be

$$\chi^{1} = \frac{1}{\sqrt{2}}\begin{pmatrix}1\\1\\0\\0\end{pmatrix}, \qquad \chi^{2} = \frac{1}{\sqrt{2}}\begin{pmatrix}0\\0\\1\\1\end{pmatrix} \tag{7.23}$$

and satisfy the relations $\chi^{j} = \Lambda^{(+)}\chi^{j}$ and by $\chi^{j\dagger}\chi^{j'} = \delta_{j,j'}$. They also have the property that

$$\chi^{j\dagger}\alpha^{\perp}\beta\chi^{j'} = i(-1)^{j}\delta_{j,j'}. \tag{7.24}$$

The two spinors χ^{1} and χ^{2} can be considered as corresponding to two "flavours" of 2-component fermions [14] called "u" and "d".

We next substitute the mode expansions (7.20) and (7.21) for ψ_+ and $\mathbf{A}^\perp$ in the expressions (7.12) to (7.14) for the conserved charges. In doing so we will again make use of the quantities

$$\{n|m\} = \frac{1}{2\pi}\int_{-\pi}^{\pi} d\xi \left\{ e^{in\xi} \frac{1}{(i\partial_\xi)} e^{im\xi} \right\}_{sym} \tag{7.25}$$

$$[k|l] = \frac{1}{2\pi}\int_{-\pi}^{\pi} d\xi \left\{ e^{ik\xi} \frac{1}{(i\partial_\xi)^2} e^{il\xi} \right\}_{sym} \tag{7.26}$$

where n and m are positive odd multiples of $\frac{1}{2}$ and k and l are integers. Their values are again given by equations (5.30) and (5.31).

7.3 The conserved charges in terms of Fock space operators

The conserved charges become

$$\mathbf{Q} = \sum_{l=\frac{1}{2}}^{\Lambda_+} \sum_{m=-\Lambda_\perp}^{\Lambda_\perp} \sum_{j=1}^{2} \left(\mathrm{b}_{lm}^{j\dagger} \mathrm{b}_{lm}^{j} - \mathrm{d}_{lm}^{j\dagger} \mathrm{d}_{lm}^{j} \right) \tag{7.27}$$

$$\mathbf{P}^+ = \frac{2\pi}{L_+} \sum_{l=\frac{1}{2}}^{\Lambda_+} \sum_{m=-\Lambda_\perp}^{\Lambda_\perp} \sum_{j=1}^{2} l \left(\mathrm{b}_{lm}^{j\dagger} \mathrm{b}_{lm}^{j} + \mathrm{d}_{lm}^{j\dagger} \mathrm{d}_{lm}^{j} \right) \tag{7.28}$$

$$\mathbf{P}^\perp = -\frac{\pi}{L_\perp} \sum_{l=\frac{1}{2}}^{\Lambda_+} \sum_{m=-\Lambda_\perp}^{\Lambda_\perp} \sum_{j=1}^{2} m \left(\mathrm{b}_{lm}^{j\dagger} \mathrm{b}_{lm}^{j} + \mathrm{d}_{lm}^{j\dagger} \mathrm{d}_{lm}^{j} \right) \tag{7.29}$$

$$\begin{aligned} \mathbf{P}^- = \frac{L_+}{2\pi} \Bigg\{ & m_0^2 \mathbf{H}_0 + \left(\frac{\pi}{L_\perp} \right)^2 \mathbf{H}_1 + \frac{g\pi}{L_\perp \sqrt{8\pi L_\perp}} \mathbf{H}_2 \\ & - \frac{i m_0 g}{\sqrt{8\pi L_\perp}} \mathbf{H}_3 + \frac{g^2}{8\pi L_\perp} \mathbf{H}_4 + \frac{g^2}{8\pi L_\perp} \mathbf{H}_5 \Bigg\} \end{aligned} \tag{7.30}$$

where

$$\mathbf{H}_0 = \sum_{l=\frac{1}{2}}^{\Lambda_+} \sum_{m=-\Lambda_\perp}^{\Lambda_\perp} \sum_{j=1}^{2} \frac{1}{l} \left(\mathrm{b}_{lm}^{j\dagger} \mathrm{b}_{lm}^{j} + \mathrm{d}_{lm}^{j\dagger} \mathrm{d}_{lm}^{j} \right) \tag{7.31}$$

$$\mathbf{H}_1 = \sum_{l=\frac{1}{2}}^{\Lambda_+} \sum_{m=-\Lambda_\perp}^{\Lambda_\perp} \sum_{j=1}^{2} \frac{m^2}{l} \left(\mathbf{b}^{j\dagger}_{lm} \mathbf{b}^{j}_{lm} + \mathbf{d}^{j\dagger}_{lm} \mathbf{d}^{j}_{lm} \right) + \sum_{l=1}^{\Lambda_+} \sum_{m=-\Lambda_\perp}^{\Lambda_\perp} \mathbf{a}^{\dagger}_{lm} \mathbf{a}_{lm} \frac{m^2}{l} \tag{7.32}$$

$$\mathbf{H}_2 = \sum_{l_1=1}^{\Lambda_+} \sum_{l_2,l_3=\frac{1}{2}}^{\Lambda_+} \sum_{m_1,m_2,m_3=-\Lambda_\perp}^{\Lambda_\perp} \sum_{j=1}^{2} \frac{1}{\sqrt{l_1}} \left(2\frac{m_1}{l_1} - \frac{m_2}{l_2} - \frac{m_3}{l_3} \right) \left(\mathbf{a}^{\dagger}_{l_1 m_1} + \mathbf{a}_{l_1 m_1} \right)$$
$$\left(\mathbf{b}^{j\dagger}_{l_2 m_2} + \mathbf{d}^{j}_{l_2 m_2} \right) \left(\mathbf{b}^{j}_{l_3 m_3} + \mathbf{d}^{j\dagger}_{l_3 m_3} \right) \delta\left(\sum \tilde{l}_i \right) \delta\left(\sum \tilde{m}_i \right) \tag{7.33}$$

$$\mathbf{H}_3 = \sum_{l_1=1}^{\Lambda_+} \sum_{l_2,l_3=\frac{1}{2}}^{\Lambda_+} \sum_{m_1,m_2,m_3=-\Lambda_\perp}^{\Lambda_\perp} \sum_{j=1}^{2} \frac{(-1)^j}{\sqrt{l_1}} \left(\frac{1}{\tilde{l}_2} + \frac{1}{\tilde{l}_3} \right) \left(\mathbf{a}^{\dagger}_{l_1 m_1} + \mathbf{a}_{l_1 m_1} \right)$$
$$\left(\mathbf{b}^{j\dagger}_{l_2 m_2} + \mathbf{d}^{j}_{l_2 m_2} \right) \left(\mathbf{b}^{j}_{l_3 m_3} + \mathbf{d}^{j\dagger}_{l_3 m_3} \right) \delta\left(\sum \tilde{l}_i \right) \delta\left(\sum \tilde{m}_i \right) \tag{7.34}$$

$$\mathbf{H}_4 = \sum_{l_1,l_2,l_3,l_4=\frac{1}{2}}^{\Lambda_+} \sum_{m_1,m_2,m_3,m_4=-\Lambda_\perp}^{\Lambda_\perp} \sum_{j,k=1}^{2} 2 \left[\tilde{l}_1 + \tilde{l}_2 | \tilde{l}_3 + \tilde{l}_4 \right] \left(\mathbf{b}^{j\dagger}_{l_1 m_1} + \mathbf{d}^{j}_{l_1 m_1} \right)$$
$$\left(\mathbf{b}^{j}_{l_2 m_2} + \mathbf{d}^{j\dagger}_{l_2 m_2} \right) \left(\mathbf{b}^{k\dagger}_{l_3 m_3} + \mathbf{d}^{k}_{l_3 m_3} \right) \left(\mathbf{b}^{k}_{l_4 m_4} + \mathbf{d}^{k\dagger}_{l_4 m_4} \right) \delta\left(\sum \tilde{m}_i \right) \tag{7.35}$$

$$\mathbf{H}_5 = \sum_{l_1,l_2=1}^{\Lambda_+} \sum_{l_3,l_4=\frac{1}{2}}^{\Lambda_+} \sum_{m_1,m_2,m_3,m_4=-\Lambda_\perp}^{\Lambda_\perp} \sum_{j=1}^{2} \frac{1}{\sqrt{l_1 l_2}} \left\{ \tilde{l}_1 + \tilde{l}_3 | \tilde{l}_2 + \tilde{l}_4 \right\} \left(\mathbf{a}^{\dagger}_{l_1 m_1} + \mathbf{a}_{l_1 m_1} \right)$$
$$\left(\mathbf{a}^{\dagger}_{l_2 m_2} + \mathbf{a}_{l_2 m_2} \right) \left(\mathbf{b}^{j\dagger}_{l_3 m_3} + \mathbf{d}^{j}_{l_3 m_3} \right) \left(\mathbf{b}^{j}_{l_4 m_4} + \mathbf{d}^{j\dagger}_{l_4 m_4} \right) \delta\left(\sum \tilde{m}_i \right) \tag{7.36}$$

Here, we have used a shorthand notation in which $\tilde{l}$ is l $(-l)$ if the momentum l is associated with a creation (destruction) operator. Apart from the different "spin" structures, the conserved charges have precisely the same form as those obtained by Tang [12] for QED in (3+1)D.

The $\mathbf{H}_0$ and $\mathbf{H}_4$ terms have already appeared in (1+1)D. The new terms $\mathbf{H}_2$, $\mathbf{H}_3$ and $\mathbf{H}_5$ allow for the absorption or emission of photons. It is noteworthy that these three new terms do not allow for flavour-changing of fermions, ie. taking a u fermion in a Fock state to a d fermion or vice versa. In contrast, in (3+1)D the corresponding terms do allow for fermion "spin-flip". $\mathbf{H}_3$ explicitly breaks flavour symmetry. This is related to the chiral-symmetry breaking term in the Lagrangian mentioned in Section 3.1.

The term $\mathbf{H}_4$ does allow for flavour-changing in the following sense. Consider Fock states $(f, \overline{f})$ with 1 fermion and 1 antifermion. There are 4 different types due to the two flavours (χ^j with $j = 1, 2$ or in the alternative notation $f = u, d$).

On acting with $\mathbf{H}_4$ these 4 different types of $(f, \overline{f})$ states get transformed among each other according to

$$(u, \overline{u}) \rightarrow (u, \overline{u}), (d, \overline{d}) \tag{7.37}$$

$$(d, \overline{d}) \rightarrow (d, \overline{d}), (u, \overline{u}) \tag{7.38}$$

$$(u, \overline{d}) \rightarrow (u, \overline{d}) \tag{7.39}$$

$$(d, \overline{u}) \rightarrow (d, \overline{u}). \tag{7.40}$$

We have a similar situation with higher Fock states. Hence we can see, for instance, that a $(u, \overline{d})$ state will only couple to Fock states with the same "net flavour", ie. the sum of the flavour label j over all the fermions and antifermions in the Fock state. We then have a decomposition of the $Q = 0$ sector of the Fock space into subsectors according to net flavour. In the numerical work we will only be concerned with $(u, \overline{d})$ and $(u, \overline{d}, \gamma)$ states. These couple to no other $(f, \overline{f})$ and $(f, \overline{f}, \gamma)$ states. We expect that in the non-relativistic limit, which which we are concerned, it does not matter which subsector we work in. Restricting ourselves to the chosen sectors drastically reduces the size of the (truncated) Fock space.

The operator $\mathbf{P}^{\perp}$ is diagonal in Fock space and measures the total transverse momentum of a Fock state. We will be working with states for which $\mathbf{P}^{\perp} = 0$. This does not make any difference as far as the invariant mass is concerned. As in the (1+1)D case, there is no explicit dependence on L_+ in the invariant mass squared $\mathcal{M}^2 = \mathbf{P}^+\mathbf{P}^- - (\mathbf{P}^{\perp})^2$. We will again work with the dimensionless operator $\mathbf{K} = \mathbf{P}^+/2\pi$. There is however an explicit dependence on $L_{\perp}$.

We now normal order the interaction terms $\mathbf{H}_2$ to $\mathbf{H}_5$. The terms $\mathbf{H}_3$ and $\mathbf{H}_4$ do not give rise to non-zero contractions and normal ordering is easy. The terms

$\mathbf{H}_4$ and $\mathbf{H}_5$ on normal ordering give rise to extra diagonal terms:

$$\mathbf{H}_4 = :\mathbf{H}_4: + \sum_{l=\frac{1}{2}}^{\Lambda_+} \sum_{m=-\Lambda_\perp}^{\Lambda_\perp} \sum_{j=1}^{2} I_l^1 \left(\mathbf{b}_{lm}^{j\dagger} \mathbf{b}_{lm}^{j} + \mathbf{d}_{lm}^{j\dagger} \mathbf{d}_{lm}^{j} \right) \tag{7.41}$$

$$\begin{aligned} \mathbf{H}_5 &= :\mathbf{H}_5: + \sum_{l=1}^{\Lambda_+} \sum_{m=-\Lambda_\perp}^{\Lambda_\perp} I_l^2 \mathbf{a}_{lm}^{\dagger} \mathbf{a}_{lm} \\ &\quad + \sum_{l=\frac{1}{2}}^{\Lambda_+} \sum_{m=-\Lambda_\perp}^{\Lambda_\perp} \sum_{j=1}^{2} \left(I_l^3 \mathbf{b}_{lm}^{j\dagger} \mathbf{b}_{lm}^{j} + I_l^4 \mathbf{d}_{lm}^{j\dagger} \mathbf{d}_{lm}^{j} \right) \end{aligned} \tag{7.42}$$

The "self-induced inertias" I_l^j obtained from normal ordering $\mathbf{H}_4$ and $\mathbf{H}_5$ are given by

$$I_l^1 = 2 \sum_{m=\Lambda_\perp}^{\Lambda_\perp} \sum_{k=\frac{1}{2}}^{\Lambda_+} \left([l-k|k-l] - [l+k|-l-k] \right) \tag{7.43}$$

$$I_l^2 = \frac{1}{l} \sum_{m=\Lambda_\perp}^{\Lambda_\perp} \sum_{k=\frac{1}{2}}^{\Lambda_+} \left(\{l-k|k-l\} - \{l+k|-l-k\} \right) \tag{7.44}$$

$$I_l^3 = \sum_{m=\Lambda_\perp}^{\Lambda_\perp} \sum_{k=1}^{\Lambda_+} \frac{1}{k} \{l-k|k-l\} \tag{7.45}$$

$$I_l^4 = \sum_{m=\Lambda_\perp}^{\Lambda_\perp} \sum_{k=1}^{\Lambda_+} \frac{1}{k} \{l+k|-l-k\}. \tag{7.46}$$

The fermion inertias I_l^1, I_l^3, and I_l^4 are all finite in Λ_+ whereas the photon inertia I_l^2 is logarithmically divergent. All four inertias are, however, linearly divergent with transverse momentum cutoff $\Lambda_\perp$ due to the unrestricted sum over transverse momenta. We will look at the divergences more carefully in the next section. Note that in normal ordering we have discarded all constant terms obtained.

We will find it convenient to work with the dimensionless form

$$\begin{aligned} \frac{\mathcal{M}^2}{g^4} &= \mathbf{K} \Big[\mu^2 \mathbf{H}_0 + \alpha^2 \nu^4 \mathbf{H}_1 + \alpha \nu^3 :\mathbf{H}_2: \\ &\quad - i\mu\nu :\mathbf{H}_3: + \nu^2 (:\mathbf{H}_4: + :\mathbf{H}_5:) + \nu^2 \mathbf{H}_I \Big] \end{aligned} \tag{7.47}$$

where $\mu = \frac{m_0}{g^2}$ is the dimensionless mass, $\nu = \frac{1}{\sqrt{8\pi L_\perp g^2}}$ and $\alpha = 8\pi^2$. $\mathbf{H}_I$ is the sum of the terms involving the self induced inertias in equations (7.42) and (7.42). g can be thought of as setting the scale for the mass spectrum.

7.4 The continuum limit and renormalization

The continuum limit, in which all momentum cutoffs are lifted and the two box sizes L_+ and $L_\perp$ are made infinite, corresponds to the limits $\nu \to 0$ and $\Lambda_+, \Lambda_\perp, K \to \infty$. The precise order in which the limits are taken is very important. If $\nu \to 0$ is taken before the others, then we end up with a trivial non-interacting theory. The correct order is to take $\Lambda_+ \to \infty$ and $\Lambda_\perp \to \infty$ before taking $K \to \infty$ and $\nu \to 0$. However we are now faced with apparent ultraviolet divergences with light cone and transverse momenta in the mass operator because of the self-induced inertias. As we show in Appendix B this ultraviolet divergence can be expected to cancel if we take the dynamics into consideration. More specifically, the one-loop light cone perturbation theory result for the fermion self-mass is linearly divergent with transverse momentum and logarithmically divergent with light cone momentum. A cancellation of all ultraviolet divergences would be required if the light cone formulation is to be equivalent to the normal spacetime formulation in which there are no ultraviolet divergences [14].

We note here that other regularization schemes than introducing momentum cutoffs are available. Burkardt [77] is currently working on a different procedure to control the divergences. Reminiscent of the Pauli-Villars regularization procedure in perturbation theory, the idea is to couple the theory to an identical theory of "ghosts" in such a way that the self-induced inertia terms disappear. The coupled theory becomes ultraviolet finite in momenta and decoupling is achieved by taking

the ghost masses to infinity, thereby recovering the original theory. Whether this program is viable computationally remains to be seen, however.

For QED in (3+1) Tang [12] used another procedure to regularize and renormalize, one familiar from perturbation theory. He used light cone perturbation theory to calculate a mass counterterm for the electron so that when inserted into the Hamiltonian, the physical electron mass is the same as the bare mass for all values of the couplings. He worked with a fixed momentum cutoff and let the cutoff dependence be taken care of by a running coupling. The self-induced inertias were simply incorporated into the mass counterterm used. With the counterterm in place he then proceeded to calculate the bound state spectrum but was restricted by computational resources. One could imagine doing the same thing in (2+1)D but must first introduce a photon mass to deconfine the fermions and make the physical fermion mass a meaningful quantity, in other words to regulate the infrared divergences in the fermion mass. Taking the photon mass to zero at the end would presumably lead us back to a confining theory. This approach will not be considered here either.

One could contrast the situation regarding taking continuum limits in the DLCQ formalism and in lattice gauge theory. In lattice gauge theory there are only two limits to take, namely the lattice size $M \to \infty$ and the lattice spacing $a \to 0$. Having more limits to take in DLCQ seems to be inevitable because of the way the light cone direction is singled out and is costly, but hopefully there are payoffs involved, too.

7.5 Numerical results

As mentioned above we work in the $(u, \overline{d})$ and $(u, \overline{d}, \gamma)$ sectors. For given integers K and $\Lambda_\perp$ we construct the Fock space as follows. For the $(u, \overline{d})$ states, partition

K into two odd half integers which will become the light cone momenta l_1 and l_2. The transverse momenta will be given simply by any combination of m_1 and m_2 which sum to zero, with each momentum being of absolute value less than the cutoff. Hence we will have a total of $K(2\Lambda_\perp + 1)$ Fock states to consider. The situation is similar for $(u, \overline{d}, \gamma)$ states except that the increase in the number of Fock states with K and $\Lambda_\perp$ is much faster.

We then have to diagonalize $\mathbf{H}_2$, $\mathbf{H}_3$ and $\mathbf{H}_4$ in this Fock space. We used the Lanczos algorithm [40] to handle large (up to approximately 3000×3000) matrices. The Lanczos algorithm usually allowed the lowest 2 eigenvalues to be determined up to 3 decimal places within 100 Lanczos steps.

We fix the dimensionless mass μ at 10 and take $2\Lambda_+ = 2000$. We chose $\nu = 0.1$, which fixes the transverse box length. With these values we studied the dependence on $\Lambda_\perp$ and K. We first did a calculation using only $(u, \overline{d})$ states. The results for the the dimensionless mass squared $\frac{\mathcal{M}^2}{g^4}$ of the lowest bound state and the mass gap $\Delta E = (\mathcal{M}_1 - \mathcal{M}_0)/g^2$ are plotted in Figures 7.1 and 7.2 against $\Lambda_\perp$ for values of $2K = 10, 30, 38$ and 50. Note that the non-relativistic limits of $\frac{\mathcal{M}^2}{g^4}$ and ΔE are, from equations (6.23) and (6.19) with $\frac{m_0}{g^2} = 10$, respectively 417.07 and 0.01094.

The dependence of the mass squared on $\Lambda_\perp$ is linear and seems to be controlled totally by the self-induced inertias. The mass gap dependence on $\Lambda_\perp$ is quite weak for large $\Lambda_\perp$ but seems to decrease, possibly to zero. In any case, the divergence does not make physical sense.

However when we coupled to $(u, \overline{d}, \gamma)$ states, the situation changed. The results for the mass squared of the lowest bound state obtained are plotted in Figure 7.3. The increase with Λ_+ is now much less marked. In other words, the dynamics of coupling to the $(u, \overline{d}, \gamma)$ states has resulted in a softening of the

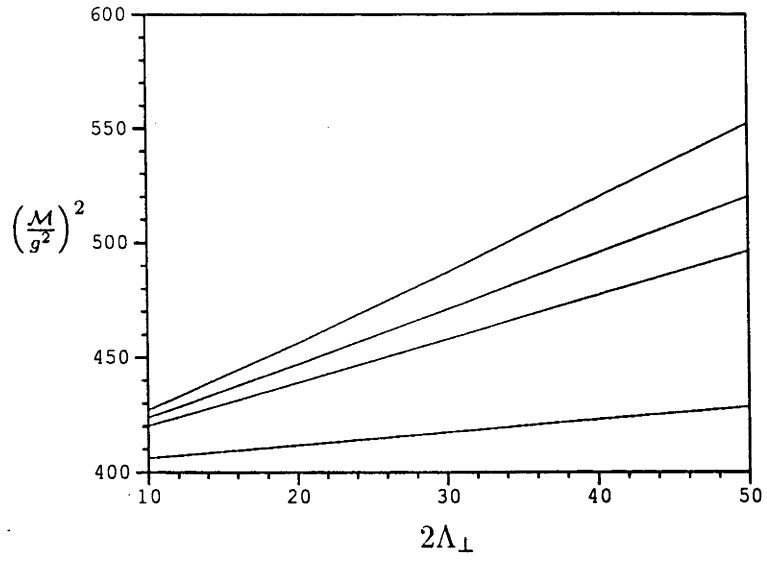

Figure 7.1: The dimensionless mass squared of the lowest bound state in the $(u, \overline{d})$ sector against transverse momentum cutoff $\Lambda_\perp$ for values of $2K = 10, 30, 38$ and 50. with $\mu = 10$ and $\nu = 0.1$. The values for fixed $\Lambda_\perp$ increase with K.

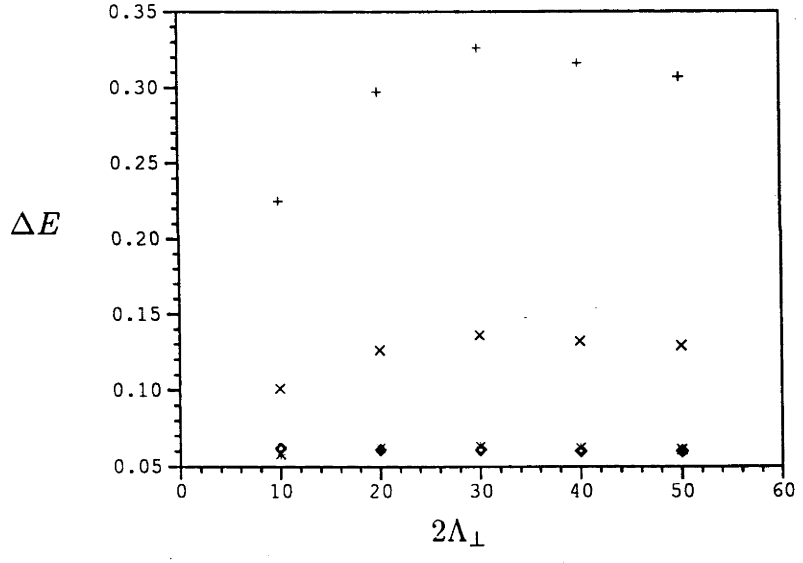

Figure 7.2: The dimensionless mass gap in the $(u, \overline{d})$ sector against transverse momentum cutoff $\Lambda_\perp$ for $2K = 10(\diamond), 30(*), 38(\times)$ and $50(+)$.

divergence. Whether it leads to a cancellation or not, ie. whether or not the mass squared plateaus out for large Λ_+, could not be determined numerically. Each increase in $\Lambda_\perp$ of 1 increases the Fock space size by about 500 so that the size is already greater than 3000 by the time we get to $2\Lambda_\perp = 20$.

It is instructive to consider the structure function $f(x)$ for the bound state.

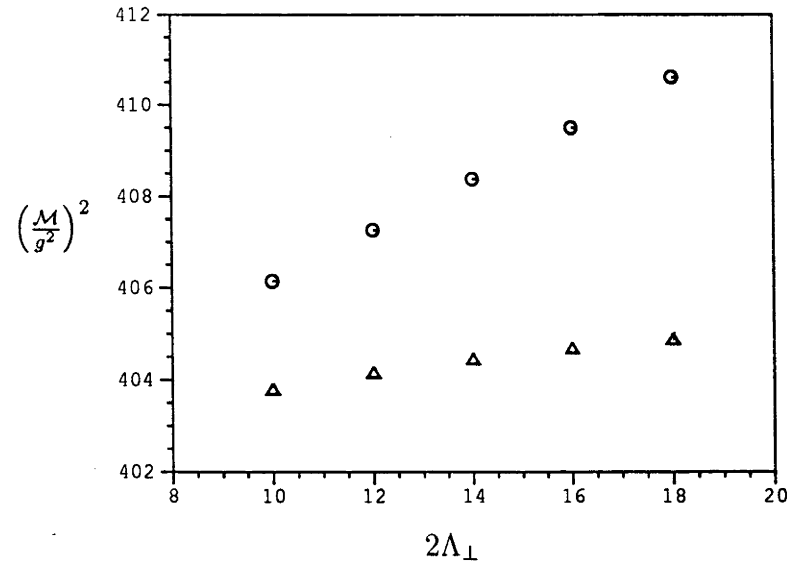

Figure 7.3: The dimensionless mass squared in the $(u, \overline{d}$ sector (o) and when coupled to the $(u, \overline{d}, \gamma)$ sector ($\triangle$) against transverse momentum cutoff $\Lambda_\perp$ for $2K = 10$, $\mu = 10$ and $\nu = 0.1$.

It is the probability to find a fermion with a total light cone momentum fraction x. If $\sum_j C^j|\Phi_j\rangle$ is the bound state wavefunction, then $f(x)$ is given by

$$f(x) \propto \sum_{i,m} \sum_j |C^j|^2 \langle \Phi_j | \mathrm{b}^{i\dagger}_{lm} \mathrm{b}^i_{lm} | \Phi_j \rangle \tag{7.48}$$

where $l = Kx$ and the sum is over all "flavours" i and all transverse momentum modes m. In the limit of large K, $f(x)$ becomes a probability density. It is a measured quantity in deep-inelastic lepton scattering. For $2K = 10$ and $2\Lambda_\perp = 10$, $f(x)$ is highly peaked at $x = 0.5$ (diagram not shown). The dominant Fock states are the ones with the fermion carrying half the total light cone momentum.

It is more instructive to consider the structure function $f^\perp(t)$, defined as the probability of finding a fermion with absolute transverse momentum t and is given by

$$f^\perp(t) = \sum_{i,l} \sum_j |C^j|^2 \langle \Phi_j | \mathrm{b}^{i\dagger}_{l,t} \mathrm{b}^i_{l,t} + \mathrm{b}^{i\dagger}_{l,-t} \mathrm{b}^i_{l,-t} | \Phi_j \rangle. \tag{7.49}$$

The results for $2K = 10$ and $\Lambda_\perp = 10$ are plotted in Figure 7.4 for the situation

with and without coupling to the $(u, \overline{d}, \gamma)$ states. There is a strong peak at $m = 0$ of approximately 1 which is not shown in the figure. The difference between the situation where we do and do allow for photons is apparent. In the former situation high transverse momentum modes become more important. This can be verified by looking directly at the eigenvector. This is strong evidence for the compensating ultraviolet divergence in the one-loop self-mass diagram at work.

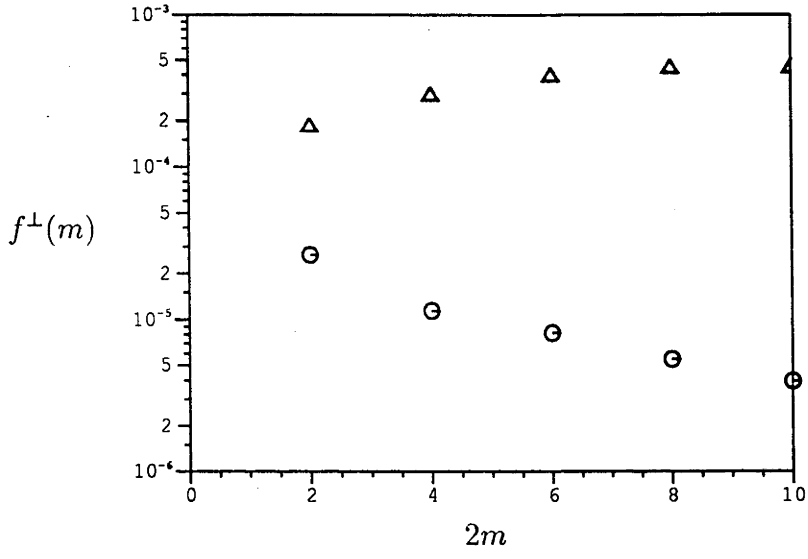

Figure 7.4: The structure function $f^{\perp}(m)$ for the lowest bound state in the $(u, \overline{d})$ sector alone (o) and when coupled to the $(u, \overline{d}, \gamma)$ sector (Δ) against transverse momentum m.

It might be thought that in addition to $\Lambda_{\perp}$ and Λ_{+} we can introduce a further Fock space cutoff to enable us to reach higher $\Lambda_{\perp}$. Such a cutoff could be a one, called Λ^2, such that all Fock states with the diagonal part of $\mathcal{M}^2$ greater than Λ^2 are discarded. Tang [12] uses Λ^2 instead of Λ^{+} and $\Lambda^{\perp}$ in his work and calls it a Lorentz invariant cutoff. The results are plotted in Figure 7.5 for the $(u, \overline{d})$ sector alone and when coupled to $(u, \overline{d}, \gamma)$. As is apparent, this results in cutting off the Fock states with higher transverse momenta which are necessary to counter the ultraviolet divergence in the self- induced inertias and will not work. In Tang's work there are no troubling self-induced inertias to contend with because they are absorbed into a mass counterterm. His approach or the Pauli-Villars approach

would seem to be more efficient than the one which we have presented in reaching the continuum limit.

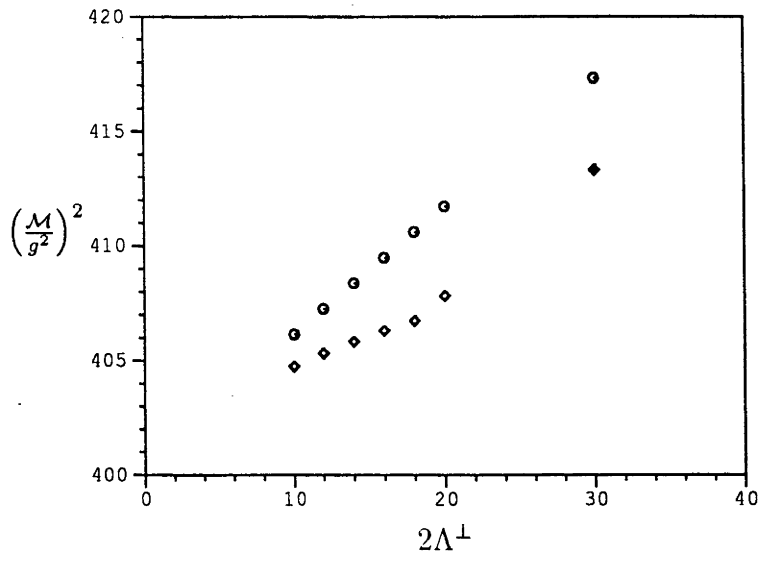

Figure 7.5: The dimensionless mass squared in the $(u, \overline{d})$ sector alone (o) and when coupled to the $(u, \overline{d}, \gamma)$ sector ($\diamond$) against transverse momentum cutoff $\Lambda_\perp$. A Lorentz invariant cutoff Λ^2 of 1000 was used in the calculations.

7.6 Conclusion

In this Chapter we have applied DLCQ to QED in (2+1)D along the same lines as the application to QED in (1+1)D. The major difference between the situation in (1+1)D and that in (2+1)D is that in the latter there is an ultraviolet divergence with transverse momentum cutoff in the self-induced inertias. This divergence is expected to cancel with the ultraviolet divergence in the one-loop self-mass diagrams. We worked in the $(f, \overline{f})$ and $(f, \overline{f}, \gamma)$ sectors and obtained numerical evidence that the (apparent) ultraviolet divergence of the mass of the lowest bound state is *softened* by the dynamics. We have not been able to show, due to limitations on matrix sizes, that the apparent ultraviolet divergence is actually *cancelled.* Hence we have not been able to obtain reliable results to compare with the non-relativistic limit results obtained in Chapter 6.

From this work it would seem that, numerically, it is dangerous to rely on ultraviolet divergences cancelling each other. A possible way out is to consider schemes in which the divergences cancel explicitly at the level of the Hamiltonian. Such a scheme, the Pauli-Villars scheme, is under active investigation [77]. Because it involves introducing extra fields, whether it is numerically viable remains to be seen. DLCQ has yet to establish its credentials as a successful competitor to lattice gauge theory but further consideration merits attention.

ADDENDUM

In this chapter, the results presented were not of sufficient precision for a detailed comparison with the non-relativistic limit obtained in Chapter 6. In particular, we did not manage to deal with a large enough Fock space basis to allow the bound state mass to converge (see figure 7.3). It would be useful to try to attempt larger-scale calculations, possibly involving stochastic methods of the type described in Chapter 4.

Before making a comparison of DLCQ results with the non-relativistic limit obtained in Chapter 6, it would be useful to check that the logarithmic potential can be derived from the light cone Hamiltonian. It is an open question whether this can be done. In fact, modifications might well have to be made to the DLCQ method to treat the non-relativistic limit satisfactorily. This is because the important light cone momentum fractions x are concentrated close to $1/2$ in that limit. Instead of going to larger "box sizes" to satisfactorily sample the peak, it might be more economical to use some sort of non-linear rescaling of the momenta.

The upsho t is that many new ideas, unfamiliar to someone used to the conventional lattice gauge theory techniques, have to be introduced to make DLCQ a useful tool in higher dimensions.

Appendix A

The values of the symmetrized brackets

In this appendix it is shown that it is possible to obtain consistently the symmetrized brackets (5.30) and (5.31).

We will be making use of the following integrals:

$$\frac{1}{2\pi}\int_{-\pi}^{\pi} d\xi \xi e^{i\alpha\xi} = \frac{\cos(\alpha\pi)}{i\alpha} \tag{A.1}$$

$$\frac{1}{2\pi}\int_{-\pi}^{\pi} d\xi \xi^2 e^{i\alpha\xi} = \frac{2\cos(\alpha\pi)}{\alpha^2} \tag{A.2}$$

$$\frac{1}{2\pi}\int_{-\pi}^{\pi} d\xi e^{i\alpha\xi} = \delta_{\alpha,0} \tag{A.3}$$

for integer α and

$$\frac{1}{2\pi}\int_{-\pi}^{\pi} d\xi r m e^{i\beta\xi} = \frac{\sin(n\pi)}{n\pi} \tag{A.4}$$

for β being an odd multiple of $\frac{1}{2}$.

We shall first calculate the bracket $\{n|m\}$ defined by

$$\{n|m\} = \frac{1}{2\pi}\int_{-\pi}^{\pi} d\xi \left\{ e^{in\xi} \frac{1}{(i\partial_\xi)} e^{im\xi} \right\}_{sym} \tag{A.5}$$

for n and m being odd multiples of $\frac{1}{2}$ and where the symmetrized bracket is defined by

$$\left\{A\frac{1}{i\partial^+}B\right\}_{sym} = \frac{1}{2}\left[A\left(\frac{1}{i\partial^+}B\right) - \left(\frac{1}{i\partial^+}A\right)B\right] \tag{A.6}$$

Now $\frac{1}{(i\partial^+)}$ is connected with eliminating ψ_- in favour of ψ_+ in equation (5.11). Hence boundary terms involved in $\frac{1}{i\partial_\xi}$ are related to boundary terms for ψ_- in the McCartor-Hornbostel approach. In general we will have

$$\frac{1}{(i\partial_\xi)}e^{in\xi} = -\frac{e^{in\xi}}{n} + A_n. \tag{A.7}$$

Substituting this into equation (A.5) and making use of integrals (A.3) and (A.4) we obtain

$$\{n|m\} = \frac{1}{n}\delta_{n+m,0} + \left(\frac{A_m\sin(n\pi)}{2n\pi} - \frac{A_n\sin(m\pi)}{2m\pi}\right). \tag{A.8}$$

We can get rid of the term within the round brackets by making the choice $A_n = 0$ for all n in (A.7) and end up with equation (5.30).

We shall now calculate the brackets $[k|l]$ defined by

$$[k|l] = \frac{1}{2\pi}\int_{-\pi}^{\pi} d\xi \left\{e^{ik\xi}\frac{1}{(i\partial_\xi)^2}e^{il\xi}\right\}_{sym} \tag{A.9}$$

for integer k and l where the symmetrized bracket is defined by

$$\left\{A\frac{1}{(i\partial^+)^2}B\right\}_{sym} = A\left(\frac{1}{(i\partial^+)^2}B\right) + \left(\frac{1}{i\partial^+}A\right)\left(\frac{1}{i\partial^+}B\right) \tag{A.10}$$

$$+\left(\frac{1}{(i\partial^+)^2}A\right)B. \tag{A.11}$$

Now $\frac{1}{(i\partial^+)^2}$ is connected with eliminating A^- and its derivatives in favour of ψ_+

in equation (5.12). In general we will have

$$\frac{1}{(i\partial_\xi)^2}e^{ik\xi} = \begin{cases} \frac{e^{ik\xi}}{k^2} + B_k\xi + C_k & k \neq 0 \\ -\frac{\xi^2}{2} + B_0\xi + C_0 & k = 0 \end{cases} . \tag{A.12}$$

Substituting this into equation (A.9), and making use of the integrals (A.1) to (A.3) we obtain

$$[k|l] = \frac{1}{n^2}\delta k + l, 0 + \left(\frac{B_l\cos(k\pi)}{ik} + \frac{B_k\cos(l\pi)}{il} - B_kB_l\right) \tag{A.13}$$

$$[k|0] = \left(\frac{B_0\cos(k\pi)}{ik} + C_k - B_kB_0\right) \tag{A.14}$$

$$[0|0] = \left(-\frac{2}{3}\pi^2 + 2C_0 - B_0^2\right). \tag{A.15}$$

where $k, l \neq 0$. In order to arrive at the result (5.31) we must get rid of all the terms within round brackets in (A.13) to (A.15). The (non-unique) choice

$$B_k = 0, \qquad C_k = -\frac{B_0\cos(k\pi)}{ik}, \qquad 2C_0 - B_0^2 = \frac{2}{3}\pi^2 \tag{A.16}$$

evidently does the job. Hence we have obtained the results (5.30) and (5.31) which are required for conservation of light cone momentum by a judicious choice of boundary terms for ψ_- and A^-.

Appendix B

The one-loop fermion self-mass

In this appendix we calculate the one-loop fermion self-mass (diagram shown in Figure B.1) using light cone perturbation theory. The rules for QCD are given in [78]. We need only make some minor modifications to these rules in order to apply them to our 4-component spinor QED in (2+1)D. The modified rules that we require are:

1. Assign a momentum k^μ to each line such that the total k^+, $k^\perp$ are conserved at each vertex, and such that $k^2 = k^+k^- - (k^\perp)^2 = m^2$. With each fermion associate an on-shell spinor

$$u^j(k) = \frac{1}{\sqrt{k^+}}\left(k^+ + \beta m + \alpha^\perp k^\perp\right) w^j \tag{B.1}$$

   where $w^1 = \frac{1}{\sqrt{2}}(1,1,0,0)^T$ and $w^2 = \frac{1}{\sqrt{2}}(0,0,1,1)^T$. The Dirac matrices matrices $\alpha^\perp$ and β are those given in equations (3.5).

2. Include a factor of $1/k^+$ for each internal line.

3. For the vertex shown below, include the factor

$$g u^{j\dagger}(k_c)\alpha^\perp u^{j'}(k_a) \tag{B.2}$$

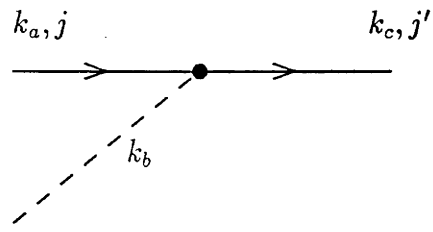

4. For each intermediate state, include the factor

$$\frac{1}{\epsilon - \sum k^- + iO_+} \tag{B.3}$$

where ϵ is the incident P^- and the sum is over all particles in the intermediate state.

5. Integrate $\int \frac{dk^+ dk^\perp}{8\pi^2}$ over each independent k and sum over internal "flavours" j.

We note the following spinor identities:

$$\begin{aligned} u^{j\dagger}(k)\beta u^{j'}(k) &= m\delta_{jj'} \\ u^{j\dagger}(p)\alpha^\perp u^{j'\dagger}(k) &= \delta_{jj'}\left[\frac{k^\perp p^+ + k^+ p^\perp + i(-1)^j(k^+ - p^+)}{\sqrt{k^+ p^+}}\right] \end{aligned}$$

which can be obtained from the Dirac matrices and the chosen spinors. The amplitude for the process is given by

$$\begin{aligned} T_{fi} &= g^2 \sum_{j''} \int \frac{dk_2^+ dk_2^\perp}{8\pi^2 k_1^+ k_2^+} \times \\ &\qquad \frac{u^{j'\dagger}(p)\alpha^\perp u^{j''}(k_2) u^{j''\dagger}(k_2) u^{j''\dagger}(k_2)\alpha^\perp u^j(p)}{p^- - k_1^- - k_2^-} \end{aligned} \tag{B.4}$$

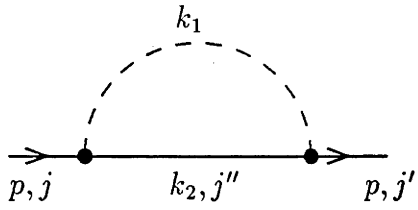

Figure A1

Figure B.1: The one-loop fermion self mass diagram.

The spinor part can be shown, making use of the above spinor identities, to be given by

$$\sum_{j''} u^{j'\dagger}(p)\alpha^{\perp}u^{j''}(k_2)u^{j''\dagger}(k_2)\alpha^{\perp}u^{j}(p) \;=\; \delta_{jj'}\left[\frac{(p^{\perp}k_2^{+}+k_2^{\perp}p^{+})^2+m^2(k_2^{+}-p^{+})^2}{p^{+}k_2^{+}}\right] \tag{B.5}$$

Eliminating

$$\begin{aligned} k_1^{+} &= p^{+}-k_2^{+}, \\ p_{-} &= \frac{m^2+(p^{\perp})^2}{p^{+}} \\ k_1^{-} &= \frac{(k_1^{\perp})^2}{k_1^{+}}=\frac{(p^{\perp}-k_2^{\perp})^2}{p^{+}-k_2^{+}} \\ k_2^{-} &= \frac{m^2+(k_2^{\perp})^2}{k_2^{+}} \end{aligned} \tag{B.6}$$

from equation (B.4) we obtain

$$T_{fi}=\delta_{jj'}g^2\int\frac{dk_2^{+}dk_2^{\perp}}{8\pi^2k_1^{+}k_2^{+}}\times \frac{\left[(p^{\perp}k_2^{+}+k_2^{\perp}p^{+})^2+m^2(k_2^{+}-p^{+})^2\right]}{\left[(m^2+(p^{\perp})^2)(p^{+}-k_2^{+})k_2^{+}-(p^{\perp}-k_2^{\perp})^2k_2^{+}p^{+}-(m^2+(k_2^{\perp})^2)(p^{+}-k_2^{+})p^{+}\right]} \tag{B.7}$$

It is now evident from power counting that T_{fi} is linearly divergent in $k_2^{\perp}$ and has a negative sign. The claim is that this ultraviolet divergence will cancel with the ultraviolet divergence in the self-induced inertias. We note that in the corresponding self-mass calculation in the conventional spacetime formulation there is no ultraviolet divergence in momentum due to symmetric integration [14].

The author in references [10] and [11] should be H.C.Pauli.

Bibliography

[1] F.E.Close, *An Introduction to Quarks and Partons*, Academic Press,1979; E.Leader and E.Predazzi, *An Introduction to Gauge Theories and the 'New Physics'*, Cambridge University Press, 1982.

[2] G.'t Hooft, Nucl. Phys. **B33** (1971) 173.

[3] D.J.Gross and F.Wilczek, Phys. Rev. Lett. **30** (1973) 1343; H.D.Politzer, Phys. Rev. **30** (1973) 1346.

[4] A.H.Mueller, in *Proceedings of the Yale Theoretical Advanced Study Institute*, eds. M.Bowick, F.Gürsey, World Scientific, 1987.

[5] C.Itzykson and J.-B.Zuber, *Quantum Field Theory*, McGraw-Hill, 1980.

[6] K.G.Wilson, Phys. Rev. **D10** (1974) 2445.

[7] "Lattice '88", Nucl. Phys. B (Proc. Suppl.) **9**(1989); "Lattice '89", in press.

[8] K.G.Wilson, *Talk presented at Lattice '89 Capri, Italy, Sept 18-21, 1989.*

[9] J.B.Kogut and L.Susskind, Phys. Rev. **D11** (1975) 395.

[10] W.Pauli and S.J.Brodsky, Phys. Rev. **D32** (1985) 1993; W.Pauli and S.J.Brodsky, Phys. Rev. **D32** (1985) 2001.

[11] T.Eller, W.Pauli and S.J.Brodsky, Phys. Rev. **D35** (1987) 1493.

[12] A.Tang, PhD Thesis, Stanford University, 1990.

[13] J.M.Cornwall and G.Tiktopoulos, Phys. Rev. **D22** (1977) 2937;
J.M.Cornwall, Phys. Rev. D22 (1980) 1452.

[14] R.Jackiw and S.Templeton, Phys. Rev. **D23** (1981) 2291;
S.Deser, R.Jackiw and S.templeton, Ann. Phys. (N.Y.) **140** (1982) 372.

[15] A.Coste and M.Lüscher, Nucl. Phys. **B323** (1989) 631.

[16] M.Göpfert and G.Mack, Comm. Math. Phys. **82** (1982) 545.

[17] P.Suranyi, Nucl. Phys. **B210** (1982) 519.

[18] J.Ambjorn, A.J.G.Hey, and S.Otto, Nucl. Phys. **B210** (1982) 347;
T.Sterling and J.Greensite, Nucl. Phys. **B220** (1983) 327;
M.Karliner and G.Mack, Nucl. Phys. **B225** (1983) 371.

[19] A.C.Irving, J.F.Owen, and C.J.Hamer, Phys. Rev. **D28** (1983) 2059.

[20] C.J.Hamer and A.C.Irving, Z. Phys. **C27** (1983) 145.

[21] D.W.Heys and D.R.Stump, Nucl. Phys. **B285** (1987) 13.

[22] G.Lana, Phys. Rev. **D38** (1988) 1954.

[23] C.J.Burden and C.J.Hamer, Phys. Rev. **D37**(1989) 479.

[24] J.B.Kogut, Rev. Mod. Phys. **51** (1979) 659;
J.B.Kogut, Phys. Rep. **67** (1980) 388;
J.B.Kogut, Rev. Mod. Phys. **55** (1983) 775.

[25] M.Creutz, *Quarks, gluons and lattices*, Cambridge University Press, 1983.

[26] R.P.Feynman and A.R.Hibbs, *Quantum Mechanics and Path Integrals*, McGraw-Hill, 1965.

[27] C.Domb and M.S.Green, eds., *Phase Transitions and Critical Phenomena, Vols. 1 - 6*, Academic, 1971 - 1976;
C.Domb and J.L.Lebowitz, eds., *Phase Transitions and Critical Phenomena, Vols. 7 - 12*, Academic, 1983 - 1988.

[28] P.Pfeuty and G.Toulose, *Introduction to the Renormalization Group and to Critical Phenomena*, Wiley, 1977.

[29] G.Parisi, *Statistical Field Theory*, Addison-Wesley, 1989.

[30] A.A.Belavin, A.M.Polyakov and A.B.Zamolodchikov, Nucl. Phys. **B241** (1984) 333.

[31] W.E.Caswell, Phys. Rev. Lett. *33* (1974) 244;
D.R.T.Jones, Nucl. Phys. *B75* (1974) 531.

[32] J.B.Kogut, D.K.Sinclair and L.Susskind, Nucl. Phys. **B114** (1976) 199;
J.B.Kogut, R.B.Pearson and J.Shigemitsu, Phys. Rev. Lett. **43** (1979) 484;
J.B.Kogut and J.Shigemitsu, Phys. Rev. Lett. **45** (1980) 410;
J.B.Kogut, R.B.Pearson and J.Shigemitsu, Phys. Lett. **98B** (1981) 63.

[33] C.J.Hamer, A.C.Irving and T.E.Preece, Nucl. Phys. **B270** (1986) 553;
C.J.Hamer, *"Hamiltonian Strong Coupling Expansions for Glueball Masses in $SU(3)$"*, Univ. of New South Wales preprint, 1989.

[34] C.J.Hamer and M.N.Barber, J. Phys. **A14** (1981) 241;
C.J.Hamer and M.N.Barber, J. Phys. **A14** (1981) 259.

[35] D.W.Heys and D.R.Stump, Nucl. Phys. **B257** (1985) 19;
S.A.Chin, C.Long and D.Robson, Phys. Rev. Lett. **57** (1986) 2779;
S.A.Chin, C.Long and D.Robson, Phys. Rev. **D37** (1988) 3001;
C.Long, D.Robson and S.A.Chin, Phys. Rev. **D37** (1988) 3006.

[36] E.Dagotto, A.Moreo, Phys.Rev. **D31** (1985) 865;
J.-W.Choe, A.Duncan and R.Roskies, Phys. Rev. **D37** (1988) 472.

[37] B.G.Nickel, unpublished (1980);
L.G.Marland, J. Phys. **A14** (1981) 2047;
A.C.Irving and C.J.Hamer, Nucl. Phys. **B230** (1984) 361;
A.C.Irving and C.J.Hamer, Nucl. Phys. **B235** (1984) 358;
A.C.Irving and C.J.Hamer, J. Phys. **A14** (1984) 1649.

[38] C.J.Burden, Phys. Lett. **B198** (1987) 525.

[39] M.N.Barber, in *Phase Transitions and Critical Phenomena*, Vol. 8, eds. C.Domb and J.L.Lebowitz, Academic Press, 1983.

[40] C.Lanczos, J. NBS. **45** (1950) 255;
R.R.Whitehead, A.Watt, B.J.Cole and I.Morrison, Adv. Nucl. Phys. vol **9** (1977) 123.

[41] C.R.Allton and C.J.Hamer, J. Phys. **A21** (1988) 2417.

[42] C.R.Allton, Australian National Univ PhD Thesis, 1989.

[43] R.J.Baxter, *Exactly solved models in Statistical Mechanics*, Academic, New York, 1982.

[44] M.Henkel, *"Applications of the Hamiltonian Limit to Critical Phenomena, Finite-size scaling and Conformal Invariance"*, in *Finite-size scaling and Numeriacl Simulation of Statistical Systems*, ed. V.Privman, World Scientific, to appear.

[45] R.D.Pisarki, Phys. Rev. **D29** (1984) 2423.

[46] L.Susskind, Phys. Rev. **D16** (1977) 3031.

[47] C.R.Allton, C.M.Yung and C.J. Hamer, Phys. Rev. **D39** (1989) 3772.

[48] C.M.Yung, C.R.Allton and C.J.Hamer, Phys. Rev. **D39** (1989) 3778.

[49] D.M.Ceperley and M.H.Kalos, in *Monte Carlo Methods in Statistical Physics* ed. K.Binder, Springer, Berlin, 1979;
D.W.Heys and D.R.Stump, Phys. Rev. **D28** (1983) 2067;
D.W.Heys and D.R.Stump, Phys. Rev. **D30** (1984) 1315.

[50] R.Blankenbecler and R.L.Sugar, Phys. Rev. **D** (1983) 1304;
D.Kung, R.Blankenbecler and R.L.Sugar, Phys. Rev. **B** (1985) 3058;
J.Potvin and T.A.DeGrand, Phys. Rev. **D30** (1984) 1285.

[51] T.A.DeGrand and J.Potvin, Phys. Rev. **D31** (1985) 871.

[52] M.P.Nightingale and H.W.J.Blote, Phys. Rev. **B33** (1986) 659.

[53] F.A.Alcaraz and M.N.Barber, unpublished (1986).

[54] S.A.Chin, J.W.Negele and S.E.Koonin, Ann. Phys. **157** (1984) 140;
S.E.Koonin, E.A.Umland, and M.R.Zirnbauer, Phys. Rev. **D33** (1986) 1795.

[55] K.Binder, in *Monte Carlo Methods in Statistical Physics* ed. K.Binder, Springer, Berlin, 1979.

[56] M.Lüscher, G.Münster and P.Weisz, Nucl. Phys. **B180** (1980) 1;
C.Itzykson, M.E.Peskin and J-B. Zuber, Phys. Lett. **95B** (1980) 259;
A., E. and P.Hasenfratz, Nucl. Phys. *B180* (1981) 353.

[57] C.J.Hamer and A.C.Irving, Nucl. Phys. **B225** (1983) 289.

[58] E.Fradkin and L.Susskind, Phys. Rev. **D17** (1978) 2637.

[59] C.Michael, J.Phys. **G13** (1987) 100.

[60] C.J.Burden, private communication (1987).

[61] A.N.Burkitt and A.C.Irving, Nucl. Phys. **B295** (1988) 525.

[62] E.Dagotto, A.Kocic and J.B.Kogut, Nucl. Phys. **B334** (1990) 279.

[63] C.J.Hamer, M. Aydin, J.Oitmaa and H-X.He, *"The 3-State Potts Model in (2+1) Dimensions"*, Univ. of New South Wales preprint, 1990;
C.J.Hamer and J.Court, *"Stochastic Truncation Approach to the Z_2 Gauge Model in (3+1) Dimensions"*, Univ. of New South Wales preprint, 1990.

[64] C.J.Hamer, Nucl. Phys. **B121** (1977) 159.

[65] I.S.Gradshteyn and I.M.Rhyzhik, *Table of Integrals, Series and Products*, Academic Press, 1980.

[66] W.A.Coppel, *Stability and Asymptotic behaviours of Differential Equations*, Heath, Boston, 1965.

[67] S.E.Koonin, *Computational Physics*, Benjamin/Cummings, 1986.

[68] D.Sen, Phys. Rev. **D41** (1990) 1227.

[69] S.Weinberg, Phys. Rev. **150** (1966) 1313.

[70] L.Susskind, Phys. Rev. **165** (1968) 1535.

[71] K.Bardakci and M.B.Halpern, Phys. Rev. **176** (1968) 1686.

[72] S.Chang and S.Ma, Phys. Rev. **180** (1969) 1506.

[73] J.B.Kogut and D.E.Soper, Phys. Rev. **D1** (1970) 2901.

[74] G.McCartor, Z.Phys. **C41** (1988) 271.

[75] K.Hornbostel, PhD thesis, Stanford University, 1988.

[76] C.J.Hamer, unpublished notes (1988).

[77] M.Burkardt, private communication (1990).

[78] G.P.Lepage, S.J.Brodsky, T.Huang and P.B.Mackenzie, in *Proceedings of the Banff Summer Institute on Particles nd Fields*, eds. A.Z.Capri and A.N.Kamal, Plenum Press, 1981;

S.J.Brodsky, in *Proceedings of the VIIIth Summer School in Nuclear and Particle Physics, Launceston, Tasmania*, eds. R.Delbourgo and J.R.Fox, World Scientific, 1987.